UNIVERSITY OF CALIFORNIA

LOS ANGELES

# Deoxygenation and the impact on ocean biogeochemistry in the Santa Barbara Channel, and the broader implication for deoxygenation policy

A dissertation submitted in partial satisfaction of the requirements for the degree Doctor of Doctor of Philosophy in Atmospheric and Oceanic Sciences

by

De'Marcus Remonte Robinson

2024

© Copyright by

De’Marcus Remonte Robinson

2024

ABSTRACT OF THE DISSERTATION

Deoxygenation and the impact on ocean biogeochemistry in the Santa Barbara Channel, and the broader implication for deoxygenation policy

by

De'Marcus Remonte Robinson

Doctor of Philosophy in Atmospheric and Oceanic Sciences

University of California, Los Angeles, 2024

Professor Tina Treude, Chair

Deoxygenation occurs along coastal environments and open ocean that affects ocean biogeochemistry and marine species. The causes of deoxygenation are multifaceted and can be influenced by various physical and biogeochemical properties in the ocean. The California Current System experiences deoxygenation along its coast and continental shelf, and effects sub-basins like the Santa Barbara Channel (SBC), located in the Southern California Bight. Here, oxygen concentrations can become hypoxic and anoxic, influencing the release of trace metals like iron from the sediment and the formation of sulfur-oxidizing bacteria mats in response to sulfide production in the sediment. Quantifying the impacts that deoxygenation has in the Santa Barbara Channel, will provide insights into ocean biogeochemistry locally, and in the California Current

System more generally, along with guidance for broader ocean policies to advance regulations to combat ocean deoxygenation. In this dissertation, I will use data from two research expedition on R/V Atlantis in 2019 and 2023 to the Santa Barbara Channel and its basin, to quantify how benthic Fe flux affects phytoplankton growth along with the spatial and temporal distribution of oxygen in the basin; and extrapolate the impact of hypoxia and anoxia on basin-wide benthic Fe flux. Lastly, I developed a framework to determine the factors that can contribute to the implementation of deoxygenation policy into the Biodiversity Beyond National Jurisdiction Treaty. Since deoxygenation can affect marine biodiversity, fisheries management, and blue economies, it is important to determine the social-human environmental factors for governance and management as it relates to deoxygenation.

**Chapter 2**. To investigate the influence of benthic Fe release from the oxygen-deficient deep basin on surface phytoplankton production, we combined benthic Fe flux measurements with numerical simulations using the Regional Ocean Model System coupled to the Biogeochemical Elemental Cycling model (ROMS-BEC). For this purpose, we updated the model Fe flux parameterization to include the new benthic flux measurements from the Santa Barbara Basin. Our simulations suggest that benthic Fe fluxes enhance surface primary production, supporting a positive feedback on benthic Fe release by decreasing oxygen in bottom waters. However, a reduction of phytoplankton Fe limitation by enhanced benthic fluxes near the coast may be partially compensated by increased nitrogen limitation further offshore, limiting the efficacy of this positive feedback.

**Chapter 3**. While numerous studies have investigated the influence of hypoxia and anoxia on nutrient cycling and microbial activity in the sediment and water column of the SBC, studies that characterize the spatial distribution of dissolved oxygen in the channel, and its temporal

variability, remain limited. I explored the spatial extent and temporal variability of dissolved oxygen in the SBC, with the goal of increasing our understanding of its dynamics and the consequences for the ocean biogeochemistry and phytoplankton productivity. To this end, I integrated historical observations of dissolved oxygen from California Cooperative Oceanic Fisheries Investigation (CalCOFI) and other programs with two highly spatially resolved oxygen surveys from recent cruises (AT42-19/2019 and AT50-11/2023) that deployed the Autonomous Underwater Vehicle (AUV) Sentry and the Remotely Operated Vehicle (ROV) Jason, equipped with oxygen sensors. This new data compilation provides the first spatially resolved characterization of dissolved oxygen across the SBC and in the bottom boundary layer.

**Chapter 4** Global deoxygenation is becoming an emerging issue in ocean policy that intersects with other ocean issues such as ocean acidification, climate impacts on marine species and marine conservation. However, deoxygenation has not appeared in international ocean policy even though the loss of oxygen transcends national and international jurisdiction. The Biodiversity Beyond National Jurisdiction Treaty (BBNJ) or "High Seas Treaty" provides an opportunity to implement deoxygenation for the High Seas. To do so we developed a framework for deoxygenation using scale and levels based on scientific understanding and consensus on the loss of oxygen that intersect with ocean governance. Our framework illustrates how ocean governance can advance ocean policy for deoxygenation that intersects with the initiative in BBNJ.

The dissertation of De'Marcus Remonte Robinson is approved.

David Valentine

David Jacobs

Daniele Bianchi

Tina Treude, Committee Chair

University of California, Los Angeles

2024

## Dedication Page

I dedicate this dissertation to my family, my church family, friends, and mentors who have supported me over this process. This dissertation reflects not only my work, but also your support and encouragement.

Thank you,

D.R.

TABLE OF CONTENTS

List of Figures

Chapter 1



Chapter 2

Appendix



Chapter 3

Appendix



Chapter 4

List of Table

List of Acronyms

°C – Degrees Celsius

2-D – Two dimensions

3-D - Three dimensions

AUV - Autonomous Underwater Vehicle

BBNJ - Biodiversity Beyond National Jurisdiction

BEC - Biogeochemical Elemental Cycling model

BFC – Benthic Flux Chamber

CA – California

CalCOFI – California Cooperative Oceanic Fisheries Investigation

CCE-LTER – California Current Ecosystem Long Term Ecological Research

CCS – California Current System

cm – Centimeters

$cm^{-3}$ – Centimeters Cubed

CUC - California Under Current

$d^{-1}$ – Per Day

d – Day

dFe – Dissolved Iron

DM - Delayed Mode

DNRA – Dissimilatory Nitrate Reduction to Ammonium

E – East

EEZ – Exclusive Economic Zone

ENSO - El Niño-Southern Oscillation

ETOPO – Earth Topographic Global Relief Model

FAIR – Finable, Accessible, Interpretable and Reusable

Fe – Iron

Fe(II) - Ferrous Iron

Fe(II)-L - Ferrous Iron Ligands

Fe(III) - Ferric Iron

Fe (III)-L – Ferric Iron Ligands

GEBCO - General Bathymetric Chart of the Ocean Database

GDAC – Global Data Assembly Centers

Gmol – Giga Mole

$GO_2DAT$ - Global Ocean Database Atlas

HAB – Harmful Algal Bloom

HABHRCA - Harmful Algal Bloom and Hypoxia Research and Control Amendments Act

IOC - Intergovernmental Oceanographic Commission

k – Rate Constant

$kg^{-1}$ – Per Kilo Grams

km – Kilo Meter

$L^{-1}$ – Per Liters

LMCT – Ligand to Metal Charge Transfer

$log_{10}$ – Logarithm base 10

LTER - Long Term Ecological Research Network

m – Meter

$m^{-2}$ – Per Square Meter

$m^{-3}$ – Per Cubic Meter

MBARI - Monterey Bay Aquarium Research Institute

mg - Milli Grams

mL – Milli Liters

mmol – Milli Mole

Mn(II) – Manganese(II)

N – North

N – Fixed Nitrogen

NDT3A - Northern Depocenter Transect Three A

NDT3B - Northern Depocenter Transect Three B

NDT3C - Northern Depocenter Transect Three C

NDRO – Northern Depocenter Radial Origin

NEPIW - North Equatorial Pacific Intermediate Water

$NO_2^-$ - Nitrite

$NO_3^-$ - Nitrate

NPP – Net Primary Production

NRT - Near Real-Time

NSF – National Science Foundation

$NH_4^+$ - Ammonium

nM - Nano Molar

$O_2$ – Oxygen

$O_2^{-\cdot}$ - Superoxide

OMZ – Oxygen Minimum Zone

p - Probability

PDF – Probability distribution function

pH – Potential of Hydrogen

Pmol – Pico Mole

$P_{O2}$ – Partial Pressure of Oxygen

$PO_4^{3-}$ - Phosphate

QF - Quality Flag

R – Correlation Coefficient

Ra – Radium

R/V – Research Vessel

ROV – Remotely Operated Vehicle

ROMS - Regional Ocean Model System

$s^{-1}$ – Per second

SBB – Santa Barbara Basin

SBC – Santa Barbara Chanel

SCB – Southern California Bight

SDRO – Southern Depocenter Radial Origin

SDT3D – Southern Depocenter Transect Three D

$SiO_2$ – Silicate

Tmol – Tera Mole

UN - United Nation

UNCLOS - United Nation Convention on the Law of the Sea

USD - United States Dollar

UV – Ultraviolet

UV - Underwater Vehicle

W – West

$yr^{-1}$ - Per Year

μm – Micrometer

μmol – Micromole

uM – Micomolar

Acknowledgements page

The research presented in this dissertation could not have been accomplished without the support of friends, family, and mentors along the way. I would like to first acknowledge and say thank you to my mentor and advisor Tina Treude, Ph.D. who provided me with her wisdom, guidance, and knowledge on the steps of the scientific process along with passing down knowledge of ocean and sediment processes that has helped me become a better scientist and person every step of the way. I would also like acknowledge and say thank you to my Ph.D. committee, Daniele Bianchi Ph.D., who is my co-advisor, David Valentine Ph.D. and David Jacobs Ph.D, who provided me their expertise, time, and insight for this work which will support the beginning of my scientific career.

I would also like to acknowledge my lab (Tina Treude's, Ph.D. Lab) that provided the necessary help and advice on research and technical assistance on experiment set-up and data analysis, along with the laughs, joys, and friendships developed along the way. I would also like to acknowledge both the UCLA Atmospheric and Oceanic Science Department, and the Earth Planetary Space Science Department for the assistance provided to me over the years from faculty, students, and staff. Even though I am in the Atmospheric and Oceanic Science Department, I spent most of my time and years in the UCLA Earth Planetary Space Science Department, and I am grateful for the people that I have met in both departments along with the relationships and friendships made.

I would also like to acknowledge the UCLA's Center for Diversity Leadership in Science (CDLS) along with alum from UCLA's The Diversity Project, that provided support outside of day-to-day life as a student, that allowed me to be more involved in the community and the work

of science. I am privileged to have worked and met some amazing people who are now close friends that have shared the graduate student experiences and life with.

I would also like acknowledge the National Oceanic and Atmospheric Administration (NOAA) California Sea Grant Office and National Sea Grant Office that accepted me as a John A. Knauss Fellow, and I would also like to acknowledge the host office, Council on Environmental Quality, that helped me develop my understanding of ocean policy. I am truly grateful for this opportunity because it has exposed me to another view of the ocean and has ultimately allowed me to think holistically about ocean research and the connection to ocean policy.

I would like to acknowledge the funding sources for my professional and research trajectory over the years: University of California – Historically Black College and University (UC-HBCU) fellowship, National Science Foundation (NSF), Center for Diversity Leadership in Science (CDLS), and the National Oceanic and Atmospheric Administration (NOAA) Sea Grant Office. Lastly, I would like to acknowledge and say thank you to the crew of the Research Vessel (R/V) *Atlantis* and (R/V) *Shearwater* along with the operators of the Remotely Operated Vehicle (ROV) *Jason*, Autonomous Underwater Vehicle (AUV) *Sentry* and Human Occupied Vehicle (HOV) *Alvin* that helped me do the science needed to understand more about our dynamic ocean and for this work.

Vita/Biographical sketch

**De'Marcus Remonte Robinson**

## Education

University of California, Los Angeles 2021

M.S Atmospheric and Oceanic Science

Florida Agricultural and Mechanical University 2018

B.S Environmental Science

## Publications

1. **Robinson, D**., Pham, A. L. D., Yousavich, D. J., Janssen, F., Wenzhöfer, F., Arrington, E. C., Gosselin, K. M., Sandoval-Belmar, M., Mar, M., Valentine, D. L., Bianchi, D., and Treude, T.: Iron "ore" nothing: benthic iron fluxes from the oxygen-deficient Santa Barbara Basin enhance phytoplankton productivity in surface waters, Biogeosciences,21, 773–788, https://doi.org/10.5194/bg-21-773-2024 , 2024.

2. Yousavich, D. J., **Robinson, D**., Peng, X., Krause, S. J. E., Wenzhöfer, F., Janssen, F., Liu, N., Tarn, J., Kinnaman, F., Valentine, D. L., and Treude, T.: Marine anoxia initiates giant sulfur-oxidizing bacterial mat proliferation and associated changes in benthic nitrogen, sulfur, and iron cycling in the Santa Barbara Basin, California Borderland, Biogeosciences, 21, 789–809, https://doi.org/10.5194/bg-21-789-2024 , 2024.

3. Krause, S. J. E., Liu, J., Yousavich, D. J., **Robinson, D**., Hoyt, D. W., Qin, Q., Wenzhöfer, F., Janssen, F., Valentine, D. L., and Treude, T.: Evidence of cryptic methane cycling and non-methanogenic methylamine consumption in the sulfate-

reducing zone of sediment in the Santa Barbara Basin, California, Biogeosciences, 20, 4377–4390, https://doi.org/10.5194/bg-20-4377-2023 , 2023.

4. Caitlin R. Fong, Kendall S. Chancellor, Julianna J. Renzi**, De'Marcus R. Robinson**, Paul H. Barber, Sennai Y. Habtes, Peggy Fong, Epibionts on Turbinaria ornata, a secondary foundational macroalga on coral reefs, provide diverse trophic support to fishes, Marine Environmental Research, Volume 141, 2018, Pages 39-43, ISSN 0141-1136, https://doi.org/10.1016/j.marenvres.2018.08.001.

**Previous appointments**

2018- Present Ph.D. Candidate, University of California, Los Angeles, Los Angeles, CA

2023-2024 Ocean Policy Fellow, John A, Knauss Marine Policy Fellowship. Host office: Council on Environmental Quality

**Selected Awards and Fellowships**

2018- 2024 UC-HBCU Fellowship

2018- 2024 Center for Diversity Leadership in Science – Early Career Fellow

2023-2024 John A. Knauss Marine Policy Fellowship – Council on Environmental Quality

2016 Third Place at NOAA EPP/MSI 8th Biennial

2015-2018 NOAA Environmental Cooperative Science Center

# Chapter 1: Introduction

## Global Deoxygenation

Oxygen is essential for marine organisms that depend on aerobic respiration. Total dissolved oxygen in the ocean amounts to 227.4 ± 1.1 Pmol, but the distribution of dissolved oxygen in the ocean is not uniform (Schmidtko et al., 2017). Variations in the distribution of oxygen can be attributed to differences in ventilations rates, seafloor bathymetry, sea surface warming, organic carbon production and remineralization rates, and surface and deep-water circulation (Fig. 1-1a). However, oxygen declined globally by 2% since the 20$^{th}$ century with more than 500 coastal environments that have undergone hypoxia since the 1950s (Breitburg et al., 2018; Evans et al., 2020; Schmidtko et al., 2017) due to nutrient loading.

The main causes of oxygen loss are attributed to eutrophication and climate change. Eutrophication occurs from the increase in nutrients from run-off into aquatic and marine systems contributing to algal blooms and high primary productivity. Algal bloom formation in marine systems can result in marine systems becoming hypoxic due to the decay from algae consumed by microorganisms through organic matter remineralization and the subsequent consumption of oxygen with enhanced respiration rates.

Climate change, due to the release of anthropogenic green-house gases into the atmosphere amplifying the greenhouse effect, contributes to increases in surface temperature, that increases stratification, and reduces ventilation and dissolved oxygen (Andrews et al., 2013; Bates and Johnson, 2020; Breitburg et al., 2018; Evans et al., 2020; Shepherd et al., 2017). The impact of deoxygenation can cause habitat compression and mortality of benthic organisms, amplification of ocean acidification, stimulate the release of nutrients like dissolved iron and phosphate, and

perturb aquatic environments from hypoxic (< 65 µM) to anoxic (0 µM) conditions (Breitburg et al., 2018; Craig, 2020; Ekau et al., 2010; Kwiatkowski et al., 2020; Morée et al., 2023; Noffke et al., 2012).

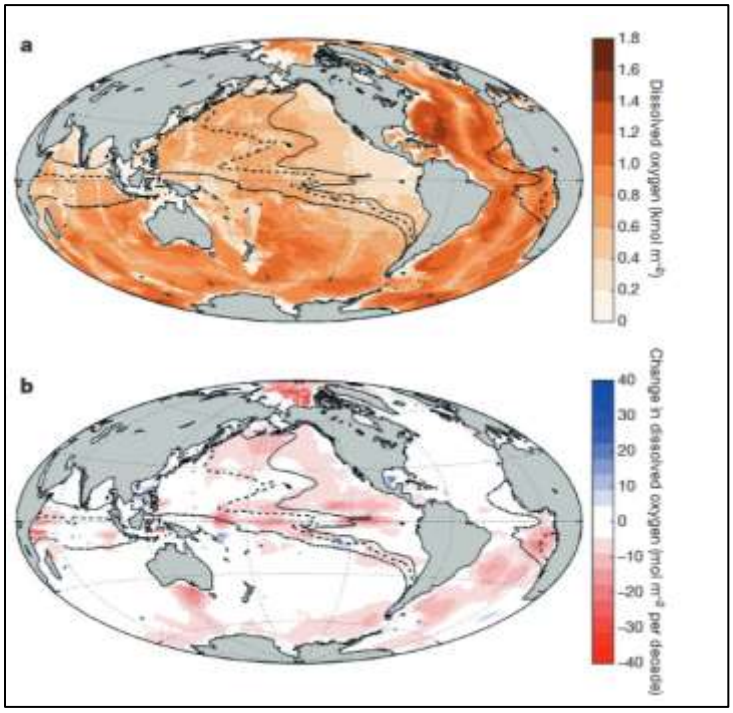


**Figure 1- 1. (**A**)** Global oxygen inventory (dissolved oxygen, color coded). Lines indicate boundaries of oxygen-minimum zones (OMZs): dashed-dotted, regions with less than 80 µmol $kg^{-1}$ oxygen anywhere within the water column; dashed lines and solid lines similarly represent regions with less than 40 and 20 µmol $kg^{-1}$ oxygen, respectively. (B) Change in dissolved oxygen per decade (color coded). Solid black lines show OMZs boundary**.** Figure from Schmidtko et al (2017).

The variability of oxygen in the surface and interior ocean is attributed to the sources and sinks of oxygen. Sources of oceanic dissolved oxygen include the production of oxygen during photosynthesis; air-sea gas exchange; wind-driven circulation causing upwelling of oxygenated water to the surface; and salinification influencing deep ventilation (Bates and Johnson, 2020; Evans et al., 2020; Pitcher et al., 2021; Shepherd et al., 2017). However the sinks, or the removal of oxygen, include oxygen consumption by biological respiration; abiotic oxidation of reduced chemicals and mineral species; surface warming that reduces the oxygen solubility; increases in

stratification influenced by surface warming that reduces mixing; reduction of diapycnal mixing due to shifts in isopycnal outcropping; and freshening that decreases ventilation (Evans et al., 2020; Laufkötter et al., 2017; Pitcher et al., 2021). Therefore, various combinations of sources and removal contribute to loss of oxygen in the ocean basin (Table 1-1, from Schmidtko et al. (2017)) .

Table 1- 1. Oxygen content and change per basin. Table from Schmidtko et al. (2017)

**Table 1 | Oxygen content and change per basin**

| Basin | Oxygen content (Pmol) | Oxygen change (Tmol per decade) | Change as percentage of global change | Volume as percentage of global ocean volume |
|---|---|---|---|---|
| Arctic Ocean | 4.7±0.2 | −73±30 | 7.6±3.1 | 1.2 |
| North Atlantic | 26.9±0.1 | −9±19 | 0.9±1.9 | 8.5 |
| Equatorial Atlantic | 15.9±0.0 | −72±20 | 7.5±2.1 | 5.7 |
| South Atlantic | 22.4±0.1 | −119±27 | 12.4±2.8 | 7.8 |
| North Pacific | 24.5±0.1 | −173±40 | 18.0±4.2 | 16.3 |
| Equatorial Pacific | 25.5±0.4 | −210±125 | 21.9±13.0 | 16.3 |
| South Pacific | 33.1±0.1 | −71±37 | 7.4±3.9 | 14.3 |
| Equatorial Indian Ocean | 10.7±0.1 | −55±49 | 5.7±5.1 | 6.6 |
| South Indian Ocean | 26.1±0.1 | −27±34 | 2.8±3.5 | 10.2 |
| Southern Ocean | 37.6±0.1 | −152±47 | 15.8±4.9 | 13.1 |
| **Total** | **227.4±1.1** | **−961±429** | **100** | **100** |

Trends that are more significant than two standard errors are marked in light grey. See Extended Data Table 1 for an extended version of this table.

The loss of oxygen is evident in many ocean basins (Fig. 1-2b). In the Arctic ocean, loss of oxygen is possibly attributed to reduced ventilation due to freshwater inputs and warming in the Canada Basin and the Beaufort Sea (Morison et al., 2012; Schmidtko et al., 2017). The Equatorial Pacific has the largest oxygen decline representing 21% of the global oxygen loss, due to low oxygen concentrations in the thermocline, that is influenced by climate modes (Pitcher et al., 2021;

Schmidtko et al., 2017). The decline of oxygen in the North Atlantic can be attributed to reduced ventilation due to changes in the meridional overturning circulation (Bates and Johnson, 2020; Schmidtko et al., 2017).

Globally, 50% of the oxygen decline happens in the upper 1000 m of the ocean (Schmidtko et al., 2017). This decline in oxygen can be attributed to microbial consumption through organic matter remineralization from phytoplankton decay, after primary production increases due to eutrophication and upwelling, and from ocean surface warming from the influence of climate change (Schmidtko et al., 2017). The remainder of the loss in oxygen, can be attributed to changes in the downward transport of oxygen-rich surface waters and upward transport of oxygen-poor waters, affecting the local distribution of oxygen, as well as changes in respiration and oxygen consumption (Evans et al., 2020; Pitcher et al., 2021; Schmidtko et al., 2017). Warming can also affect ocean transport properties in the thermocline, by enhancing stratification that reduces the mixed layer depth and diapycnal mixing. The reduction restricts transportation of oxygen through reduced ventilation and poleward outcropping of isopycnals (Evans et al., 2020). The decline of oxygen can also occur along the continental shelf, enclosed seas and coastal environments, harboring areas, or zones of low oxygen called oxygen minimum zones (OMZ) (Fig. 1-2).


**Figure 1- 2**. Distribution of oxygen minimum zones in the world oceans: open ocean (orange), continental shelves (yellow), enclosed seas (purple), and coastal environments (green). Figure from Pitcher et al. (2021).

OMZs are areas in the open ocean, or in coastal areas, where oxygen declines to hypoxic and anoxic conditions within the water column (Canfield and Kraft, 2022; Pitcher et al., 2021). Some of the larger OMZs are located on western boundaries of continents, where wind-driven circulation induces Ekman transport across the surface, resulting in nutrient transport from the deep ocean to the surface through coastal upwelling (Fig. 1-3). The upwelling of nutrients to the surface contributes to photosynthesis by phytoplankton, which assimilates inorganic carbon along with nitrate, phosphate, iron, and other nutrients. Aerobic respiration by microbial communities consumes dead organic matter from phytoplankton and other organisms within the oceanic food web, and recycles inorganic nutrients within the surface ocean, the ocean interior, and deeper depths as part of the biological pump. Simultaneously, microbial aerobic respiration consumes oxygen everywhere in the ocean, but rapidly within the subsurface below the photic zone where oxygen consumption outcompetes oxygen production from photosynthesis contributing to formation of hypoxic or anoxic waters (Long et al., 2021).

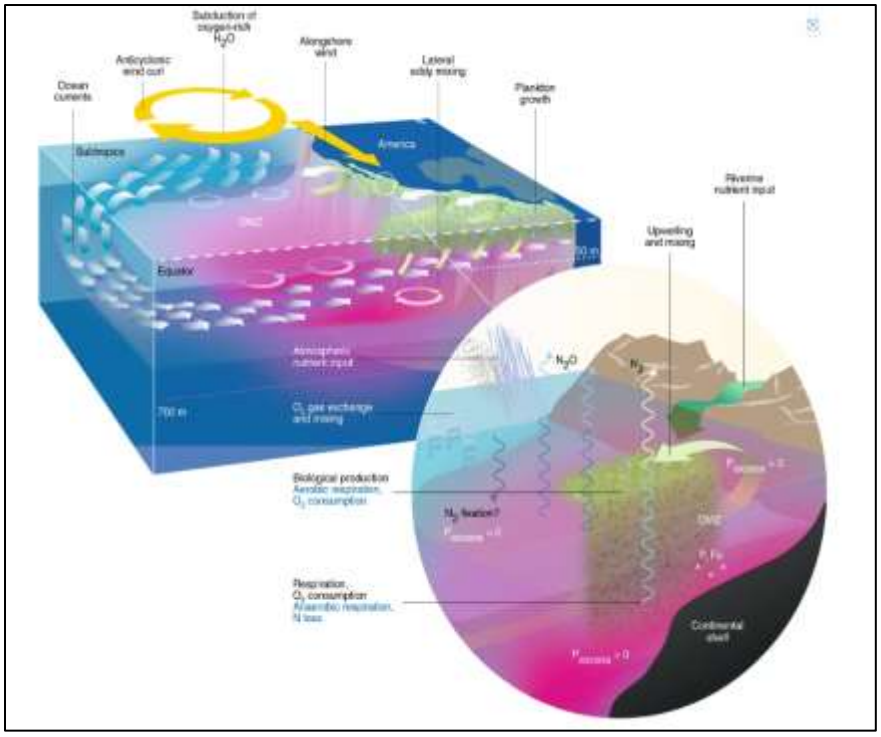


**Figure 1- 3**. Schematic illustration of the formation of oxygen minimum zones and thermocline ventilation. Figure from Oschlies et al. (2018).

OMZs are often characterized by weak ventilation and sluggish horizontal transport, especially in the Eastern Tropical Pacific, the world's largest OMZ (Pitcher et al., 2021; Tiano et al., 2014) in the Eastern Tropical North Atlantic, Peru and Northern Central Pacific, North Indian Ocean, and California Current System (Pitcher et al., 2021).

Coastal system can also experience hypoxia, when exposed to high nutrient loads and freshwater inflow from estuaries (Fennel and Testa, 2019) (Fig. 1-4). Coastal hypoxia is often seasonal, occurring during periods of strong stratification, typically resulting from freshwater inputs and warming in the summer, and are often terminated when vertical mixing from storms and wind stress erodes density stratification and resupplies oxygen (Fennel and Testa, 2019).

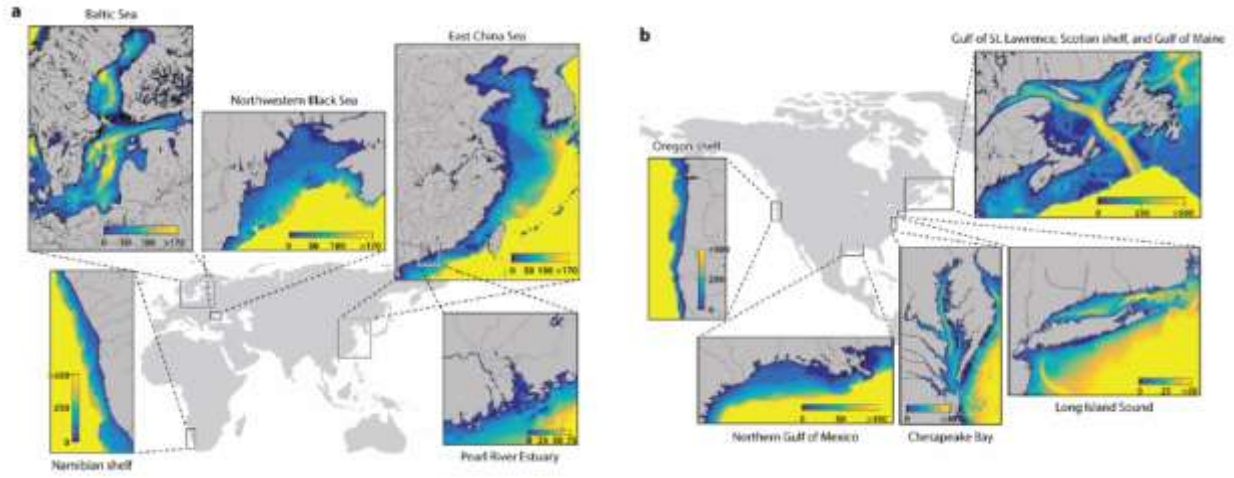


**Figure 1- 4.** Bathymetry of selected coastal systems. (A) the Baltic Sea, the northwestern Black Sea, the East China Sea, the Namibian shelf, and the Pearl River Estuary. (B): the Oregon shelf, the northern Gulf of Mexico, Chesapeake Bay, the Gulf of St. Lawrence along with the Scotian shelf and Gulf of Maine, and Long Island Sound. The color shows depth (in meters). Figure from Fennel and Testa (2019).

The Baltic Sea, Chesapeake Bay, Gulf of Mexico and South China Sea receive excess nutrients from river input that contributes to hypoxia formation (Fennel and Testa, 2019). The frequency and retention of hypoxia is dependent on surface circulation, bathymetry, biogeochemistry and nutrient loading from estuaries. For instance, the Baltic Sea is composed of several basins that maintain a permanent stratification causing long-term hypoxia and anoxia with sporadic decadal oxygenation events (Conley et al., 2011; Fennel and Testa, 2019; Reissmann et al., 2009). The temporal and physical effect in the Baltic Sea is different compared to the Chesapeake Bay, where hypoxia can be interrupted seasonally by storms and changes in nutrient loading and ocean circulation (Fennel and Testa, 2019). For river dominated marginal seas like the Gulf of Mexico and the East China Sea, large amount of nutrients comes from major rivers that are transported into the Gulf of Mexico and East Chaina Sea. However, in the East China Sea, the Kuroshio Current has a more dominating influence on nutrient transport than the Changjiang River that transports freshwater into sea. This freshening through river discharge effects vertical stratification, contributing to bottom boundary layer hypoxia both in the Gulf of Mexico and South

China Sea along with oxygen consumption in the water column and sediments (Fennel and Testa, 2019).

**Methods for the determination of dissolved oxygen concentration in the ocean**

Global deoxygenation is a current and future problem, and being able to quantify and measure oxygen concentration throughout the ocean is important for understanding more about the spatial distribution and temporal variability of oxygen and the effect deoxygenation has on various ocean ecosystems. Measuring oxygen in the ocean can be performed utilizing various instruments that includes iodometric titration (Winker titration), electrochemical sensors (e.g., Clark-type $O_2$ sensors), and optical sensors (optode sensors) (Grégoire et al., 2021 and references therein). Winkler titration requires discrete sampling of water samples from the ocean environment. The titration is based on the oxidation of Mn-(II) by oxygen in an alkaline solution. Oxygen can then be determined through titration of thiosulfate when iodide, or triodide is formed from the oxidation of Mn-(II) or spectrophotometrically after reacting with the color reagent (Grégoire et al., 2021; Labasque et al., 2004; Langdon, 2010). Winkler titration is the oldest method to measure oxygen in the ocean (Grégoire et al., 2021; Winkler, 1888). Another method involves electrochemical sensors, that are commonly used especially for marine sediments. Driven by partial pressure differences, dissolved oxygen diffuses through a membrane into an electrolyte, then oxygen reacts with a cathode and generates a measurable electrical current (Grégoire et al., 2021; Revsbech et al., 2009)). Lastly, optical sensors, or optodes, are a popular method to measure oxygen, as optodes do not consume oxygen during measurements. Instead, measurements are based on luminescence quenching, a process where the partial pressure of a gas can permeate the sensing foil in the cylinder that contains a luminescent substance that reacts, so that dissolved oxygen can be measured (Grégoire et al., 2021; Lehner et al., 2015). Each one of these methods

can be utilized for a specific oceanographic purpose to assist in oxygen concentration determinations in the ocean (Table. 1-2) (Grégoire et al., 2021)).

**Table 1-2.** Ocean observing platforms and methods for the determination of dissolved oxygen concentrations in the ocean. Global Data Assembly Centres (GDAC), Delayed Mode (DM), Near Real-Time (NRT), Quality Flag (QF), and Findable, Accessible, Interoperable and Reusable (FAIR)

| Observing platform | Methods | Spatial and temporal scales resolved | Spatial and temporal coverage | Community-agreed calibration and best practices | Community-agreed QF | Secondary community-agreed correction | GDAC | (N)RT/DM | FAIR |
|---|---|---|---|---|---|---|---|---|---|
| Profiling floats | Sensors | Horizontal: 10–$10^2$km Vertical: $10^{-3}$ km 5–10 days | $10^2$–$10^3$ km 3–5 years | With the atmosphere [1] | Yes [2,3] | Yes *In situ* Drift [4] | Yes [5] | NRT and DM | Yes |
| Gliders | Sensors | Horizontal:$10^{-1}$-1 km Vertical: $10^{-3}$ km Hourly-daily | 1-$10^2$ km Several days-weeks | In progress[6] | No | No | Yes [7] | NRT and DM | Yes |
| Ship-based Repeat Hydrography | Winkler + Sensors | Horizontal: 10 km Vertical: $10^{-3}$ km Decadal | $10^2$–$10^3$ km Multi-decadal | At sea or in delayed mode using Winkler | Yes [8] | Yes [9] | Yes[10] | DM | Yes |
| Moored fixed point observatories | Mainly optical sensors | Hourly | Multi-year | Yes [11] | Yes [12] | No | Yes [13] | NRT & DM | No |
| Ship-based Fixed-point Observatories | Winkler + Sensors | Monthly | Multi-year | No[14] | Yes[8] | Yes | Yes [10] | DM | Yes |
| Ship-based underway observations | Optical sensors | Sub-weekly to monthly | 10–$10^2$ km | No[15] | No | No | No | DM | No |
| Coastal/benthic | Winkler + Sensors | Vertical: $10^{-6}$ - $10^{-4}$ km Temporal:punctual | 10-$10^2$ km | Yes [16] | No | No | No [17] | DM | No |

**Iron in the ocean**

Iron is an essential micronutrient for phytoplankton growth in the ocean, that impacts carbon, phosphorus, and nitrogen dynamics in the euphotic zone (Tagliabue et al., 2017). Major external and internal sources of iron to the ocean and water column include, (1) rivers, (2) aeolian wind-driven deposition, (3) hydrothermal venting, and (4) sediment below oxygen-deficient waters (Barbeau, 2006; Rijkenberg et al., 2014; Tagliabue et al., 2017). Removal of iron in the water column includes biological uptake, oxidative precipitation, flocculation, which is the aggregation of colloidal particles from sediments, and scavenging by sinking particles (Jensen et al., 2020). However, in the sediment, Fe is only removed through sediment resuspension, or benthic Fe flux, discussed later; however, iron in the sediments can undergo redox transformations, changing the composition of iron through oxidative and reductive processes either biotically or abiotically (Aller et al., 2023; Canfield, 1989; Esther et al., 2015; Huang et al., 2021; Lovley et al., 1993; Schippers and Jørgensen, 2002; Weber et al., 2006). These sources and sinks of iron contribute to the cycling of iron in the ocean between the sediment and water column (Dale et al., 2015; Huang et al., 2021; Kappler et al., 2021; Tagliabue et al., 2017).

In the ocean, iron can be found as ferrous iron (Fe(II)) and ferric iron (Fe(III)). Fe(II) can be produced either from the reduction of iron(III)oxide minerals by iron-reducing bacteria in the sediments, reduction from Fe(III)-ligands such as siderophores that are secreted by microorganisms, or through photoreduction from the reaction between superoxides and Fe(III) (Huang et al., 2021). Aqueous Fe(II) that is produced can be oxidized abiotically, biotically, or become adsorbed on (oxyhydr)oxide surfaces. Fe(III) on the other hand can exist as colloid, soluble (<0.2 or 0.45 μm), particulate iron in the sediment or water column; or as iron oxide minerals in the sediment (Barbeau, 2006; Gledhill, 2012; Huang et al., 2021). Fe(II) oxidation,

i.e., Fe(III) production, is controlled by pH, the availability of oxygen and other electron acceptors, and the meditation by iron-oxidizing bacteria (Jensen et al., 2020).

*Fe (lll) reduction and ligands*

Fe(III) reduction can occur abiotically and biotically (Esther et al., 2015; Huang et al., 2021). In anoxic sediments, Fe(III) reduction can be facilitated by dissimilatory iron-reducing bacteria during the oxidation of organic compounds or hydrogen. The process of transferring electrons from the electron donor to Fe(III) occurs extracellularly either through direct contact, electron shuttling, ligands, or the use of pili (Fig. 1-5). The two bacteria that are commonly associated with iron reducers are *Geobacteria* and *Shewanella.* The close interaction between iron-reducing bacteria and the iron oxide surface is facilitated by a biofilm composed of an extra polymetric substance for electron transfer (Esther et al., 2015; Melton et al., 2014).

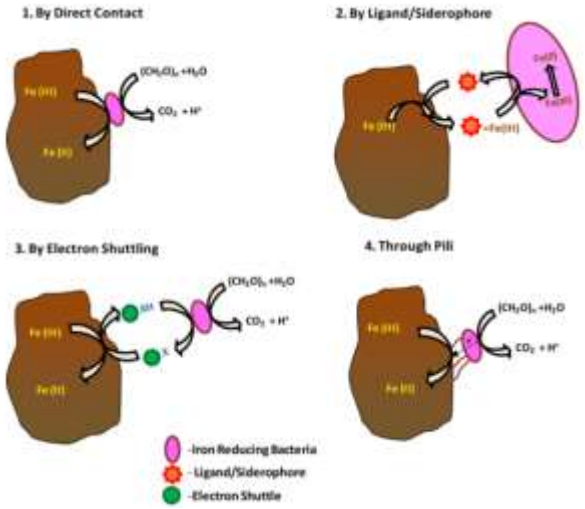


**Figure 1- 5**. Schematic illustrating solid phase Fe (III)-dissimilatory iron reducing bacteria electron transfer mechanisms. Figure from Esther et al. (2015)

However, Fe(III) can also undergo photoreduction either by direct ligand-to-metal transfer, or photochemically using reactive oxygen species that can reduce Fe(III), or oxidize Fe(II) ((Lueder et al., 2020). The photochemical reduction of Fe(III) in aquatic systems in circumneutral

pH can occur due to ligands that bind with Fe(III). Higher light intensities with lower wavelength leads to a faster Fe(III) photoreduction rate (Lueder et al., 2020). The photochemical reaction with oxygen produces superoxide ($O_2^{-\cdot}$) radicals that react with Fe(III)-ligands. The photochemical equations below depict the various processes of the photoreduction of Fe(III) and oxidation of Fe(II). The photochemical equations are as follows Equation 1-5 (Lueder et al., 2020):

$$\text{Fe (III)-L} + O_2^{-\cdot} \rightarrow \text{Fe(II)-L} + O_2 \quad [1]$$

$$\text{Fe(III)} + O_2^{-\cdot} \rightarrow \text{Fe(II)} + O_2 \quad [2]$$

$$\text{Fe(II)} + O_2 \rightarrow \text{Fe(III)} + O_2^{-\cdot} \quad [3]$$

$$\text{Dissolved organic matter} + \textit{light} + O_2 \rightarrow O_2^{-\cdot} \quad [4]$$

where the Fe(III)-ligand complex can be reduced by superoxide radicals producing Fe(II)-Ligand complexes, or (Eq. 2) by the reduction of Fe(III), which dissociated from a ligand prior to reduction by superoxide. Superoxide can be produced from oxygen reacting with Fe(II) (Eq. 3), or by photochemical reaction of dissolved organic matter and oxygen (Lueder et al., 2020). The production of biological available Fe(II)-L or Fe(II) through photoreduction is a source of iron for phytoplankton in the surface ocean (Fig. 1-6).

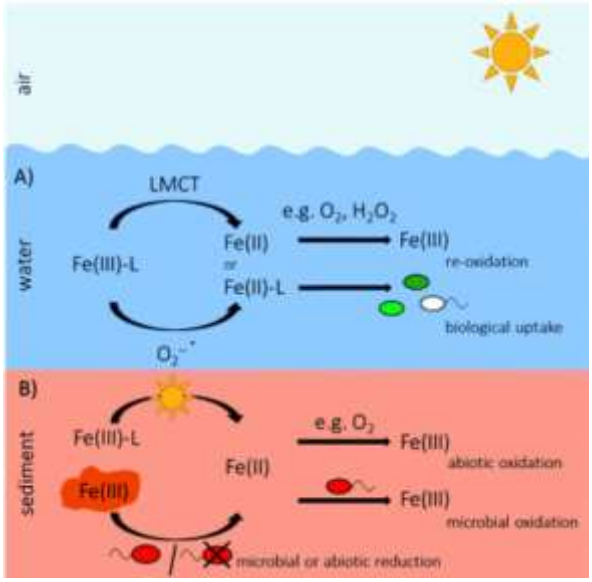


**Figure 1- 6**. (A) Illustration of photoreduction in the water column of Fe(III)–L through ligand-to-metal-charge transfer (LMCT) reaction or by superoxide ($O_2^{-\bullet}$). (B) Fe(II) production in sediments by either Fe(III) photoreduction, or by biotic or abiotic iron (III) reduction. Figure from (Lueder et al. (2020).

*Fe (II) oxidation*

At a pH < 4 and > 8, Fe(II) can exist as aqueous Fe(II), where the rate of oxidation is independent of pH, but oxidation rate of Fe(II) is dependent when pH is between 4 and 7 (Morgan and Lahav, 2007). Under acidic conditions, aqueous Fe(II) is thermodynamically stable with a negative redox potential, but during oxidation of Fe(II), any chemical toxins, or organic compounds can be reduced either biologically or abiotically making the substance less toxic or more degradable (Huang et al., 2021; Morgan and Lahav, 2007). The dependency of Fe(II) stability on pH and oxygen can be described using a general 1$^{st}$ order rate law (Morgan and Lahav, 2007; Stumm and Lee, 1961) as seen in Equation 4:

$$-\frac{d[Fe(II)]}{dt} = k[Fe(II)][O_2] \quad [4]$$

a. $k = -\frac{dlog[Fe(II)]}{dt}$

where k is the rate constant for Fe(II) oxidation; d[Fe(II)]/dt is the rate of oxidation depended on the present of Fe(II) anions; and [$O_2$] is the concentration of oxygen. The oxidations of Fe(II) results in the formation of iron(III)(oxyhyroxides) that dominate during oxic condition. (Fig. 1-7).

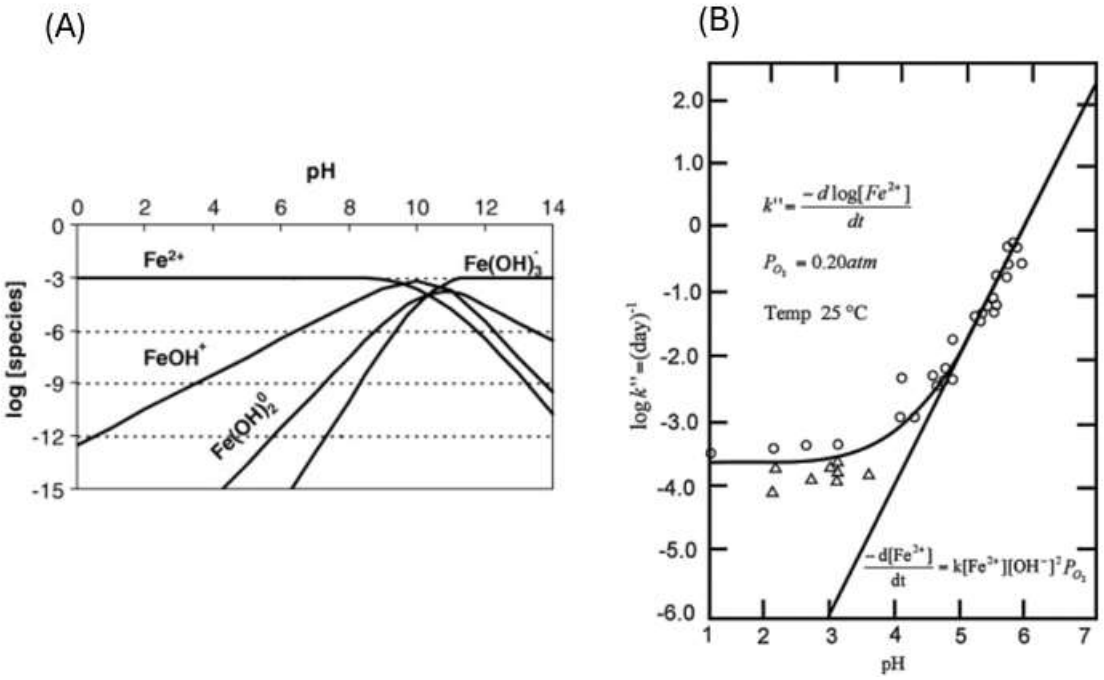


**Figure 1- 7.** (A) Log species–pH diagram of soluble ferrous hydroxide species at infinite dilution. (B) Oxidation rate of ferrous iron species as a function of pH ($P_{O2}$=0.20bar). At low pH the oxidation rate is independent of pH, while at higher pH values (>5). Both figures from Morgan and Lahav (2007).

Fe(II) can be oxidized by microorganisms in the presence of oxygen. Fe(II) oxidation can be mediated in acidic conditions (pH < 4) by aerobic acidophilic organisms, in hydrothermal vent environments, and by anoxygenic photosynthetic microorganism (Pronk and Johnson, 1992; Widdel et al., 1993). At circumneutral pH, Fe(II) can also be oxidized with nitrate and nitrite microbially (Huang et al., 2021; Melton et al., 2014). Additionally, the oxidation of iron (II) sulfides has been shown to be coupled to nitrate reduction by *Thiobacillus denitrificans* and other

microorganisms, but the oxidation of iron (II) sulfides can also occur abiotically (Kappler et al., 2021; Melton et al., 2014).

*Benthic Fe flux*

The flux of dissolved Fe(II) from shelves and continental margins are a source of Fe to the water column through abiotic and biotic processes mentioned previously. The diffusive flux of Fe(II) from the sediment can occur under hypoxic and (more pronounced) under anoxic conditions (Aller et al., 2023; Esther et al., 2015; Severmann et al., 2010). Once Fe(II) is in the water column, Fe(II) can either undergo oxidation when oxygen concentrations are high enough to cause the oxidation of Fe(II) to Fe(III), followed by the precipitation of Fe(III) minerals on particulate organic matter, or stay as dissolved Fe(II) (dFe) and become assimilated by phytoplankton (Barbeau, 2006; Hawco et al., 2021; Kappler et al., 2021; Tagliabue et al., 2017). The physical mechanisms of iron transport through the water column are unclear, but possibly varies by location. In upwelling regions, dFe transport can be assumed to occur through diapycnal mixing and upwelling to the surface. Other transport mechanisms includes bottom boundary layer turbulence, that can cause resuspensions, or tidal wave influence at the bottom boundary (Severmann et al., 2010).

Various in-situ and ex-situ methodologies exist to determine benthic Fe fluxes. These methodologies include (Aller et al., 2023): (1) using a two-point ex-situ porewater gradient profile of Fe(II) in the sediment with the application of Fick's First Law of Diffusion, (2) deploying in-situ benthic flux chambers to determine the change in dissolved Fe(II) in the enclosed water over time, (3) estimating a maximum Fe flux from measurements of dissolved Fe(ll) production rates in sediments at steady state, or (4) using $^{224}$Ra as a tracer either in the sediment or water column and correlate $^{224}$Ra to Fe(II).

*Benthic Flux chamber*

A benthic flux chamber quantifies the concentration of dissolved Fe (dFe) over time. The general construction of benthic flux chambers utilizes a polycarbonate material for the chamber walls with a stirrer for ventilation to prevent stagnation and the development of concentration gradients (Kononets et al., 2021, and references therein). For water injection and collection, syringes are used that connect to tubing along with various sensors. Chambers can be modified with multiple sensors to measure oxygen concentrations, turbidity and conductivity (Kononets et al., 2021). Syringes attached to the chamber are activated on a pre-programed timer that withdraws a volume of water (from bottom water. Once chambers are recovered, analysis of dissolved iron (Grasshoff and Ehrhardt, 1999) from the collected volume of the water from the syringes are measured and can be determined  spectrophotometrically.

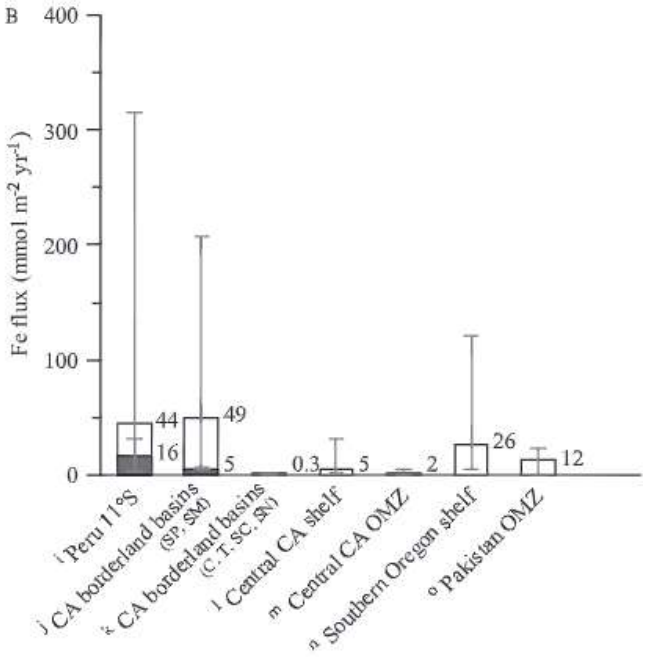


**Figure 1- 8.** Benthic Fe fluxes determined at various locations. Figure from Noffke et al. (2012)

Several studies have utilized benthic flux chambers to measure Fe flux from sediments on shelves and continental margins below OMZs. The estimated global benthic Fe flux amounts to $150 \pm 75$ Gmol $yr^{-1}$ in which $109 \pm 55$ Gmol $yr^{-1}$ is contributed by continental margin sediments (of which 72 Gmol $yr^{-1}$ from the shelf and 37 Gmol $yr^{-1}$ from slope sediments) and 41 Gmol $yr^{-1}$ from the deep sea (>2000 m) (Dale et al., 2015). Along the Oregon-California coast, benthic Fe flux ranged from 0-300 μmol $m^{-2}$ $d^{-1}$, and has been compared to sediment carbon oxidation demand, denitrification and biological productivity in the sediment (Dale et al., 2015; Fuchsman et al., 2015; Severmann et al., 2010). Along the oxygen minimum zone on the Peruvian margin, the highest benthic Fe flux was recorded between 200-600 m at 316 mmol $m^{-2}$ $yr^{-1}$ (Fig. 1-8). Recently, fluxes of Fe from the sediment have been used for the Regional Ocean Modeling System Biogeochemical Elemental Cycle model, to simulate benthic Fe flux along the California margin (Deutsch et al., 2021; Severmann et al., 2010) for iron cycling in the Biogeochemical Elemental Cycle Model (Fig. 1-9) using an equation relating parametrized sediment Fe release as a function of bottom water.

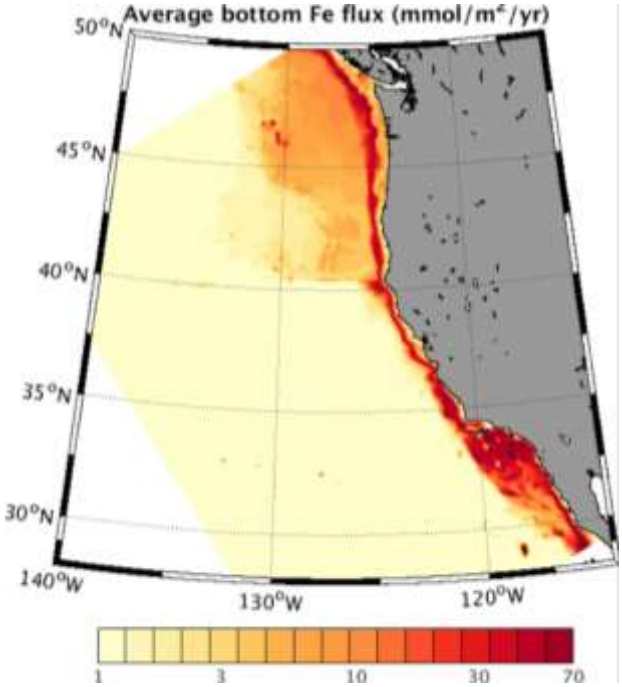


**Figure 1- 9.** Parameterized fluxes of iron between the water column and sediments along the California shelf. Figure from Deutsch et al. (2021).

**Deoxygenation along the US west coast**

*California Current System*

The California Current System (CCS), located off the coasts of Washington, Oregon, and California, is a typical eastern boundary upwelling system, where seasonal upwelling supports a highly diverse and productive marine ecosystem (Fig. 1-10) (Chavez and Messié, 2009; Carr and Kearns, 2003). The CCS can be split into three main parts: the main equatorward California Current offshore, a subsurface poleward undercurrent fringing the continental shelf, and a recirculation pattern known as the Southern California Eddy in the Southern California Bight (Kämpf and Chapman, 2016).

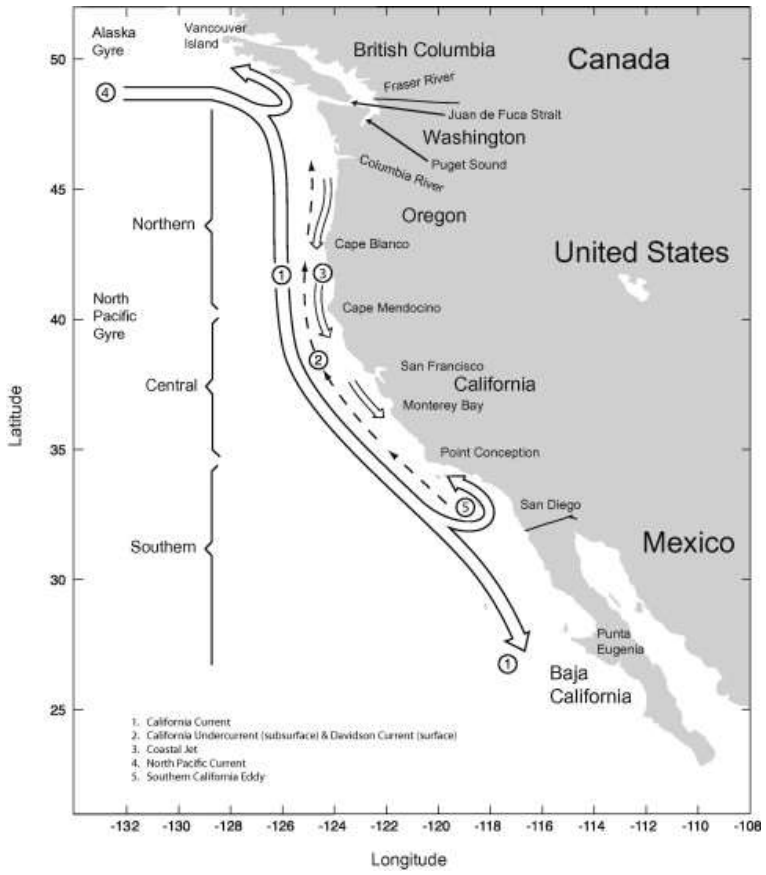


**Figure 1- 10.** Map of the California Current System. Figure from Checkley and Barth (2009).

Unlike the Eastern Tropical Pacific that has a core with the lowest oxygen concentration in the interior of the OMZ, oxygen in the CCS, more specifically the Southern California Bight, is depleted from the sea surface to seafloor, due to the California border land where oxygen can become hypoxic, or anoxic forming a permanent OMZ, or fluctuate interannually, stimulated by high productivity and remineralization (Pitcher et al., 2021) (Fig. 1-11).

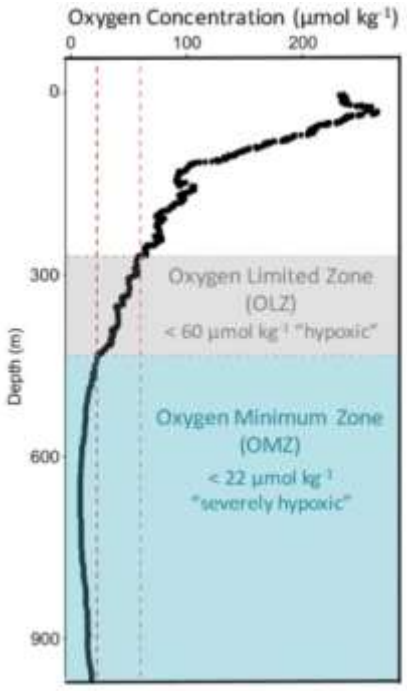


**Figure 1- 11.** A conceptual diagram for the Southern California Bight showing a decline of oxygen in the Bight. Figure from Pitcher et al. (2021).

The decline in oxygen in the CCS can be attributed to loss of oxygen in the California Under Current (CUC) and the California Current System that effects various regions including the Southern California Bight (-0.87 to -1.7 µmol $kg^{-1}$ $yr^{-1}$), Newport Oregon Line (-024-0.86 µmol $kg^{-1}$ $yr^{-1}$), and Central California (-1.92 µmol $kg^{-1}$ $yr^{-1}$)(Evans et al., 2020). The physical transport of low oxygen in the California Current System is attributed to the loss of oxygen in the tropical pacific that merges into the CUC, along with a decline of dissolve oxygen in the Northern Pacific possibly driven by variability in the Pacific Decadal Oscillation (Bograd et al., 2015). The causes of the decline in oxygen is due to increased organic matter remineralization in the North Equatorial Pacific Intermediate Water (NEPIW) (Evans et al., 2020). The NEPIW is responsible for 50% of the deoxygenation that occurs in the CCS from the deep Pacific Subarctic Upper Waters due to remineralization and increased subsurface stratification (Evans et al., 2020).

Oxygen decline has also been observed in the Southern California Bight due to low concentrations in dissolved oxygen that is advected from the CUC (Bograd et al., 2008). The decline in oxygen is attributed to the shoaling of hypoxic oxygen minimum layer. The largest decline in dissolved oxygen happens in the upper ocean between 200-300 m with a large decline of dissolved oxygen in the Santa Barbara Basin at 500 m (Bograd et al., 2008). The trend in the decline of dissolved oxygen is largest at the surface (0-100 m) with a loss of 2.13 $\mu$mol $O_2$ $kg^{-1}$ $yr^{-1}$ (.00558 $\mu$mol $O_2$ $kg^{-1}$ $d^{-1}$) while at 400-500 m oxygen decline is 0.1 − -0.7 $\mu$mol $O_2$ $kg^{-1}$ $yr^{-1}$ (0.0002-0.001 $\mu$mol $O_2$ $kg^{-1}$ $d^{-1}$) (Bograd et al., 2008).

The impact of deoxygenation along the CCS effects ocean biogeochemistry and phytoplankton productivity along the coast (Deutsch et al., 2021). Thermocline water with weak ventilation upwells and enters into the CCS transporting high nutrient concentrations like nitrate, low oxygen concentrations and high pH along the California coast. Nitrate limitation is observed along the Central California Current and Southern California Current near shore for diatom growth while dFe is usually not a limiting factor (Deutsch et al., 2021). However, in the Northern California System, Fe is more limiting than nitrogen, due to the Pacific Subarctic Waters that transport high nitrate concentration into the northern CCS (Deutsch et al., 2021). For small phytoplankton like picophytoplankton, nutrients are not a limiting factor, but instead irradiance (Deutsch et al., 2021) due to the low half-saturation of light for small phytoplankton. Upwelled nutrients produce a nitracline that deepens cross-shore of the CCS. This nitracline stimulates a deep chlorophyll maximum and follows the deep isopycnal from the shallow shore (Deutsch et al., 2021; Hawco et al., 2021).

Iron in the CCS influences the decline of nitrate and stimulates phytoplankton growth. The sources of Fe to the CCS include sediment-derived Fe, atmospheric Fe deposition, and freshwater

(river) Fe input, (Biller et al., 2013; Deutsch et al., 2021). Fe has an exponential relationship with oxygen where Fe(II) production is dependent on the oxygen conditions. Under anoxic and hypoxic condition Fe(II) is produced and sustained through biotic and abiotic processes, but Fe(II) is oxidized under fully oxic conditions. With the shoaling of hypoxic waters along shore, oxygen can stimulate the release of Fe(II) from the sediment into the CCS (Bograd et al., 2008; Severmann et al., 2010). The shoaling of hypoxic water along with decline of oxygen in the CCS overlaps with high benthic Fe flux along the coast (Fuchsman et al., 2015; Severmann et al., 2010). This benthic Fe is assumed to contribute to phytoplankton productivity along the coast that further stimulating phytoplankton productivity in the surface (King and Barbeau, 2007; Severmann et al., 2010).

In the CCS, the trace metal iron has been identified as a limiting factor for the growth of phytoplankton (Hogle et al., 2018). Fe is an essential micronutrient that also has a considerable influence on the dynamics of phosphorus and nitrogen in the euphotic zone (Tagliabue et al., 2017). Similar to other nutrients, Fe can be possibly transported to the surface by upwelling and circulation. However, Fe supply is generally low in oxygenated environments relative to other macronutrients, reflecting rapid scavenging of insoluble iron-oxide minerals by sinking particles that eventually accumulate in the sediment (Bruland et al., 2001, 2014; Firme et al., 2003; Till et al., 2019). While earlier studies suggested that Fe inputs to the CCS are dominated by rivers and aeolian deposition (Biller and Bruland, 2013; Johnson et al., 2003), more recent work highlights a combination of sources, including benthic Fe fluxes (Severmann et al., 2010; Noffke et al., 2012; Tagliabue et al., 2017; Wallmann et al., 2022) that is redistributed in coastal waters and open ocean by ocean currents (Bray et al., 1999; Boiteau et al., 2019; García-Reyes and Largier, 2010).

Under hypoxic or anoxic bottom conditions in the ocean, Fe(II) produced in the sediment during microbial organic matter degradation coupled to Fe(III) reduction, diffuses across the

sediment–water interface and accumulates in the water column (Furrer and Wehrli, 1993; Dale et al., 2015; Severmann et al., 2010; Wallmann et al., 2022). In the CCS, this benthic Fe flux is likely to exceed atmospheric deposition (Deutsch et al., 2021) and may ultimately make its way to the surface by upwelling and vertical mixing, supporting high rates of photosynthesis.

The impact of nutrients in the CCS stimulates the occurrence of *Pseudo-nitzschia*, a type of harmful algae found along the west coast that produces domoic acid, a neurotoxin that can negatively impact wildlife and fisheries and put human life at risk through amnesic shellfish poisoning (Moreno et al., 2022). Under nitrogen limitation, domoic acid production is shut off. Domic acid production commonly occurs in oligotrophic waters. But when nitrogen is sufficient, domoic acid is stimulated especially during the photoperiod, or the longer period of time in a day that an organism is exposed to light (Moreno et al., 2022). The effect of deoxygenation has a wide range of impacts in the California Current System. Deoxygenation in the CCS has been observed to impact ocean biogeochemistry, sediment geochemistry, and phytoplankton productivity. The decline of oxygen can be attributed to nutrient transport, ocean circulation and changes in oxygen outside the CCCS within the Pacific Ocean.  The connection of the California Current can have impacts on sub basin in the CCS like the Santa Barbabra Basin

*Santa Barbara Basin*

The effects of upwelling and deoxygenation in the CCS also impacts sub-basins in the CCS including the Santa Barbara Basin (SBB) (Bograd et al., 2002; Bray et al., 1999; Qin et al., 2022). The SBB, is one of 14 sub-basins within the Southern California Borderland, and is located between the Channel Islands and the California coast. The SBB frequently experiences seasonal anoxia in bottom water in summer and fall, with irregular oxygen flushing of dense, hypoxic water below the western sill depth (475 m) during winter and spring (Goericke et al., 2015; Sholkovitz and Soutar, 1975; White et al., 2019). This seasonal flushing reflects either changes in upwelling strength and frequency, or changes in stratification at the sill depth, although the exact cause of the flushing is still unclear (Goericke et al., 2015; Sholkovitz and Gieskes, 1971; White et al., 2019).

Lack of oxygen in the deeper parts of the basin supports anaerobic microbial processes in the bottom water and sediment (White et al., 2019), including sediment iron reduction (Goericke et al., 2015), causing the release of Fe(II) into the water column (Severmann et al., 2010). Ventilation events that re-oxygenate the deep basin, as well as mixing by the vigorous submesoscale circulation (Kessouri et al., 2020), could allow upwelling of this Fe above the sill depth and ultimately to the surface, providing a linkage between benthic processes and upper water-column biogeochemistry. Increased surface primary production supported by this Fe source would in turn drive higher remineralization and oxygen loss in deep waters, thus providing positive feedback to benthic Fe release. However, with a dearth of benthic Fe flux measurements in the SBB, gaps remain in our understanding of the dynamics and impact of benthic Fe flux in the Southern California Borderland, particularly with respect to its magnitude, dependence on bottom water oxygen, and ability to reach the euphotic zone and influence primary production.

The seasonal variability of hypoxia and anoxia between 1986-2020 in the bottom water illustrates the decline in flushing frequency along with oxygen depletion, which in turn minimizes nitrate concentration, resulting in complete nitrate deficiency (0 μM) in 2005, 2010, 2012, and 2013 (Goericke et al., 2015; Qin et al., 2022; Valentine et al., 2016). Since 2000, the frequency of low oxygen (< 0.5 μM) events outside the springtime upwelling season have increased significantly ($p<0.05$) below 520 m. During springtime upwelling, oxygen concentrations increases to 20 μM before returning to 1 μM because of an increase in remineralization (Goericke et al., 2015). It is unclear quantitatively how much of the CCS effects oxygen decline, benthic flux of nutrients and increase remineralization in the SBB, but CCS can assume to have broad impacts in the basin.

## References


Aller, R. C., Dwyer, I. P., Perger, D. A. S., Heilbrun, C., Volkenborn, N., and Wehrmann, L. M.: Estimating benthic Fe and reactive solute fluxes, Mar. Chem., 249, 104221, https://doi.org/10.1016/j.marchem.2023.104221, 2023.

Andrews, O. D., Bindoff, N. L., Halloran, P. R., Ilyina, T., and Le Quéré, C.: Detecting an external influence on recent changes in oceanic oxygen using an optimal fingerprinting method, Biogeosciences, 10, 1799–1813, https://doi.org/10.5194/bg-10-1799-2013, 2013.

Barbeau, K.: Photochemistry of Organic Iron(III) Complexing Ligands in Oceanic Systems, Photochem. Photobiol., 82, 1505–1516, https://doi.org/10.1111/j.1751-1097.2006.tb09806.x, 2006.

Bates, N. R. and Johnson, R. J.: Acceleration of ocean warming, salinification, deoxygenation and acidification in the surface subtropical North Atlantic Ocean, Commun. Earth Environ., 1, 1–12, https://doi.org/10.1038/s43247-020-00030-5, 2020.

Biller, D. V., Coale, T. H., Till, R. C., Smith, G. J., and Bruland, K. W.: Coastal iron and nitrate distributions during the spring and summer upwelling season in the central California Current upwelling regime, Cont. Shelf Res., 66, 58–72, https://doi.org/10.1016/j.csr.2013.07.003, 2013.

Bograd, S. J., Schwing, F. B., Castro, C. G., and Timothy, D. A.: Bottom water renewal in the Santa Barbara Basin, J. Geophys. Res. Oceans, 107, 9-1-9–9, https://doi.org/10.1029/2001JC001291, 2002.

Bograd, S. J., Castro, C. G., Di Lorenzo, E., Palacios, D. M., Bailey, H., Gilly, W., and Chavez, F. P.: Oxygen declines and the shoaling of the hypoxic boundary in the California Current, Geophys. Res. Lett., 35, https://doi.org/10.1029/2008GL034185, 2008.

Bograd, S. J., Buil, M. P., Lorenzo, E. D., Castro, C. G., Schroeder, I. D., Goericke, R., Anderson, C. R., Benitez-Nelson, C., and Whitney, F. A.: Changes in source waters to the Southern California Bight, Deep Sea Res. Part II Top. Stud. Oceanogr., 112, 42–52, https://doi.org/10.1016/j.dsr2.2014.04.009, 2015.

Bray, N. A., Keyes, A., and Morawitz, W. M. L.: The California Current system in the Southern California Bight and the Santa Barbara Channel, J. Geophys. Res. Oceans, 104, 7695–7714, https://doi.org/10.1029/1998JC900038, 1999.

Breitburg, D., Levin, L. A., Oschlies, A., Grégoire, M., Chavez, F. P., Conley, D. J., Garçon, V., Gilbert, D., Gutiérrez, D., Isensee, K., Jacinto, G. S., Limburg, K. E., Montes, I., Naqvi, S. W. A., Pitcher, G. C., Rabalais, N. N., Roman, M. R., Rose, K. A., Seibel, B. A., Telszewski, M., Yasuhara, M., and Zhang, J.: Declining oxygen in the global ocean and coastal waters, Science, 359, eaam7240, https://doi.org/10.1126/science.aam7240, 2018.

Canfield, D. E.: Reactive iron in marine sediments, Geochim. Cosmochim. Acta, 53, 619–632, https://doi.org/10.1016/0016-7037(89)90005-7, 1989.

Canfield, D. E. and Kraft, B.: The ‘oxygen’ in oxygen minimum zones, Environ. Microbiol., 24, 5332–5344, https://doi.org/10.1111/1462-2920.16192, 2022.

Conley, D. J., Carstensen, J., Aigars, J., Axe, P., Bonsdorff, E., Eremina, T., Haahti, B.-M., Humborg, C., Jonsson, P., Kotta, J., Lännegren, C., Larsson, U., Maximov, A., Medina, M. R., Lysiak-Pastuszak, E., Remeikaité-Nikiené, N., Walve, J., Wilhelms, S., and Zillén, L.: Hypoxia is increasing in the coastal zone of the Baltic Sea, Environ. Sci. Technol., 45, 6777–6783, https://doi.org/10.1021/es201212r, 2011.

Craig, R. K.: The New United Nations High Seas Treaty: A Primer, Nat. Resour. Environ., 34, 48–50, 2020.

Dale, A. W., Nickelsen, L., Scholz, F., Hensen, C., Oschlies, A., and Wallmann, K.: A revised global estimate of dissolved iron fluxes from marine sediments: GLOBAL BENTHIC IRON FLUXES, Glob. Biogeochem. Cycles, 29, 691–707, https://doi.org/10.1002/2014GB005017, 2015.

Deutsch, C., Frenzel, H., McWilliams, J. C., Renault, L., Kessouri, F., Howard, E., Liang, J.-H., Bianchi, D., and Yang, S.: Biogeochemical variability in the California Current System, Prog. Oceanogr., 196, 102565, https://doi.org/10.1016/j.pocean.2021.102565, 2021.

Ekau, W., Auel, H., Pörtner, H.-O., and Gilbert, D.: Impacts of hypoxia on the structure and processes in pelagic communities (zooplankton, macro-invertebrates and fish), Biogeosciences, 7, 1669–1699, https://doi.org/10.5194/bg-7-1669-2010, 2010.

Esther, J., Sukla, L. B., Pradhan, N., and Panda, S.: Fe (III) reduction strategies of dissimilatory iron reducing bacteria, Korean J. Chem. Eng., 32, 1–14, https://doi.org/10.1007/s11814-014-0286-x, 2015.

Evans, N., Schroeder, I. D., Pozo Buil, M., Jacox, M. G., and Bograd, S. J.: Drivers of Subsurface Deoxygenation in the Southern California Current System, Geophys. Res. Lett., 47, https://doi.org/10.1029/2020GL089274, 2020.

Fennel, K. and Testa, J. M.: Biogeochemical Controls on Coastal Hypoxia, Annu. Rev. Mar. Sci., 11, 105–130, https://doi.org/10.1146/annurev-marine-010318-095138, 2019.

Fuchsman, C. A., Devol, A. H., Chase, Z., Reimers, C. E., and Hales, B.: Benthic fluxes on the Oregon shelf, Estuar. Coast. Shelf Sci., 163, 156–166, https://doi.org/10.1016/j.ecss.2015.06.001, 2015.

Gledhill, M.: The organic complexation of iron in the marine environment: a review, Front. Microbiol., 3, https://doi.org/10.3389/fmicb.2012.00069, 2012.

Goericke, R., Bograd, S. J., and Grundle, D. S.: Denitrification and flushing of the Santa Barbara Basin bottom waters, Deep Sea Res. Part II Top. Stud. Oceanogr., 112, 53–60, https://doi.org/10.1016/j.dsr2.2014.07.012, 2015.

Grasshoff, K. and Ehrhardt, M.: Methods of seawater analysis, 3rd, completely rev. and extended ed. ed., Wiley-VCH, Weinheim, New York, xxxii, 600 pp., 1999.

Grégoire, M., Garçon, V., Garcia, H., Breitburg, D., Isensee, K., Oschlies, A., Telszewski, M., Barth, A., Bittig, H. C., Carstensen, J., Carval, T., Chai, F., Chavez, F., Conley, D., Coppola, L., Crowe, S., Currie, K., Dai, M., Deflandre, B., Dewitte, B., Diaz, R., Garcia-Robledo, E., Gilbert, D., Giorgetti, A., Glud, R., Gutierrez, D., Hosoda, S., Ishii, M., Jacinto, G., Langdon, C., Lauvset, S. K., Levin, L. A., Limburg, K. E., Mehrtens, H., Montes, I., Naqvi, W., Paulmier, A., Pfeil, B., Pitcher, G., Pouliquen, S., Rabalais, N., Rabouille, C., Recape, V., Roman, M., Rose, K., Rudnick, D., Rummer, J., Schmechtig, C., Schmidtko, S., Seibel, B., Slomp, C., Sumalia, U. R., Tanhua, T., Thierry, V., Uchida, H., Wanninkhof, R., and Yasuhara, M.: A Global Ocean Oxygen Database and Atlas for Assessing and Predicting Deoxygenation and Ocean Health in the Open and Coastal Ocean, Front. Mar. Sci., 8, 2021.

Hawco, N. J., Barone, B., Church, M. J., Babcock-Adams, L., Repeta, D. J., Wear, E. K., Foreman, R. K., Björkman, K. M., Bent, S., Van Mooy, B. A. S., Sheyn, U., DeLong, E. F., Acker, M., Kelly, R. L., Nelson, A., Ranieri, J., Clemente, T. M., Karl, D. M., and John, S. G.: Iron Depletion in the Deep Chlorophyll Maximum: Mesoscale Eddies as Natural Iron Fertilization Experiments, Glob. Biogeochem. Cycles, 35, https://doi.org/10.1029/2021GB007112, 2021.

Huang, J., Jones, A., Waite, T. D., Chen, Y., Huang, X., Rosso, K. M., Kappler, A., Mansor, M., Tratnyek, P. G., and Zhang, H.: Fe(II) Redox Chemistry in the Environment, Chem. Rev., 121, 8161–8233, https://doi.org/10.1021/acs.chemrev.0c01286, 2021.

Jensen, L. T., Morton, P., Twining, B. S., Heller, M. I., Hatta, M., Measures, C. I., John, S., Zhang, R., Pinedo-Gonzalez, P., Sherrell, R. M., and Fitzsimmons, J. N.: A comparison of marine Fe and Mn cycling: U.S. GEOTRACES GN01 Western Arctic case study, Geochim. Cosmochim. Acta, 288, 138–160, https://doi.org/10.1016/j.gca.2020.08.006, 2020.

Kämpf, J. and Chapman, P.: The California Current Upwelling System, in: Upwelling Systems of the World: A Scientific Journey to the Most Productive Marine Ecosystems, edited by: Kämpf, J. and Chapman, P., Springer International Publishing, Cham, 97–160, https://doi.org/10.1007/978-3-319-42524-5_4, 2016.

Kappler, A., Bryce, C., Mansor, M., Lueder, U., Byrne, J. M., and Swanner, E. D.: An evolving view on biogeochemical cycling of iron, Nat. Rev. Microbiol., 19, 360–374, https://doi.org/10.1038/s41579-020-00502-7, 2021.

King, A. and Barbeau, K.: Evidence for phytoplankton iron limitation in the southern California Current System, Mar. Ecol. Prog. Ser., 342, 91–103, https://doi.org/10.3354/meps342091, 2007.

Kononets, M., Tengberg, A., Nilsson, M., Ekeroth, N., Hylén, A., Robertson, E. K., van de Velde, S., Bonaglia, S., Rütting, T., Blomqvist, S., and Hall, P. O. J.: In situ incubations with the Gothenburg benthic chamber landers: Applications and quality control, J. Mar. Syst., 214, 103475, https://doi.org/10.1016/j.jmarsys.2020.103475, 2021.

Kwiatkowski, L., Torres, O., Bopp, L., Aumont, O., Chamberlain, M., Christian, J. R., Dunne, J. P., Gehlen, M., Ilyina, T., John, J. G., Lenton, A., Li, H., Lovenduski, N. S., Orr, J. C., Palmieri, J., Santana-Falcón, Y., Schwinger, J., Séférian, R., Stock, C. A., Tagliabue, A., Takano, Y., Tjiputra, J., Toyama, K., Tsujino, H., Watanabe, M., Yamamoto, A., Yool, A., and Ziehn, T.: Twenty-first century ocean warming, acidification, deoxygenation, and upper-ocean nutrient and primary production decline from CMIP6 model projections, Biogeosciences, 17, 3439–3470, https://doi.org/10.5194/bg-17-3439-2020, 2020.

Labasque, T., Chaumery, C., Aminot, A., and Kergoat, G.: Spectrophotometric Winkler determination of dissolved oxygen: re-examination of critical factors and reliability, Mar. Chem., 88, 53–60, https://doi.org/10.1016/j.marchem.2004.03.004, 2004.

Langdon, C.: Determination of Dissolved Oxygen in Seawater by Winkler Titration Using The Amperometric Technique., https://doi.org/10.25607/OBP-1350, 2010.

Laufkötter, C., John, J. G., Stock, C. A., and Dunne, J. P.: Temperature and oxygen dependence of the remineralization of organic matter, Glob. Biogeochem. Cycles, 31, 1038–1050, https://doi.org/10.1002/2017GB005643, 2017.

Lehner, P., Larndorfer, C., Garcia-Robledo, E., Larsen, M., Borisov, S. M., Revsbech, N.-P., Glud, R. N., Canfield, D. E., and Klimant, I.: LUMOS - A Sensitive and Reliable Optode System for Measuring Dissolved Oxygen in the Nanomolar Range, PLOS ONE, 10, e0128125, https://doi.org/10.1371/journal.pone.0128125, 2015.

Long, A. M., Jurgensen, S. K., Petchel, A. R., Savoie, E. R., and Brum, J. R.: Microbial Ecology of Oxygen Minimum Zones Amidst Ocean Deoxygenation, Front. Microbiol., 12, 748961, https://doi.org/10.3389/fmicb.2021.748961, 2021.

Lovley, D. R., Giovannoni, S. J., White, D. C., Champine, J. E., Phillips, E. J. P., Gorby, Y. A., and Goodwin, S.: Geobacter metallireducens gen. nov. sp. nov., a microorganism capable of coupling the complete oxidation of organic compounds to the reduction of iron and other metals, Arch. Microbiol., 159, 336–344, https://doi.org/10.1007/BF00290916, 1993.

Lueder, U., Barker Jørgensen, B., Kappler, A., and Schmidt, C.: Photochemistry of iron in aquatic environments, Environ. Sci. Process. Impacts, 22, 12–24, https://doi.org/10.1039/C9EM00415G, 2020.

Melton, E. D., Swanner, E. D., Behrens, S., Schmidt, C., and Kappler, A.: The interplay of microbially mediated and abiotic reactions in the biogeochemical Fe cycle, Nat. Rev. Microbiol., 12, 797–808, https://doi.org/10.1038/nrmicro3347, 2014.

Morée, A. L., Clarke, T. M., Cheung, W. W. L., and Frölicher, T. L.: Impact of deoxygenation and warming on global marine species in the 21st century, Biogeosciences, 20, 2425–2454, https://doi.org/10.5194/bg-20-2425-2023, 2023.

Moreno, A. R., Anderson, C., Kudela, R. M., Sutula, M., Edwards, C., and Bianchi, D.: Development, calibration, and evaluation of a model of *Pseudo-nitzschia* and domoic acid

production for regional ocean modeling studies, Harmful Algae, 118, 102296, https://doi.org/10.1016/j.hal.2022.102296, 2022.

Morgan, B. and Lahav, O.: The effect of pH on the kinetics of spontaneous Fe(II) oxidation by O2 in aqueous solution – basic principles and a simple heuristic description, Chemosphere, 68, 2080–2084, https://doi.org/10.1016/j.chemosphere.2007.02.015, 2007.

Morison, J., Kwok, R., Peralta-Ferriz, C., Alkire, M., Rigor, I., Andersen, R., and Steele, M.: Changing Arctic Ocean freshwater pathways, Nature, 481, 66–70, https://doi.org/10.1038/nature10705, 2012.

Noffke, A., Hensen, C., Sommer, S., Scholz, F., Bohlen, L., Mosch, T., Graco, M., and Wallmann, K.: Benthic iron and phosphorus fluxes across the Peruvian oxygen minimum zone, Limnol. Oceanogr., 57, 851–867, https://doi.org/10.4319/lo.2012.57.3.0851, 2012.

Pitcher, G. C., Aguirre-Velarde, A., Breitburg, D., Cardich, J., Carstensen, J., Conley, D. J., Dewitte, B., Engel, A., Espinoza-Morriberón, D., Flores, G., Garçon, V., Graco, M., Grégoire, M., Gutiérrez, D., Hernandez-Ayon, J. M., Huang, H.-H. M., Isensee, K., Jacinto, M. E., Levin, L., Lorenzo, A., Machu, E., Merma, L., Montes, I., Swa, N., Paulmier, A., Roman, M., Rose, K., Hood, R., Rabalais, N. N., Salvanes, A. G. V., Salvatteci, R., Sánchez, S., Sifeddine, A., Tall, A. W., Plas, A. K. van der, Yasuhara, M., Zhang, J., and Zhu, Z.: System controls of coastal and open ocean oxygen depletion, Prog. Oceanogr., 197, 102613, https://doi.org/10.1016/j.pocean.2021.102613, 2021.

Pronk, J. T. and Johnson, D. B.: Oxidation and Reduction of Iron by Acidophilic Bacteria, Geomicrobiol. J., 10, 153–171, https://doi.org/10.1080/01490459209377918, 1992.

Qin, Q., Kinnaman, F. S., Gosselin, K. M., Liu, N., Treude, T., and Valentine, D. L.: Seasonality of water column methane oxidation and deoxygenation in a dynamic marine environment, Geochim. Cosmochim. Acta, 336, 219–230, https://doi.org/10.1016/j.gca.2022.09.017, 2022.

Reissmann, J. H., Burchard, H., Feistel, R., Hagen, E., Lass, H. U., Mohrholz, V., Nausch, G., Umlauf, L., and Wieczorek, G.: Vertical mixing in the Baltic Sea and consequences for eutrophication – A review, Prog. Oceanogr., 82, 47–80, https://doi.org/10.1016/j.pocean.2007.10.004, 2009.

Revsbech, N. P., Larsen, L. H., Gundersen, J., Dalsgaard, T., Ulloa, O., and Thamdrup, B.: Determination of ultra-low oxygen concentrations in oxygen minimum zones by the STOX sensor, Limnol. Oceanogr. Methods, 7, 371–381, https://doi.org/10.4319/lom.2009.7.371, 2009.

Rijkenberg, M. J. A., Middag, R., Laan, P., Gerringa, L. J. A., Aken, H. M. van, Schoemann, V., Jong, J. T. M. de, and Baar, H. J. W. de: The Distribution of Dissolved Iron in the West Atlantic Ocean, PLOS ONE, 9, e101323, https://doi.org/10.1371/journal.pone.0101323, 2014.

Schippers, A. and Jørgensen, B. B.: Biogeochemistry of pyrite and iron sulfide oxidation in marine sediments, Geochim. Cosmochim. Acta, 66, 85–92, https://doi.org/10.1016/S0016-7037(01)00745-1, 2002.

Schmidtko, S., Stramma, L., and Visbeck, M.: Decline in global oceanic oxygen content during the past five decades, Nature, 542, 335–339, https://doi.org/10.1038/nature21399, 2017.

Severmann, S., McManus, J., Berelson, W. M., and Hammond, D. E.: The continental shelf benthic iron flux and its isotope composition, Geochim. Cosmochim. Acta, 74, 3984–4004, https://doi.org/10.1016/j.gca.2010.04.022, 2010.

Shepherd, J. G., Brewer, P. G., Oschlies, A., and Watson, A. J.: Ocean ventilation and deoxygenation in a warming world: introduction and overview, Philos. Trans. R. Soc. Math. Phys. Eng. Sci., 375, 20170240, https://doi.org/10.1098/rsta.2017.0240, 2017.

Stumm, W. and Lee, G. F.: Oxygenation of Ferrous Iron, Ind. Eng. Chem., 53, 143–146, https://doi.org/10.1021/ie50614a030, 1961.

Tagliabue, A., Bowie, A. R., Boyd, P. W., Buck, K. N., Johnson, K. S., and Saito, M. A.: The integral role of iron in ocean biogeochemistry, Nature, 543, 51–59, https://doi.org/10.1038/nature21058, 2017.

Tiano, L., Garcia-Robledo, E., Dalsgaard, T., Devol, A. H., Ward, B. B., Ulloa, O., Canfield, D. E., and Peter Revsbech, N.: Oxygen distribution and aerobic respiration in the north and south eastern tropical Pacific oxygen minimum zones, Deep Sea Res. Part Oceanogr. Res. Pap., 94, 173–183, https://doi.org/10.1016/j.dsr.2014.10.001, 2014.

Valentine, D. L., Fisher, G. B., Pizarro, O., Kaiser, C. L., Yoerger, D., Breier, J. A., and Tarn, J.: Autonomous Marine Robotic Technology Reveals an Expansive Benthic Bacterial Community Relevant to Regional Nitrogen Biogeochemistry, Environ. Sci. Technol., 50, 11057–11065, https://doi.org/10.1021/acs.est.6b03584, 2016.

Weber, K. A., Achenbach, L. A., and Coates, J. D.: Microorganisms pumping iron: anaerobic microbial iron oxidation and reduction, Nat. Rev. Microbiol., 4, 752–764, https://doi.org/10.1038/nrmicro1490, 2006.

Widdel, F., Schnell, S., Heising, S., Ehrenreich, A., Assmus, B., and Schink, B.: Ferrous iron oxidation by anoxygenic phototrophic bacteria, Nature, 362, 834–836, https://doi.org/10.1038/362834a0, 1993.

Winkler, L. W.: Die Bestimmung des im Wasser gelösten Sauerstoffes, Berichte Dtsch. Chem. Ges., 21, 2843–2854, https://doi.org/10.1002/cber.188802102122, 1888.

**Chapter 2: Iron "ore" nothing: benthic iron fluxes from the oxygen-deficient.**

**Santa Barbara Basin enhance phytoplankton productivity in surface waters.**

**De'Marcus Robinson**[1], Anh L.D. Pham[1], David J. Yousavich[2], Felix Janssen[3], Frank Wenzhöfer[3], Eleanor C. Arrington[4], Kelsey M. Gosselin[5], Marco Sandoval-Belmar[1], Matthew Mar[1], David L. Valentine[4], Daniele Bianchi[1], Tina Treude[1,2]

[1]Department of Atmospheric and Oceanic Sciences, University of California Los Angeles, Los Angeles, CA, USA

[2]Department of Earth, Planetary, and Space Sciences, University of California Los Angeles, Los Angeles, CA, USA

[3]HGF-MPG Joint Research Group for Deep-Sea Ecology and Technology, Alfred Wegener Institute, Helmholtz Centre for Polar and Marine Research, Bremerhaven, Germany

[4]Department of Earth Science and Marine Science Institute, University of California, Santa Barbara, CA 93106, USA

**Abstract**

The trace metal iron (Fe) is an essential micronutrient that controls phytoplankton productivity, which subsequently affects organic matter cycling with feedback on the cycling of macronutrients. Along the continental margin of the U.S. West Coast, high benthic Fe release has been documented, in particular from deep anoxic basins in the Southern California Borderland. However, the influence of this Fe release on surface primary production remains poorly understood. In the present study from the Santa Barbara Basin, in-situ benthic Fe fluxes were determined along a transect from shallow to deep sites in the basin. Fluxes ranged between 0.23 and 4.9 mmol $m^{-2}$ $d^{-1}$, representing some of the highest benthic Fe fluxes reported to date. To investigate the influence of benthic Fe release from the oxygen-deficient deep basin on surface phytoplankton production, we combined benthic flux measurements with numerical simulations using the Regional Ocean Model System coupled to the Biogeochemical Elemental Cycling model (ROMS-BEC). For this purpose, we updated the model Fe flux parameterization to include the new benthic flux measurements from the Santa Barbara Basin. Our simulations suggest that benthic Fe fluxes enhance surface primary production, supporting positive feedback on benthic Fe release by decreasing oxygen in bottom waters. However, a reduction of phytoplankton Fe limitation by enhanced benthic fluxes near the coast may be partially compensated by increased nitrogen limitation further offshore, limiting the efficacy of this positive feedback.

## Introduction

The California Current System (CCS), located off the coasts of Washington, Oregon, and California, is a typical Eastern Boundary Upwelling System, where seasonal upwelling supports a highly diverse and productive marine ecosystem (Chavez and Messié, 2009; Carr and Kearns, 2003). The CCS can be split into three main parts: the main equatorward California Current offshore, a subsurface poleward undercurrent fringing the continental shelf, and a recirculation pattern known as the Southern California Eddy in the Southern California Bight.

In the CCS, both upwelling and large-scale circulation provide essential nutrients to the euphotic zone, where they fuel high rates of net primary production (NPP). While seasonal upwelling dominates north of Point Conception, advection by the CCS provides a major route for nutrient supply to the Santa Barbara Channel in the Southern California Bight (Bray et al., 1999). Following phytoplankton blooms, sinking and degradation of organic matter lead to oxygen consumption and widespread oxygen loss in subsurface waters (Brander et al., 2017; Chavez and Messié, 2009). Along the southern California coast, this oxygen depletion is exacerbated by regional circulation patterns that include transport of low-oxygen waters of tropical origin along the poleward undercurrent (Evans et al., 2020; Pozo Buil and Di Lorenzo, 2017). Oxygen decline is particularly apparent in deep, isolated basins such as those found in the Southern California continental borderland, where the presence of shallow sills limits ventilation of deep waters, and anoxic conditions are often encountered near the bottom (Reimers et al., 1990; Goericke et al., 2015; White et al., 2019).

In the CCS, the trace metal iron (Fe) has been identified as a limiting factor for the growth of phytoplankton (Hogle et al., 2018). Fe is an essential micronutrient that has also a considerable

influence on the dynamics of phosphorus and nitrogen in the euphotic zone (Tagliabue et al., 2017). Similar to other nutrients, Fe is transported to the surface by upwelling and circulation. However, Fe supply is generally low in oxygenated environments relative to other macronutrients, reflecting rapid scavenging of insoluble iron-oxide minerals by sinking particles that eventually accumulate in the sediment (Bruland et al., 2001, 2014; Firme et al., 2003; Till et al., 2019). While early studies suggested that Fe inputs to the CCS are dominated by rivers and aeolian deposition (Biller and Bruland, 2013; Johnson et al., 2003), more recent work highlights a combination of sources, including benthic fluxes (Severmann et al., 2010; Noffke et al., 2012; Tagliabue et al., 2017; Wallmann et al., 2022) and ocean currents, which help redistributing Fe in coastal waters (Bray et al., 1999; Boiteau et al., 2019; García-Reyes and Largier, 2010).

Benthic release of Fe(II), the reduced and soluble form of Fe, has been recognized as a potential source of Fe to the surface ocean along the continental shelf and slope of the CCS, including the deep basins of the California borderland (John et al., 2012; Severmann et al., 2010). Under hypoxic or anoxic bottom waters, Fe(II) produced in the sediment during microbial organic matter degradation coupled to Fe(III) reduction diffuses across the sediment-water interface and accumulates in the water column (Furrer and Wehrli, 1993; Dale et al., 2015; Severmann et al., 2010; Wallmann et al., 2022). In the CCS, this benthic Fe flux is likely to exceed atmospheric deposition (Deutsch et al., 2021), and may ultimately make its way to the surface by upwelling and vertical mixing, supporting high rates of photosynthesis.

The interaction between low bottom water oxygen, Fe(II) release, and transport by the ocean circulation is particularly important in the Santa Barbara Basin (SBB), an oxygen-deficient basin located between the Channel Islands and mainland California in the Southern California Bight. The SBB frequently experiences seasonal anoxia in the bottom water in fall, with irregular

oxygen flushing of dense, hypoxic water below the western sill depth (470 m) during winter and spring (Goericke et al., 2015; Sholkovitz and Soutar, 1975; White et al., 2019; Qin et al., 2022). This seasonal flushing reflects either changes in upwelling strength and frequency, or changes in stratification at the sill depth, although the exact cause of the flushing is still unclear (Goericke et al., 2015; Sholkovitz and Gieskes, 1971; White et al., 2019). Lack of oxygen in the deeper parts of the basin supports anaerobic microbial processes in the bottom water and sediment (White et al., 2019), including benthic Fe reduction (Goericke et al., 2015), causing the release of Fe(II) into the water column (Severmann et al., 2010). Ventilation events that re-oxygenate the deep basin, as well as mixing by the vigorous submesoscale circulation (Kessouri et al., 2020), could allow upwelling of this Fe above the sill depth and ultimately to the surface, providing a linkage between benthic processes and upper water-column biogeochemistry. Increased surface primary production supported by this Fe source would in turn drive higher remineralization and oxygen loss in deep waters, thus providing a positive feedback to benthic Fe release. However, with a dearth of benthic Fe flux measurements in the SBB, gaps remain in our understanding of the dynamics and impact of benthic Fe flux in the Southern California Borderland, particularly with respect to its magnitude, dependence on bottom water oxygen, and ability to reach the euphotic zone and influence primary production.

In this study, we explore the connection between benthic Fe flux and surface primary production in the CCS, by investigating the influence of enhanced benthic Fe fluxes from low-oxygen waters with a combination of field observations and experiments with a numerical model. We focus on the SBB, where we provide a new set of benthic Fe flux estimates determined by in-situ benthic flux chamber measurements. We combine these new observations with existing data (Severmann et al., 2010) to revise the representation of benthic Fe fluxes in UCLA's Regional

Ocean Modeling System coupled to the Biogeochemical Elemental Cycling (ROMS-BEC) model (Deutsch et al., 2021). We then use the model to evaluate the effect of benthic Fe fluxes on surface nutrient consumption and NPP, and compare their impact to that of aeolian Fe deposition in the SBB and beyond.

## 2. Materials and Methods

### 2.1 Study Site

Fieldwork in the SBB was conducted between Oct 29 and Nov 11, 2019, during the R/V Atlantis cruise AT42-19. Sampling occurred during the anoxic, non-upwelling season along one bimodal transect with six stations total at depths between 447 and 585 m (Fig. 2-1, Table 1).

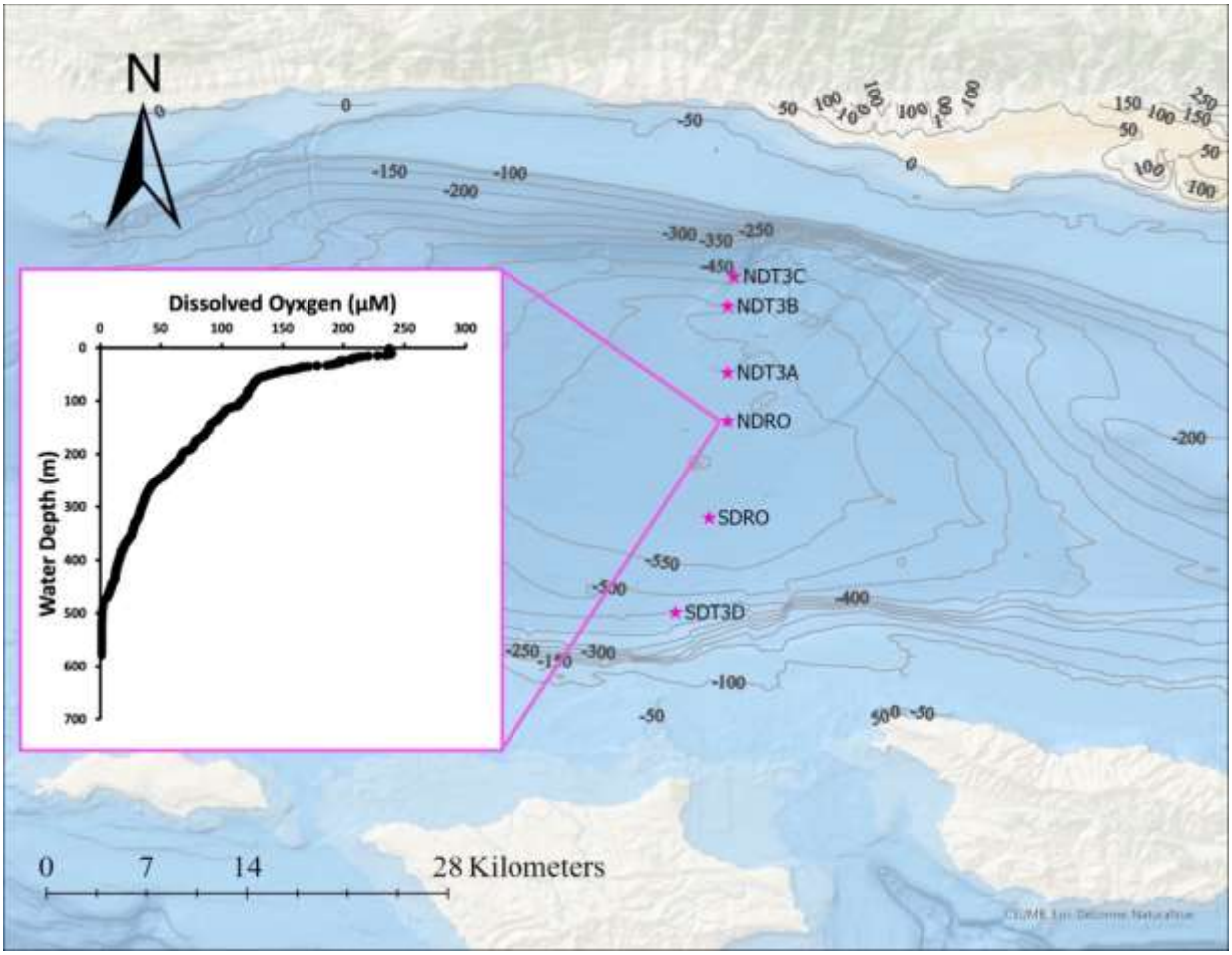


**Figure 2- 1.** Station locations in the SBB during the AT42-19 expedition with R/V Atlantis. NDT3 (with stations A, B, C) = Northern Depocenter Transect Three, NDRO = North Depocenter Radial Origin, SDRO = Southern Depocenter Radial Origin, SDT3 (with station D) = Southern Depocenter Transect Three. The small insert figure displays dissolved oxygen concentrations in the water column at the NDRO station profiled by an optical oxygen sensor attached to the AUV Sentry. The profile was measured at the following position: Latitude 34.2618 N, Longitude -120.0309 E. The map was created using ArcGIS Ocean Basemap,

with bathymetric contour lines representing depth information taken from the General Bathymetric Chart of the Ocean (GEBCO) database.

Transects were divided into northern (NDT3 = Northern Depocenter Transect Three) and southern (SDT3 = South Depocenter Transect Three) sites based on basin geography (Fig. 2-1). Stations were labeled alphabetically from A (deepest) to D (shallowest) according to their location along the transect, except for the deepest stations at the bottom of the basin, which were labeled Northern Depocenter Radial Origin (NDRO) and Southern Depocenter Radial Origin (SDRO).

### 2.2 Benthic Flux Chambers

Custom-built cylindrical benthic flux chamber systems (Treude et al., 2009) were deployed by the ROV Jason at the six stations (Fig. 2-1). Polycarbonate chambers (19 cm inner diameter) were installed in a small lightweight frame made from fiber-reinforced plastics. A stirrer (Type K/MT 111, K.U.M. Umwelt- und Meerestechnik, Kiel, Germany) was used to keep the water overlying the sediment enclosed by the chamber well mixed. One or two replicate chamber systems were deployed at each site. Since sediment in the SBB is quite soft and poorly consolidated, especially towards the deeper stations, frames were fitted with platforms attached to the feet of the frame and with buoyant syntactic foam to reduce sinking into the sediment. A syringe sampler was equipped with 6 glass sampling syringes that were connected with 50 cm long plastic tubes (2.5mm inner diameter, Vygon, Aachen, Germany). Each sampling syringe withdrew 50 mL of the overlying seawater at pre-programmed times. A seventh syringe was used to inject 50 mL of de-ionized water shortly after chambers were deployed to calculate chamber volume from the salinity-drop recorded with a conductivity sensor (type 5860, Aanderaa Data Instruments, Bergen, NO) in the overlying water, following the approach described in (Kononets et al., 2021). Water samples were analyzed for Fe(II) on the ship using a Shimadzu UV-Spectrophotometer (UV-1800),

equipped with a sipper unit, following the procedure of (Grasshoff and Ehrhardt, 1999). Fe fluxes were calculated from the slope of linear fits of Fe concentration time series vs. time (Fig. S2-1), multiplied by the chamber volume, and divided by the surface area of the sediment (Kononets et al., 2021).

### 2.3 Numerical model (ROMS-BEC)

To explore the impacts of benthic Fe fluxes on surface primary production, we used a well-established ocean biogeochemical model of the CCS (Renault et al., 2016; Deutsch et al., 2021). The physical model component consists of the Regional Ocean Modeling System (ROMS), (Shchepetkin, 2015; Shchepetkin and McWilliams, 2005) a primitive-equation, hydrostatic, topography-following ocean model. As in prior work, the model domain spans the entire U.S. West Coast, from Baja California to Vancouver Island, with a horizontal resolution of 4 km, enough to resolve the mesoscale circulation (Capet et al., 2008). The baseline model configuration was run over the period 1995–2017 with interannually varying atmospheric forcings. We refer the reader to earlier publications (Renault et al., 2021; Deutsch et al., 2021) for a complete description of the model configuration, setup, forcings and boundary conditions used in this study.

ROMS is coupled online to the Biogeochemical Elemental Cycling (BEC) model (Moore et al., 2004), adapted for the U.S. West Coast by (Deutsch et al., 2021). BEC solves the equations for the evolution of six nutrients (nitrate ($NO_3^-$), ammonium ($NH_4^+$), nitrite ($NO_2^-$), silicate ($SiO_2$), phosphate ($PO_4^{3-}$), and iron (Fe)), three phytoplankton groups (small phytoplankton, diatoms, and diazotrophs), a single zooplankton group, inorganic carbon, oxygen ($O_2$), and dissolved organic matter (carbon, nitrogen, phosphorus, and iron). Nutrient and carbon cycles are coupled by a fixed stoichiometry, except for silica and Fe, which use variable stoichiometries (Deutsch et al., 2021;

Moore et al., 2001, 2004). The Fe cycle in BEC includes four separate pools: dissolved inorganic Fe (dFe), dissolved and particulate organic Fe, and Fe associated with mineral dust. Of these, only dissolved organic and inorganic Fe are explicitly tracked as state variables, while particulate Fe is treated implicitly by resolving vertical sinking particle fluxes (Moore et al., 2001; Moore and Braucher, 2008). Four main processes control the cycle of Fe in the model: atmospheric deposition, biological uptake and remineralization, scavenging by sinking particles, and release by sediment. The atmospheric dFe deposition is based on the dust climatology of (Mahowald et al., 2006), and dissolution rates from (Moore and Braucher, 2008). Different from (Deutsch et al., 2021), we re-evaluated the dependence of benthic dFe fluxes on bottom water $O_2$ concentrations in the California margin based on a merged dataset that combines our measurements from the SCB, with those presented in (Severmann et al., 2010) (see Section 2.5). The model Fe scavenging scheme removes dFe from the water column at a rate proportional to sinking particle fluxes and dFe concentrations, assuming a uniform concentration of 0.6 nM of Fe-binding ligands (Moore et al., 2004; Moore and Braucher, 2008). Accordingly, scavenging rates increase strongly at dFe concentrations greater than 0.6 nM, and vice versa rates decrease strongly below 0.5 nM (Fig. S2-2). Note that, while simplistic, this formulation is still widely adopted by global ocean biogeochemistry models (Tagliabue et al., 2014, 2016), although improvements have been proposed (Moore and Braucher, 2008; Aumont et al., 2015; Pham and Ito, 2019, 2018).

As shown in previous work, the model captures the main patterns of physical and biogeochemical variability in the CCS, providing a representation of nutrient cycles and NPP in good agreement with observations (Renault et al., 2021; Deutsch et al., 2021). We further evaluate the model against an extended set of dissolved Fe measurements for the CCS (see Sections **2.4** and **3.1**).

### 2.4 Fe dataset along the U.S. West Coast

To assess the ability of the model to capture observed patterns in dFe along the U.S. West Coast, we gathered available dFe concentration measurements from published studies, including a global compilation (Tagliabue et al., 2016), regional programs such as CalCOFI, CCE-LTER, IRNBRU and MBARI cruises (Bundy et al., 2016; Hogle et al., 2018; Johnson et al., 2003; King and Barbeau, 2011), and other individual studies (Biller and Bruland, 2013; Boiteau et al., 2019; Bundy et al., 2014, 2015, 2016; Chappell et al., 2019; Chase, 2002; Chase et al., 2005; Firme et al., 2003; Hawco et al., 2021; John et al., 2012; Till et al., 2019). In the final compilation, we define dFe as the sum of the dissolved Fe and dissolvable Fe, based on the definitions used in each publication. Different studies used different filter sizes to define the dFe pool, most commonly 0.20, 0.40, and 0.45 μm, and different sampling methods, such as bottles, pump systems and/or surface tows. In some studies, samples were briefly acidified before being analyzed. Despite the differences in sampling and measurement approaches, we found that these datasets generally agreed with each other, suggesting that the final compilation accurately represents the dFe distribution along the U.S. West Coast. The final dataset includes observations from 1980 to 2021, with most samples collected between 1997 and 2015, and from the upper 100 m of the water column.

### 2.5 Experimental Design

To evaluate the impact of Fe fluxes from low-$O_2$ sediment in the SBB on surface biogeochemistry, we designed a suite of model sensitivity experiments with ROMS-BEC in which external sources of Fe are modified relative to a baseline simulation. Accordingly, we run the following model experiments:

***High-flux**:* This experiment is the baseline model simulation, using a Fe flux parameterization calculated as an exponential fit to a data set of benthic Fe fluxes consisting of the new benthic measurements from AT42-19 and previous observations from the U.S. West Coast (Severmann et al., 2010) (see Section 3.2), thus updating the parameterization by (Deutsch et al., 2021). Benthic Fe release follows the equation:

$$\log_{10}(\mathrm{Fe}) = 2.86 - 0.01 \cdot O_2 \quad [1]$$

Where $O_2$ is the concentration of oxygen in mmol $m^{-3}$ and (Fe) is the Fe flux in μmol $m^{-2}$ $d^{-1}$. This revised formulation is only applied in the SBB where we performed our measurements, while a different formulation, solely based on data by (Severmann et al., 2010) is used outside of the SBB:

$$\log_{10}(\mathrm{Fe}) = 2.6178 - 0.0128\ O_2 \quad [2]$$

For this parameterization, we corrected a model bias that resulted in modeled bottom $O_2$ concentrations greater than 30 mmol $m^{-3}$ over most of the deep basins where observations indicated lower concentrations, down to oxygen-free conditions (Fig. S2-3). We therefore reduced modeled bottom water $O_2$ concentrations in the Southern California Borderland by 30 mmol $m^{-3}$, based on the average difference between model and observed $O_2$ in the region. This correction is crucial to producing realistic benthic Fe fluxes under the anoxic conditions observed in the SBB, rather than fluxes at $O_2$ concentrations of 30 mmol $m^{-3}$.

***Hypoxia-off:*** The purpose of this experiment is to evaluate the importance of enhanced Fe fluxes under low-$O_2$ conditions in the SBB. Benthic Fe fluxes are calculated as in *High-flux* experiment (Equation 2), but they are capped at a constant value when $O_2$ decreased below a threshold of 65 mmol $m^{-3}$, which we chose as representative of hypoxic conditions (Deutsch et al.,

2011). This change is applied only to in the SBB, and effectively bounds the benthic Fe release at 1.48 μmol $m^{-2}$ $d^{-1}$ when $O_2$ drops below the threshold for hypoxia.

***Dust-off*:** The purpose of this experiment is to evaluate the importance of aeolian Fe deposition in the CCS, and to compare it with the benthic Fe fluxes. In this experiment, the atmospheric Fe deposition is set to zero; all other settings are identical to the *High-flux* experiment.

The baseline (*High-flux*) model simulation is run from 1995 to 2017. The other two model sensitivity experiments (*Hypoxia-off* and *Dust-off)* are branched off from the *High-flux* simulation in year 2008 and run separately for 10 additional years (2008-2017). All model experiments use the same set of forcings and initial conditions. Results from the final 3 years (2015-2017) of the *Hypoxia-off* and *Dust-off* simulations are averaged and analyzed by comparing differences in biogeochemical fields (Fe, $NO_3^-$, and NPP) to the final 3 years of the *High-flux* run.

## 3. Results

### 3.1 In-situ benthic Fe fluxes and model parameterization

Benthic Fe fluxes from in-situ benthic chamber measurements during the AT42-19 expedition are shown in Table 1. High Fe flux was recorded at the anoxic depocenter stations (4.90 and 3.92 mmol $m^{-2}$ $d^{-1}$ at SDRO and 3.49 mmol $m^{-2}$ $d^{-1}$ at NDRO). Fe fluxes at the shallower hypoxic stations (NDT3C, NDT3B, and SDT3D) were an order of magnitude lower. The Fe flux at the hypoxic NDT3A station between NDRO and NDT3B was approximately half the flux observed at the depocenter.

**Table 2-1.** Station details and geochemical parameters determined during the AT42-19 expedition. Benthic Fe fluxes were determined using in-situ benthic chambers. Dissolved $O_2$ concentrations were measured in the water column at 10 m above the seafloor using a Seabird optode sensor attached to the ROV Jason. At stations with two benthic chamber deployments (NDT3A and SDRO), $O_2$, geographical coordinates, and depth were averaged as there were only minimal differences between the two chamber deployments.

| Station | Fe Flux [mmol $m^{-2}$ $d^{-1}$] | $O_2$ [mmol $m^{-3}$] | Latitude [N] | Longitude [E] | Depth [m] |
|---|---|---|---|---|---|
| NDT3C | 0.23 (n=1) | 5.3 | 34.3526 | -120.0160 | 499 |
| NDT3B | 0.36 (n=1) | 6.8 | 34.3336 | -120.0188 | 535 |
| NDT3A | 1.73; 1.20 (n=2) | 9.6 | 34.2921 | -120.0258 | 572 |
| NDRO | 3.49 (n=1) | 0.0 | 34.2618 | -120.0309 | 581 |
| SDRO | 4.90; 3.92 (n=2) | 0.0 | 34.2011 | -120.0446 | 586 |
| SDT3D | 0.58 (n=1) | 9.6 | 34.1422 | -120.0515 | 446 |

Trends in the Fe fluxes suggest modulation by $O_2$ concentration, water depth, and/or bathymetry. We also note that observed oxygen concentration represents a snapshot of bottom water conditions, while Fe fluxes likely reflect the oxygenation history at any given site. We observed a decrease in the Fe flux with a decrease in water depth (Fig. 2-2). There was also a slight trend of higher Fe fluxes with lower $O_2$ concentrations (most pronounced when $O_2$ reaches zero); however, since $O_2$ concentrations were relatively low at all stations (<10 mmol $m^{-3}$) it is difficult to distill a clear pattern based on the small dataset. Notably, the NDT3A station showed a high Fe flux despite exhibiting the same $O_2$ concentration as the shallower station SDT3D. Basin bathymetry may also contribute to observed differences in the flux. For instance, the deeper depocenter and A-station showed higher averaged fluxes than the B, C, and D stations**.** We further noticed differences between the north and south extension of the transect. The southern stations (SDRO and SDT3D) showed a higher Fe flux than the northern stations (NDRO and NDT3C).

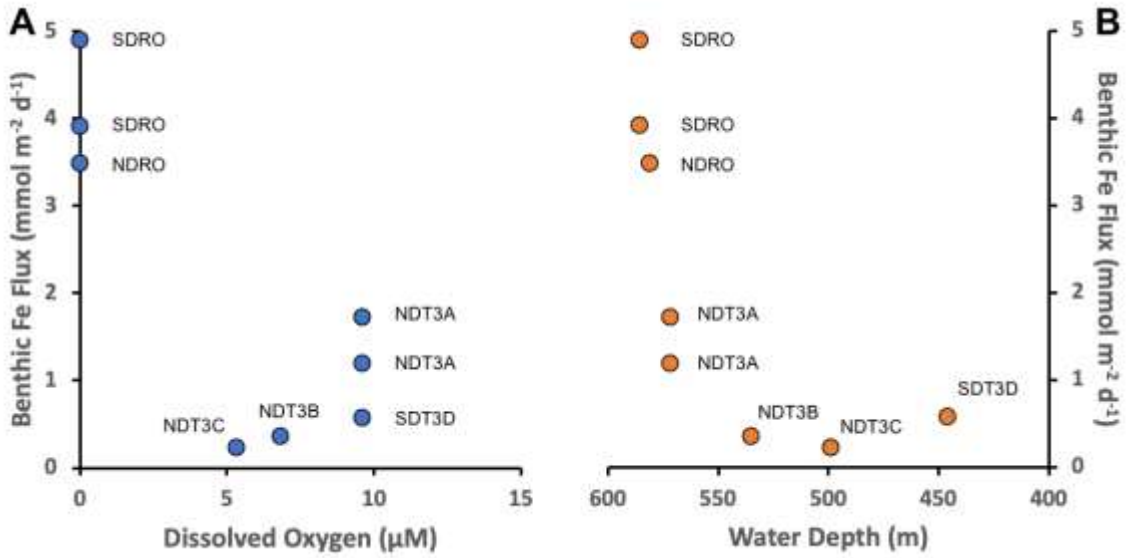


**Figure 2- 2.** Benthic in-situ Fe fluxes. A: Fluxes as a function of $O_2$. B: Fluxes as a function of (station) water depth. Note that water depth is shown from deep to shallow depths. See Table 1 for station details.

We combined Fe fluxes determined during AT42-19 with previous estimates along the CCS, as compiled by (Severmann et al., 2010), and analyzed them as a function of bottom water $O_2$ (Fig. 2-3). Pooled together, the measurements can be described reasonably well by an exponential increase of Fe fluxes with declining bottom water $O_2$ (Severmann et al., 2010), although significant variability around an exponential fit remains. This is consistent with the Fe flux parameterization adopted in the ROMS-BEC model (Deutsch et al., 2021). Several observations from the AT42-19 cruise (red dots) in (Fig. 2-3) exceed the range of previous measurements (blue dots) in (Fig. 2-3), likely owing to the anoxic or near-anoxic conditions in the water. Relative to the exponential fit to the dataset by (Severmann et al., 2010) (yellow line in Fig. 2-3, see Equation 2) the revised fit to the pooled data (purple line in Fig. 2-3, see Equation 1) expands Fe fluxes by approximately a factor of two at $O_2$ concentrations close to zero, but decreases the magnitude of the Fe fluxes at concentrations above approximately 130 mmol $m^{-3}$.

### 3.2 Model evaluation: High flux simulation

The *High-flux* simulation captures the magnitude and patterns of the observed dFe distribution in the upper ocean (Fig. 2-4), consistently with our knowledge of the ocean Fe cycle. In both model and observations, dFe concentrations are low at the surface, as a result of phytoplankton uptake, and increase gradually in subsurface waters due to organic matter remineralization in the water column and at the seafloor, and benthic Fe fluxes from the sediment (Fig. S2-4). The highest dFe concentrations are found along the coast, likely related to high surface productivity and shallow carbon export and remineralization, combined with basin bathymetry and $O_2$ deficiency. In the open ocean, dFe concentrations are low in both model and observations, reflecting a combination of phytoplankton uptake, scavenging by sinking particles, and low external inputs.

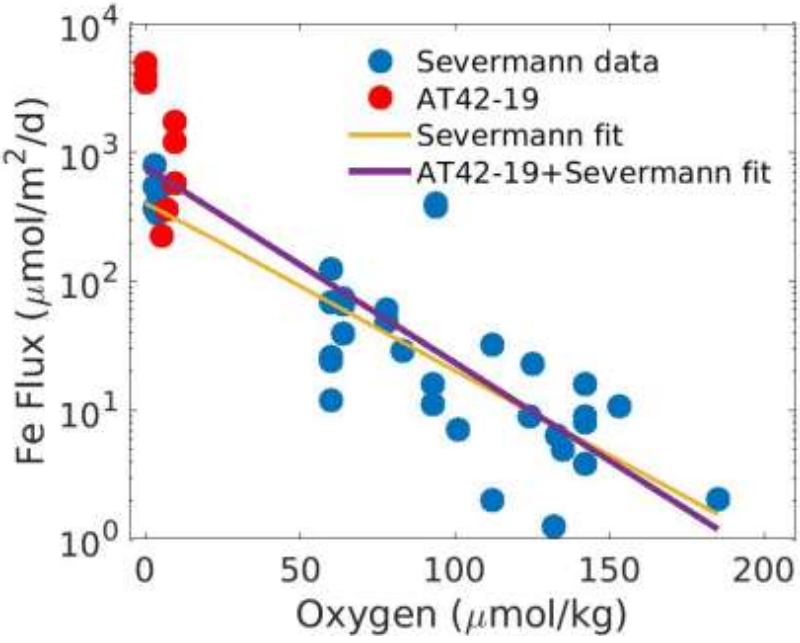


**Figure 2- 3**. Combined benthic Fe flux data as a function of bottom oxygen. Blue dots show data from the compilation by (Severmann et al., 2010); red dots measurements from the AT42-19 cruise. The yellow line shows an exponential fits to the dataset by (Severmann et al., 2010) equation 2. The purple line

shows an exponential fit to the combined dataset equation 1. Note the logarithmic scale used for the y-axis.

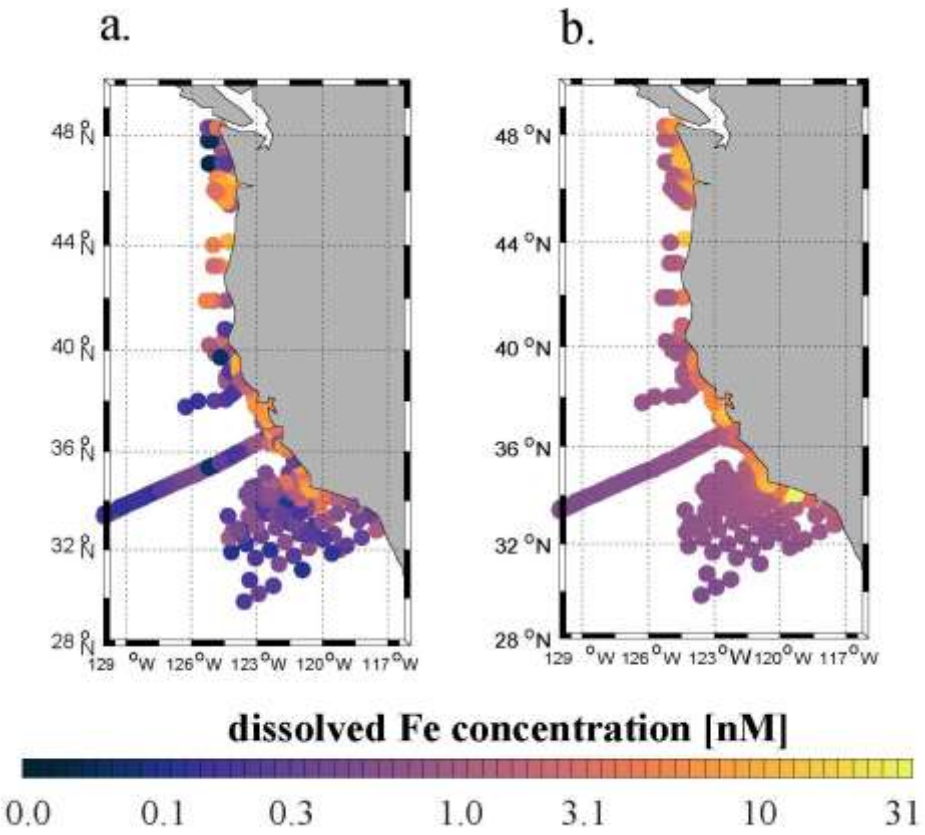


**Figure 2- 4** (a) Observed dFe concentrations (nM) from the U.S. West Coast compilation (see Section **2.4**) averaged between 0 and 100 m depth. (b) Annual mean modeled dFe concentrations (nM) averaged between 0 and 100 m depth, sampled at the same locations as the observations in panel (a).

Observational limitations prevent a more detailed validation of subsurface dFe patterns. Measurements of dFe concentrations in subsurface and deep waters (> 100 m) are currently very sparse in the CCS region and Southern California Borderland. Most of the dFe measurements for the SBB come from limited sampling conducted quarterly as part of selected CalCOFI (California Cooperative Oceanic Fisheries Investigations) cruises (King and Barbeau, 2011). These samples mostly focus on the mixed layer and are too sparse in space and time to capture the effects of deep-

water renewal events that ventilate the anoxic basins and allow uplifting and transport of deep waters towards the surface.

The agreement of the model dFe with observations (correlation coefficient $R=0.22$, $p<0.01$) is similar to that of other ocean biogeochemical models (Tagliabue et al., 2016). The model tends to underestimate the sharp dFe gradient between coastal and open ocean waters, overestimating dFe in the open ocean and producing too uniform concentrations offshore and at depth (Fig. 2-4). These biases are likely related to the simple Fe scavenging scheme, which assumes a constant Fe-binding ligand concentration of 0.6 nM. The small number and episodic nature of in-situ measurements may also explain some of the mismatches between model and observations.

At the scale of the CCS, the *High-flux* simulation produces lower surface dFe in the southern part of the domain (33°N to 36°N), and higher surface concentration in the northern part (40°N to 45°N) and near the central coast (Fig. 2-5a). While these patterns reflect a combination of internal Fe cycling and external inputs, the elevated dFe in the northern CCS, in particular offshore, can be partly attributed to higher aeolian deposition in that region (Fig. S2-5) as well as coastal inputs from the Juan De Fuca strait (Deutsch et al., 2021).

The model reproduces the typical signature of coastal upwelling, with higher concentrations of $NO_3^-$ nearshore in the central coast (36°N-40°N) and low concentrations in the Southern California Bight and offshore Fig. 5b. Similarly, the model reproduces high values of NPP near the coast, in particular along the central coast, and rapidly decreasing values offshore (Fig. 2-5c). Relative to previous modeling work (Deutsch et al., 2021) our simulations generate somewhat lower surface $NO_3^-$ concentrations close to the coast, and sharper NPP gradients between the nearshore and offshore regions, which are consistent with the rapid decrease in

primary productivity and chlorophyll shown by both satellite-based estimates and *in situ* data (Deutsch et al., 2021). These changes likely reflect the higher benthic Fe fluxes in our simulations (Equation 1), which increase phytoplankton productivity and promote nutrient drawdown near the coast.

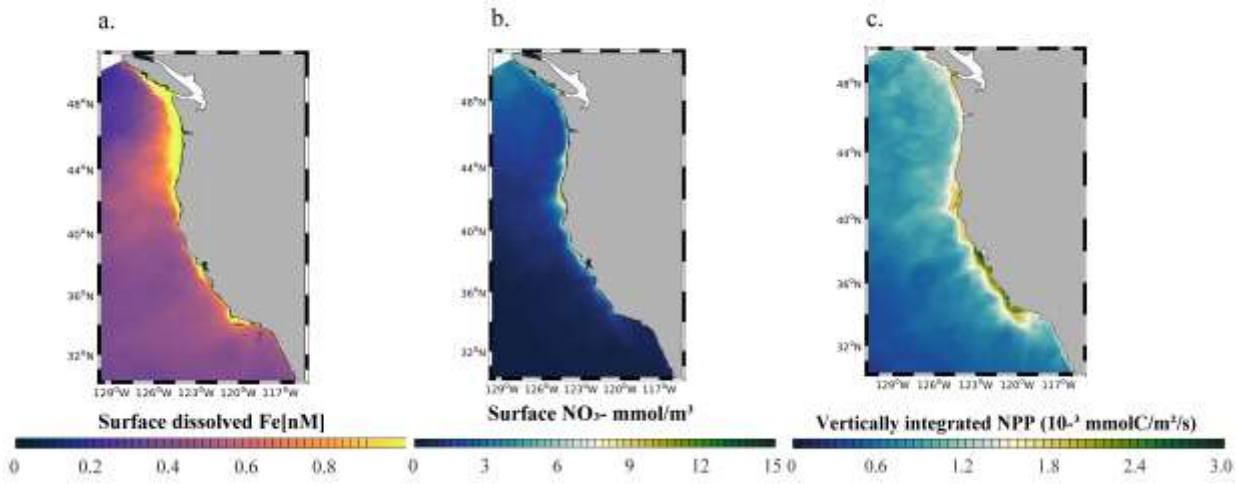


**Figure 2- 5.** (a) Surface dFe concentration, (b) surface $NO_3^-$ concentration, and (c) vertically integrated net primary production (NPP) from the High-flux model simulation.

### 3.3 Hypoxia-off: Impact of benthic Fe flux from low-oxygen bottom water

We quantify the importance of benthic Fe fluxes from low-$O_2$ bottom waters in the Southern California Borderland by analyzing results from the *Hypoxia-off* experiment, in which we cap the high benthic Fe flux at a constant value (1.48 μmol $m^{-2}$ $d^{-1}$) when $O_2$ declines below hypoxic conditions (65 mmol $m^{-3}$, see Section 2.5) (Fig 2-6).

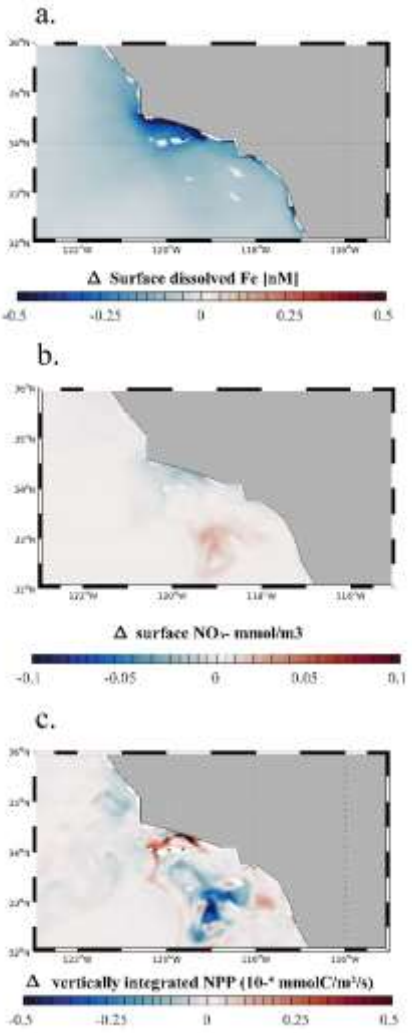


**Figure 2- 6** (a) Surface dFe anomalies, (b) Surface $NO_3^-$ anomalies, and (c) vertically integrated net primary production (NPP) from the Hypoxia-off model run relative to the High-flux model run. The maps focus on the region around the SBB.

As expected, a decrease in benthic Fe flux from the anoxic basins in the *Hypoxia-off* simulation leads to a decrease in the surface dFe concentration (Fig. 2-6a). This decrease is particularly significant along the coast of the SBB, but also extends slightly into the open ocean (Fig S2-6). This trend indicates that dFe released from low- $O_2$ sediment is effectively transported to the surface and offshore, where it can affect primary production. The decrease in surface dFe caused by reduced benthic release causes a decline in NPP near the coast (Fig. 2-6c), where phytoplankton rely the most on benthic-derived Fe. NPP also shows a patchy increase in some regions, especially between 32°N and 33°N and between 34°N and 35°N. This patchy increase can be explained by the relative importance of Fe vs. N limitation along a cross-shore productivity gradient. While near the SBB coast, phytoplankton is frequently Fe limited (up to 50% of the time in the model), especially following upwelling events, it tends to be almost exclusively N-limited moving offshore (Deutsch et al., 2021). This limitation pattern is consistent with observations from (King and Barbeau, 2011), who show that N:Fe ratios decrease moving from the coast to the open ocean (i.e., N is likely more limiting than Fe offshore). As Fe limitation reduces NPP near the coast in the *Hypoxia-off* experiment, $NO_3^-$ utilization also declines, so that more $NO_3^-$ can accumulate in surface waters (Fig. 2-6b). Shallow transport of excess $NO_3^-$ in mesoscale eddies can further fertilize offshore waters (Damien et al., 2023), releasing local N limitation and fueling an increase in NPP (Fig. 2-6c).

### 3.4 Dust-off: Role of atmospheric Fe deposition

We evaluate the importance of aeolian Fe sources in the *Dust-off* simulation, in which atmospheric Fe deposition is set to zero. In this experiment, surface dFe decreases everywhere in the CCS, but the decrease is particularly evident in the open ocean and the northern part of the domain (Fig. 2-7a). This dFe decrease leads to a widespread reduction in NPP in the northern

CCS (40°N to 48°N, Fig. 2-7c), with stronger negative anomalies away from the coast. The decline in NPP is accompanied by a broad decrease in $NO_3^-$ utilization, particularly evident offshore, where phytoplankton rely mostly on Fe delivery by dust. In contrast, we observe a broad increase in NPP in the southern CCS (south of 40°S) and in coastal areas, likely reflecting increased availability of $NO_3^-$ transported southward by the broad California Current. The response of NPP in coastal areas and the southern CCS when the dust deposition of Fe is set to zero demonstrates that phytoplankton in those regions relies mostly on benthic Fe fluxes, rather than dust deposition, as the main source of Fe.

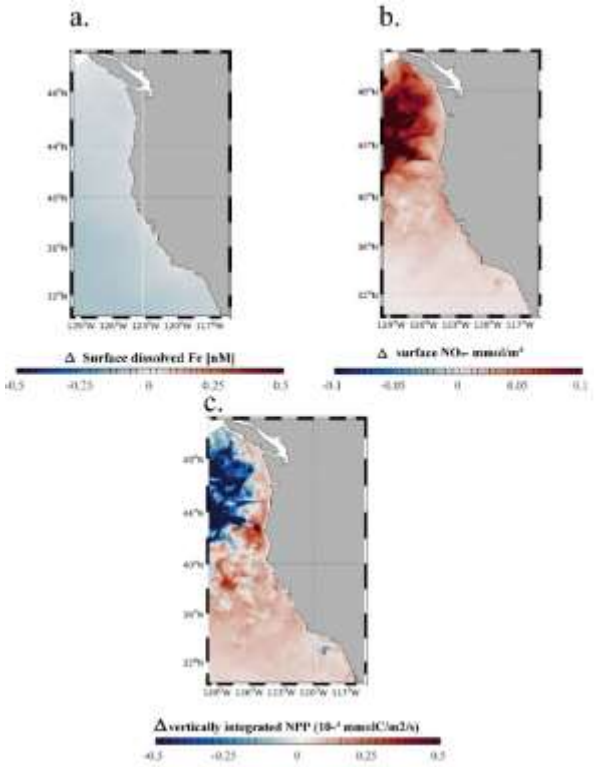


**Figure 2- 7** (a) Surface dissolved Fe, (b) surface $NO_3^-$ anomalies, and (c) vertically integrated net primary production (NPP) from the Dust-off model run relative to the High-flux model run.

# 4. Discussion

## 4.1 Benthic Fe flux feedbacks on SBB biogeochemistry

The influence of bottom water $O_2$ concentration on the exchange of solutes between the sediment and the water column has been well documented (Soetaert et al., 2000; Sommer et al., 2016; Testa et al., 2013). Under hypoxic or anoxic bottom water conditions, organic matter sedimentation sustains anaerobic respiration at the sediment-water interface and in the sediment (Furrer and Wehrli, 1993; Middelburg and Levin, 2009a). Reduced compounds accumulate in pore waters forming chemical gradients (Widdows and Brinsley, 2002) that result in the flux of solutes such as Fe(II) out of the sediment, and their accumulation in bottom water (Jørgensen and Nelson, 2004; McMahon and Chapelle, 1991; Middelburg and Levin, 2009b; Yao et al., 2016). Similar conditions are observed in the SBB, where high sedimentation rates, water column denitrification below the sill depth, and high pore-water concentrations of sulfide and Fe(II) have been observed (Behl and Kennett, 1996; Bray et al., 1999; Goericke et al., 2015; Sholkovitz and Soutar, 1975; Sigman et al., 2003; White et al., 2019).

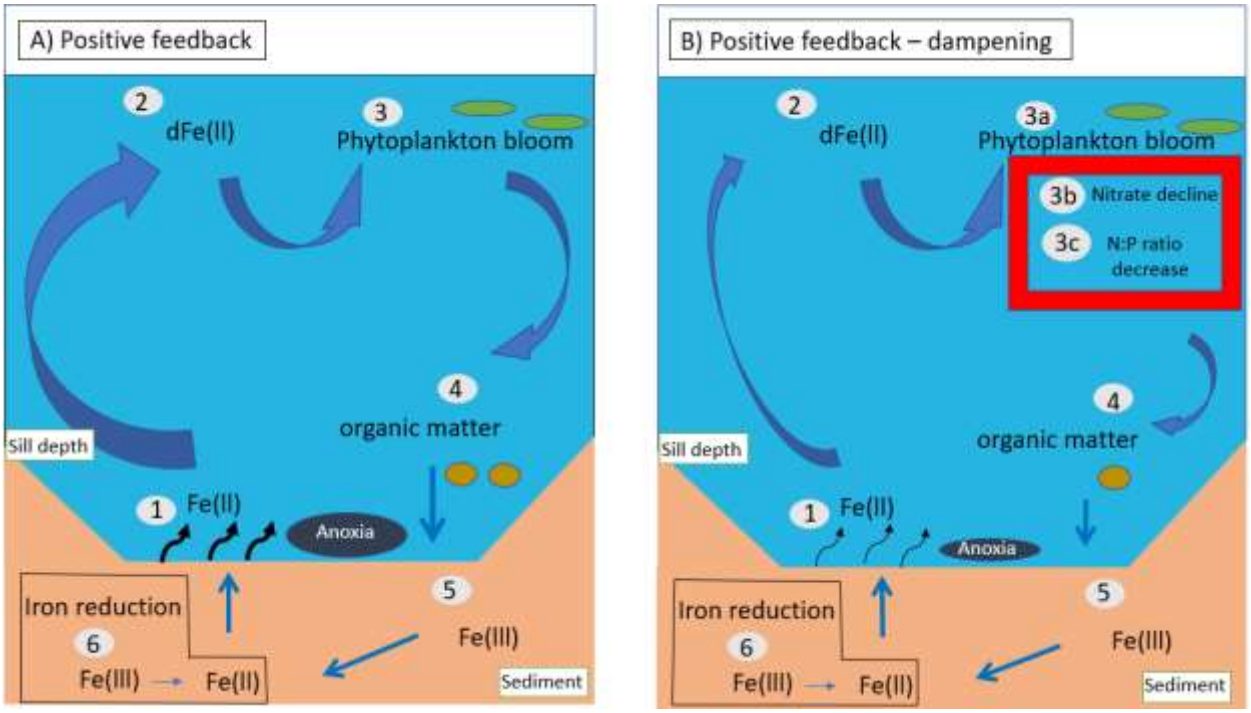


**Figure 2- 8.** Schematic illustrating feedback loops between benthic Fe release, nutrient cycles, and productivity in the Santa Barbara Basin. (a) Positive feedback loop: 1. Benthic Fe is released into the oxygen poor bottom water. 2. Upwelled Fe reaches the surface ocean increasing dissolved Fe concentrations. 3. Dissolved Fe is assimilated by phytoplankton, fueling blooms and production of organic matter and siderophores, ligands used to chelate ferric iron. 4. Organic matter is exported from the surface to the deep ocean. 5. Organic matter accumulates at the sediment-water interface. 6. During remineralization, iron-reducing bacteria reduce Fe(III) to Fe(II), increasing benthic dFe release. (b) Positive feedback loop – dampening: 1-3 (not including 3b and 3c) and 4-6 are identical to (a). Parts 3b and 3c illustrate the decline of $NO_3$- at the surface caused by the release of Fe limitation, which together with fixed-N loss in anoxic sediment would limit the increase in primary production and export production. Together with enhanced release of phosphate from anoxic sediment, this could also reduce the N:P ratio of phytoplankton. Ultimately, these processes inhibit a further increase of the benthic Fe(II) release, dampening the positive feedback.

The intense flux of dFe from the sediment suggests the potential for biogeochemical feedbacks in the SBB and more broadly in the CCS (as shown by Figs. 2- 5 – 7). Under a positive feedback scenario (illustrated in Fig. 8a), anoxic and nearly anoxic bottom water conditions facilitate Fe(II) diffusion from the sediment into the bottom water. In the SBB, this Fe eventually reaches the surface via upwelling and mixing processes, which are likely enhanced in the presence of complex bathymetry and islands in the Southern California Bight (Kessouri et al., 2020). This additional dFe input fertilizes coastal waters and increases primary production. Newly formed

organic matter eventually sinks towards the seafloor as a rain of organic particles, supporting low-oxygen concentrations in the bottom water, and fueling anaerobic respiration, including Fe reduction, in the sediment. This chain of processes thus represents a positive feedback loop that maintains high Fe(II) release from the sediment, as long as the bottom water remains hypoxic or anoxic (Mills et al., 2004; Noffke et al., 2012; Sañudo-Wilhelmy et al., 2001; Dale et al., 2015; Wallmann et al., 2022).

Our simulations also indicate the potential for complex biogeochemical responses between Fe, $NO_3^-$ and NPP, which could limit the effects of these feedbacks. Specifically, the positive feedback loop is damped in our conceptual model by increased $NO_3^-$ limitation and elevated N-loss in anoxic sediments under oxygen-deficient bottom waters at higher Fe supply (illustrated by Fig. 2-8b), which would in turn limit the increase in NPP. Transport of N-depleted coastal waters can further reduce NPP offshore, counteracting the positive feedback. In addition, the positive feedback would be also damped by Fe scavenging, which is magnified at high dissolved Fe concentrations, unless Fe-binding ligands also increase. This damping effect is particularly strong in our model, where a constant ligand concentration of 0.6 nM is used, above which scavenging rapidly increases (Section 2). Such a negative feedback between scavenging and benthic Fe fluxes is consistent with the global modeling study by Somes et al. (2021).

Additional processes may further modulate these feedback loops. Increased anoxia in bottom water and sediment favors the removal of fixed N by denitrification (Goericke et al., 2015; White et al., 2019). Upwelling of $NO_3^-$-depleted waters would then reduce surface productivity by increasing N limitation (Gruber and Deutsch, 2014). Release of Fe(II) from the sediment could also impact phosphate dynamics. Phosphate is scavenged by Fe during oxidation of Fe(II) in the water column and sediment because of the ability of Fe(III) minerals to bind it. After burial,

phosphate is released due to reduction of solid Fe(III) minerals to dissolved Fe(II), and diffuses upward to be either re-adsorbed by Fe(III) at the oxic sediment-water interface, or released to the bottom water under anoxic conditions (Dijkstra et al., 2014). The latter scenario is consistent with our in-situ benthic flux chamber measurements revealing increased phosphate release from the sediment with increased depth in the SBB (Yousavich et al., 2023). Higher release of phosphate into the water column, and transport to the surface, could decrease the N:P ratio of phytoplankton, especially downstream of waters where denitrification occurred (Deutsch et al., 2007). In the presence of N limitation, these conditions could favor the activity of nitrogen-fixing microorganisms (Mills et al., 2004; Noffke et al., 2012; Sañudo-Wilhelmy et al., 2001), which could further modulate surface NPP (Deutsch et al., 2007).

### 4.2 Contribution of physical transport on surface Fe

Our numerical experiments suggest that Fe released into the deep SBB can reach surface waters and fertilize them. This finding highlights the critical role of bottom water upwelling and mixing in the deep basins of the Southern California Borderland. There is ample literature describing seasonal surface circulation and bottom water renewal and their effect on nutrients in the SBB (Bray et al., 1999; Hendershott and Winant, 1996; Sholkovitz and Gieskes, 1971). However, the frequency and rate of seasonal bottom water flushing events, and the processes responsible for vertical mixing and upwelling across hundreds of meters remain poorly understood (Shiller et al., 1985; Sholkovitz and Gieskes, 1971; White et al., 2019). It is likely that interaction between wind-driven upwelling events and submesoscale eddies, which are particularly intense inside the Santa Barbara Channel (Kessouri et al., 2020), favors upward mixing of deep bottom water in the wake of flushing events, connecting deep bottom waters to the surface.

### 4.3 Quantifying expansion of anoxia in the SBB

Changes in source waters and global $O_2$ loss have contributed to decreasing $O_2$ levels throughout the Southern California Bight and the SBB (Zhou et al., 2022). With the outlook of a continuing decline in oceanic $O_2$ (Bopp et al., 2013; Kwiatkowski et al., 2020), quantifying the expansion of hypoxic and anoxic zones in the SBB is vital to understand the dynamics and fate of Fe(II) and other reduced compounds, such as ammonium and hydrogen sulfide, in deep low-oxygen waters. In the SBB, bottom water renewal events have experienced a decline in frequency and magnitude, driving an expansion of hypoxic and anoxic conditions in deep waters (White et al., 2019). This expansion has led to an increase in anaerobic reactions, such as denitrification in the water column (White et al., 2019) as well as Fe reduction, sulfate reduction, and dissimilatory nitrate reduction to ammonium (DNRA) in the sediment (Valentine et al., 2016; Treude et al., 2021; Sommer et al., 2016). Expansion of low $O_2$ waters could intensify the positive feedback loop between Fe release, NPP and $O_2$ loss (Fig. 2-8). However, to date, despite growing evidence for more frequent anoxia, there is no clear quantitative record of the vertical or horizontal expansions of oxygen-deficient waters in the SBB.

## 5. Conclusion

Our field campaign in the SBB measured a remarkably high flux of Fe(II) from the sediment (0.23 – 4.9 mmol $m^{-2}$ $d^{-1}$), greater than in previous studies from this region (Severmann et al., 2010) and from other oxygen minimum zones (Dale et al. 2015; Homoky et al. 2021). While these observations are based on snapshots of $O_2$ and Fe fluxes, they have implications for the temporal variability of Fe supply. High benthic Fe fluxes are observed during the anoxic fall season, while seasonal flushing in winter and spring likely decreases them by increasing bottom water $O_2$ and Fe oxidation and retention near the sediment.

Using a series of simulations with an ocean biogeochemical model, we show that this high Fe release from deep, low-oxygen sediment can reach the surface and impact nutrients and productivity in the SBB and the Southern California Bight, where Fe is often limiting (Hogle et al., 2018). We also highlight the impacts of coastal Fe inputs on waters further offshore. While phytoplankton in coastal areas directly benefits from Fe fertilization, increased $NO_3^-$ utilization in coastal waters can increase N-limitation of phytoplankton further downstream in open-ocean areas. Thus, benthic Fe fluxes can modulate Fe and $NO_3^-$ limitation in ways that partially counteract one another along the cross-shore productivity gradient of the CCS. Our simulations also suggest that Fe inputs from atmospheric deposition are mostly important in the open ocean north of 40°N, where phytoplankton rely on Fe delivery by dust. However, we also show that changes in atmospheric Fe deposition can affect ocean productivity in the southern CCS by altering $NO_3^-$ utilization further downstream. Our results support the idea that benthic Fe fluxes are the major source of Fe in the southern CCS and are supplemented by atmospheric deposition in northwestern and offshore waters, leading to relatively high NPP coastwide.

We suggest that benthic Fe fluxes from deep anoxic basins reach the surface in the SBB, contributing to feedbacks between Fe and $NO_3^-$ limitation and NPP. Specifically, high Fe fluxes from low-oxygen sediment support higher NPP near the coast, in turn leading to increased respiration and $O_2$ loss at depth, maintaining high Fe release. This positive feedback is damped by increased $NO_3^-$ limitation, which reduces NPP downstream of coastal regions. This benthic-pelagic coupling demonstrates the importance of sediment-derived Fe fluxes on the coastal ecosystem of the CCS, and the role of vertical transport processes in connecting deep environments to surface waters along continental margins. Our results are thus consistent with previous work from the Peruvian coastal upwelling (Wallmann et al., 2022), suggesting that oceanic $O_2$ loss could drive an increase in benthic Fe fluxes, enhancing local productivity and leading to further $O_2$ loss. This positive feedback could be stabilized by loss of fixed nitrogen under expanded anaerobic conditions.

It is likely that feedbacks of the type highlighted by (Wallmann et al., 2022) and our work in the SBB are at play more broadly along low-oxygen upwelling systems and coastal OMZ. Further studies should focus on the coupling between benthic processes and Fe and nutrient cycling in these regions. For example, fixed nitrogen loss by denitrification and enhanced release of phosphorous under low-oxygen bottom water are likely to further modulate these interactions. Seasonal studies based on stable isotope, radiotracer, and geochemical techniques are required to track the fate and transport of nutrients in low-$O_2$ coastal regions, clarifying the dynamics and sensitivities of the underlying microbial metabolisms. Ocean biogeochemical models for regional and global studies should incorporate new observations of benthic fluxes and their sensitivity to bottom $O_2$ and other environmental variables. This would expand the ability of models to better

capture the effects of long-term oceanic $O_2$ loss, and the feedbacks between benthic nutrient fluxes and surface productivity.

**Acknowledgements**

We thank the captain and crew of R/V Atlantis, the crew of ROV Jason, the crew of AUV Sentry, and the science party of research cruise AT42-19 for their technical and logistical support. We thank Q. Qin, M. O'Beirne, A. Mazariegos, X. Moreno, and A. Eastman for assisting with shipboard analyses. Funding for this work was provided by the US National Science Foundation, NSF OCE-1829981 (to TT), OCE-1756947 and OCE-1830033 (to DLV), and OCE-2023493 (to DB and ALP). Computational resources were provided by the Expanse system at the San Diego Supercomputer Center through allocation TG-OCE170017 from the Extreme Science and Engineering Discovery Environment (XSEDE), which was supported by National Science Foundation grant 1548562.

**Code availability**

The physical and biogeochemical codes used for our simulations can be accessed at: https://github.com/UCLA-ROMS/Code.

The model output can be accessed through Zenodo: (link will be provided before publication)

**Data availability**

In-situ benthic Fe flux data are accessible through the Biological & Chemical Oceanography Data Management Office (BCO-DMO) under the following DOI: 10.26008/1912/bco-dmo.896706.1.

**Author contributions.**

DR, TT, DB, and AP conceived this study. DM, DJY, FJ, FW, ECA, KMG, DLV and TT conducted the sampling at sea. DJY transformed and interpreted ROV Jason data. FJ and FW constructed and managed benthic flux chambers. DYJ and DR analyzed Fe(II) and assisted with the flux calculation. MM provided the compiled Fe measurements along the U.S. West Coast. AP and MS performed the model simulations. DR, DB, AP and TT wrote the manuscript with input from all co-authors.

**Competing interests**

Some authors are members of the editorial board of Biogeosciences. The peer-review process was guided by an independent editor, and the authors have no other competing interests to declare.

**Supplementary Material**

# Iron "Ore" Nothing: Benthic iron fluxes from the oxygen-deficient Santa Barbara Basin enhance phytoplankton productivity in surface waters

**De'Marcus Robinson**[1*], Anh D. Pham[1], David J. Yousavich[2], Felix Janssen[3], Frank Wenzhöfer[3], Eleanor C. Arrington[4], Kelsey M. Gosselin[5], Marco Sandoval Belmar[1], Matthew Mar[1], David L. Valentine[4], Daniele Bianchi[1], Tina Treude[1,2*]

[1]Department of Atmospheric and Oceanic Sciences, University of California Los Angeles, Los Angeles, CA, USA

[2]Department of Earth, Planetary and Space Sciences, University of California Los Angeles, Los Angeles, CA, USA

[3]HGF-MPG Joint Research Group for Deep-Sea Ecology and Technology, Alfred Wegener Institute, Helmholtz Centre for Polar and Marine Research, Bremerhaven, Germany

[4]Department of Earth Science and Marine Science Institute, University of California, Santa Barbara, CA 93106, USA

[5]Interepartment Graduate Program in Marine Science, University of California, Santa Barbara, CA 93106, USA

*Correspondence: De'Marcus Robinson, demarcus1.robinson@atmos.ucla.edu; Tina Treude, ttreude@g.ucla.edu

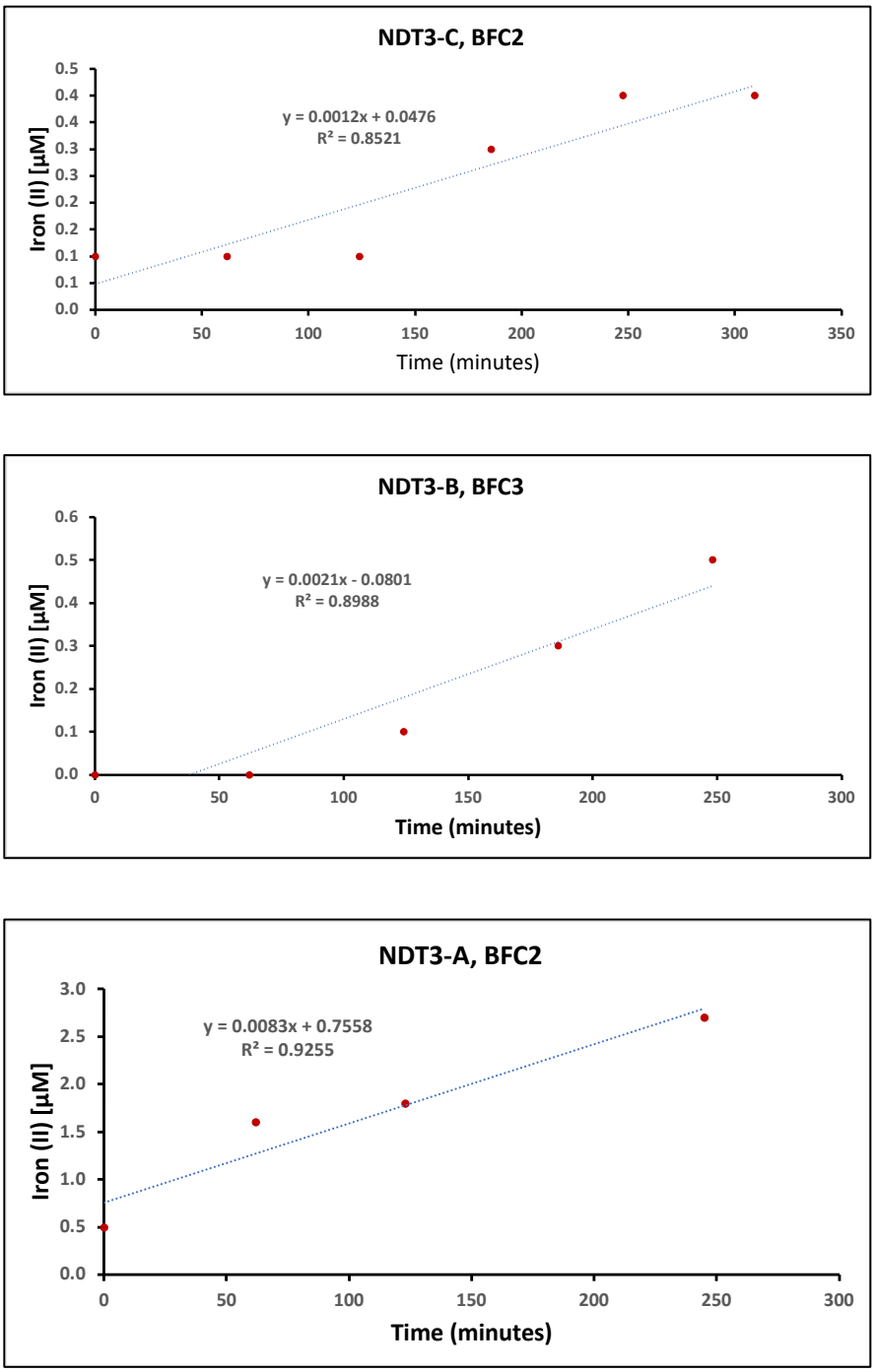


**Figure S2- 1.** Development of dissolved Fe(II) concentration in the supernatant water of benthic flux chambers (BFC) deployed at the studied stations in the Santa Barbara Basin during the AT42-19 expedition (see also data in **Table 1**). The increase (slope) in Fe(II) over time was used for the calculation of benthic Fe(II) fluxes.

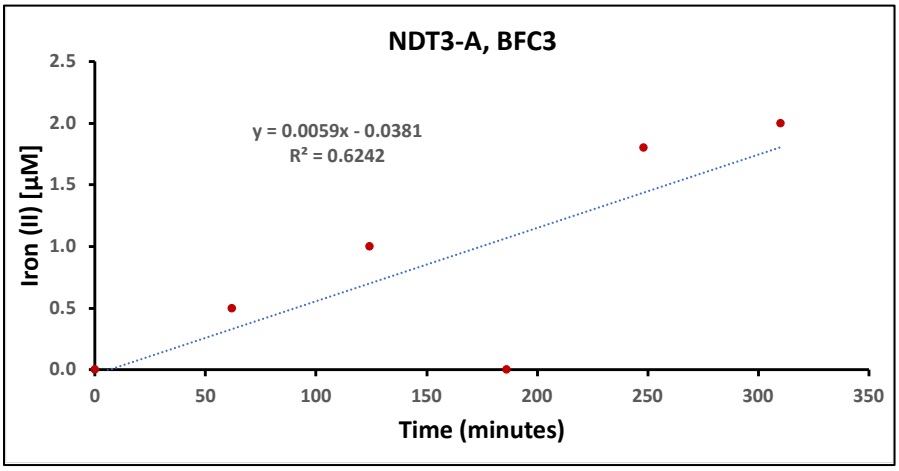


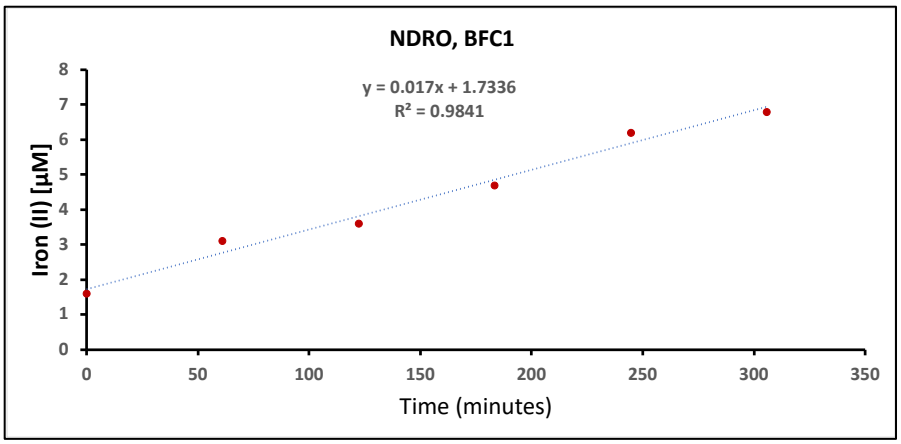


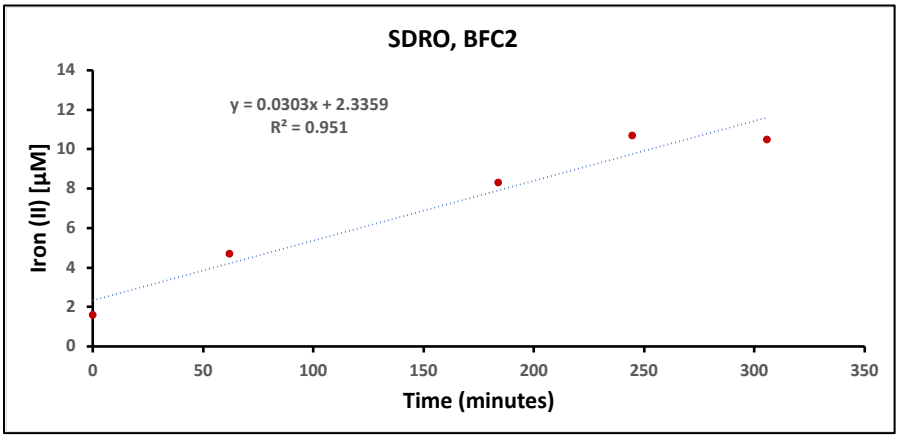


**Figure S1.** Continued.

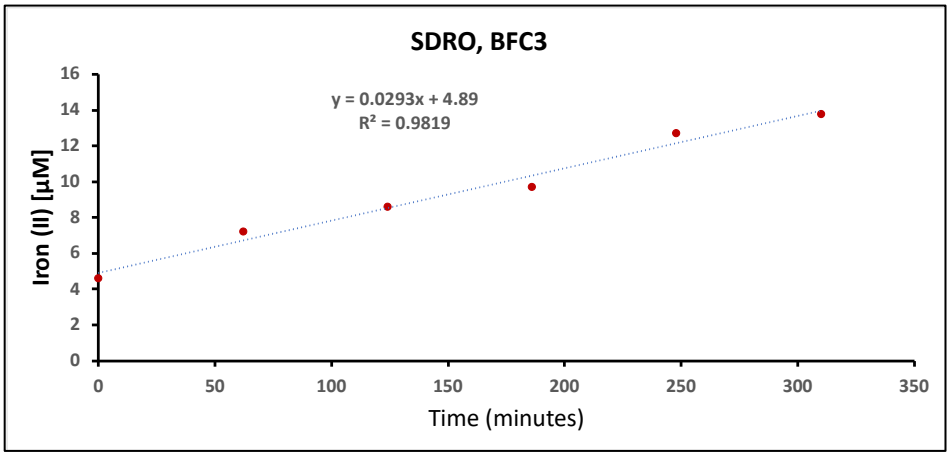


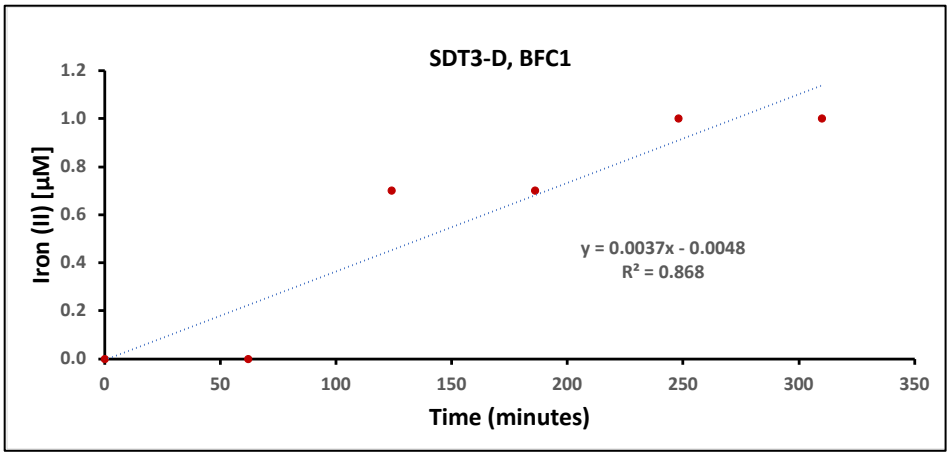


**Figure S1.** Continued.

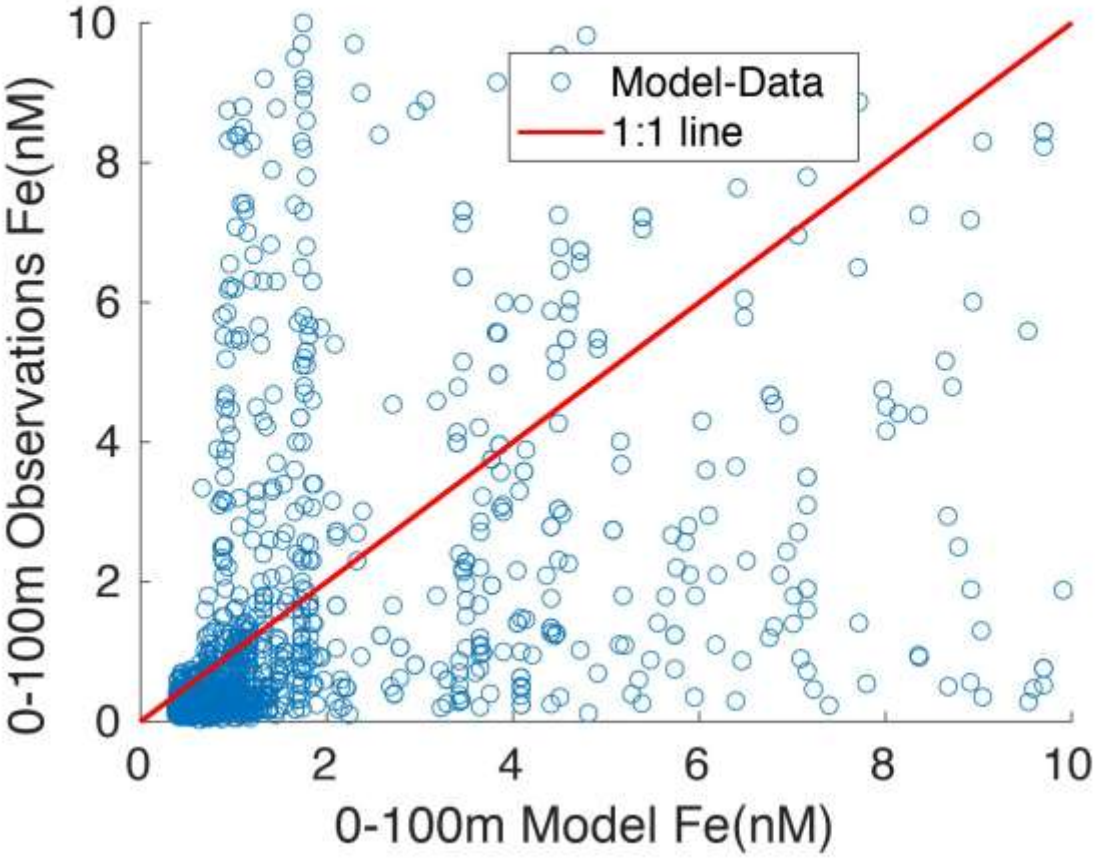


**Figure S2- 2.** Scatter plot for the dissolved iron concentrations in the upper 100 m of the ocean from field measurements along the US West Coast (y-axis) and from the ROMS-BEC model, where we have field measurements (x-axis). Model data are sampled seasonally according to field measurements. R = 0.5

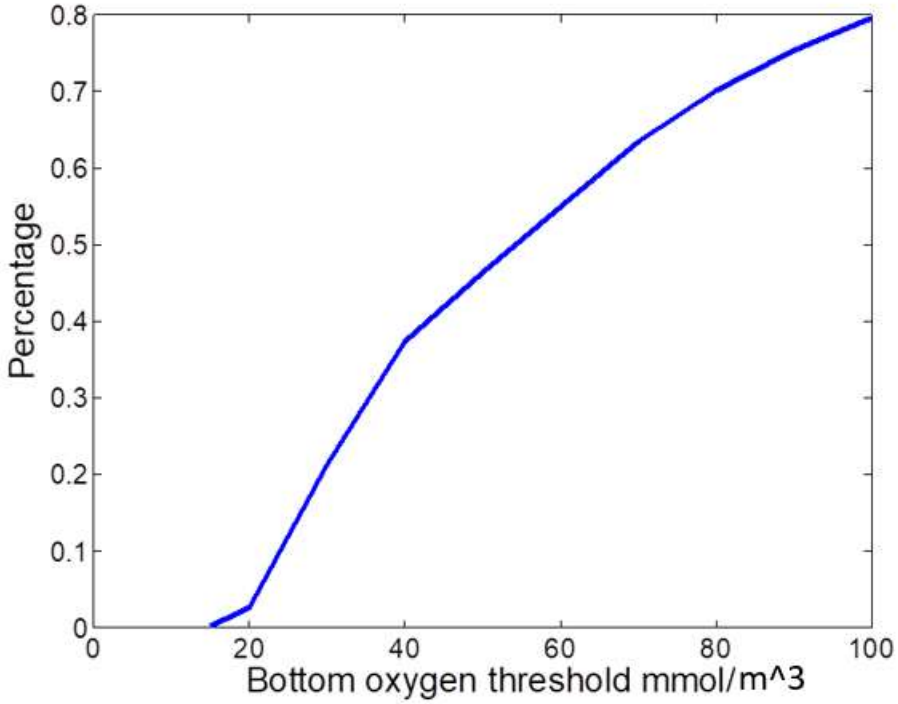


**Figure S2- 3.** Modeled Oxygen concentration throughout the domain where 80 percent of the oxygen concentration is between 20 to 100 µM.

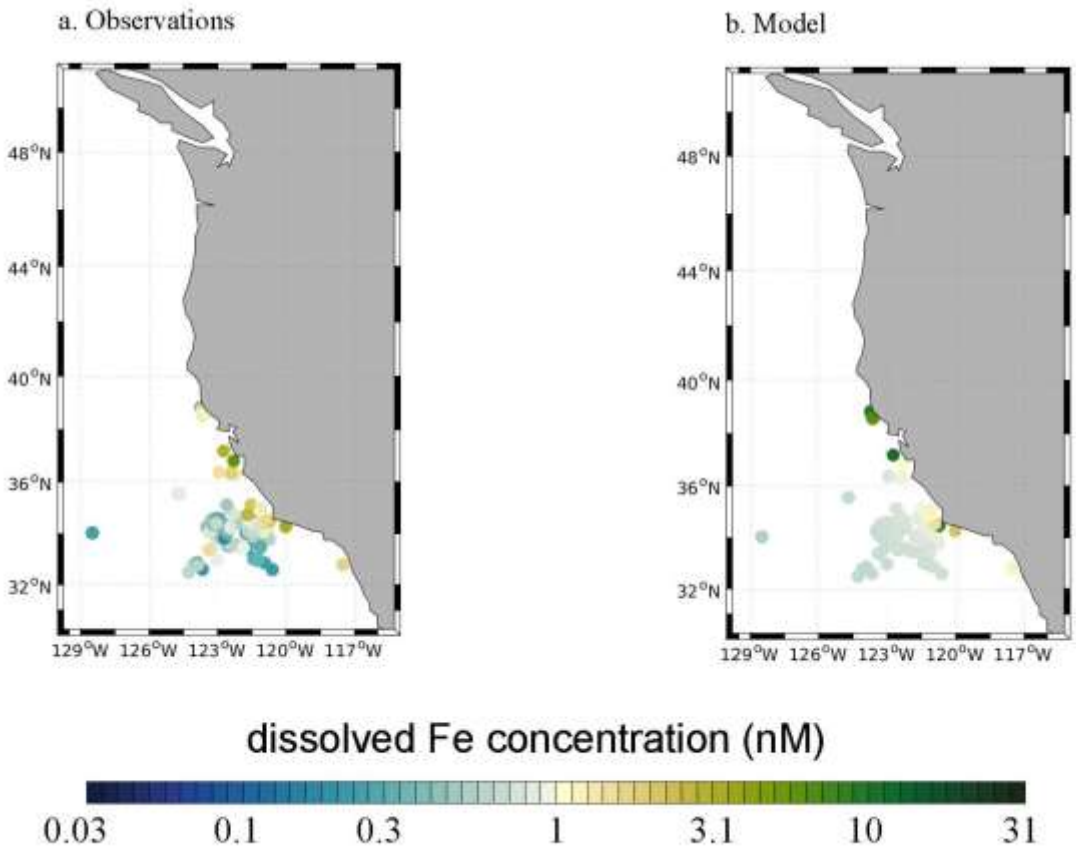


**Figure S2- 4.** Dissolved iron (dFe) concentrations averaged between 100-200 m: (a) measured data (see manuscript section 2.4), (b) model results.

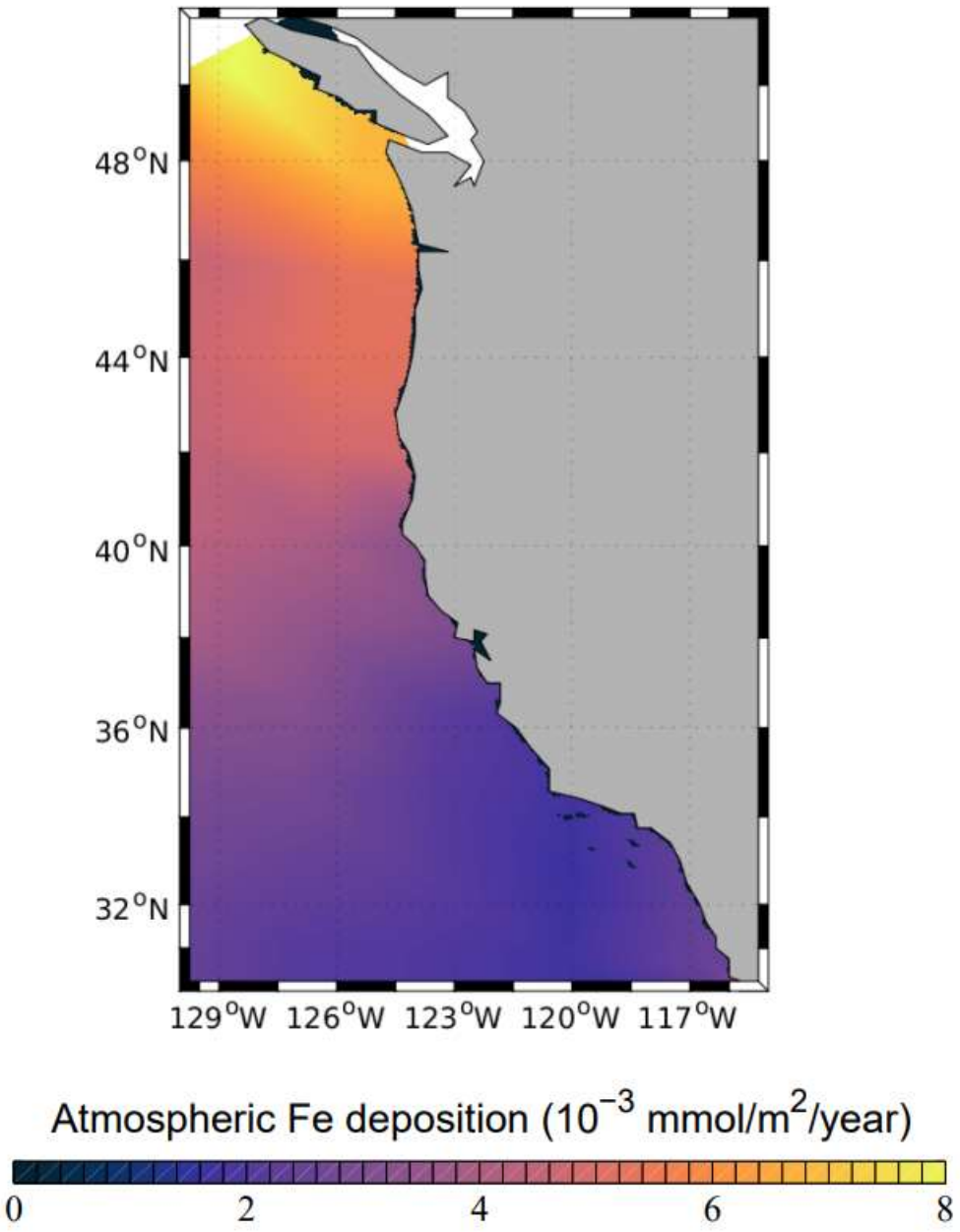


**Figure S2- 5.** Atmospheric dFe deposition into the surface ocean of the CCS (32-48N). Higher atmospheric dFe deposition is observed north of 42°N.

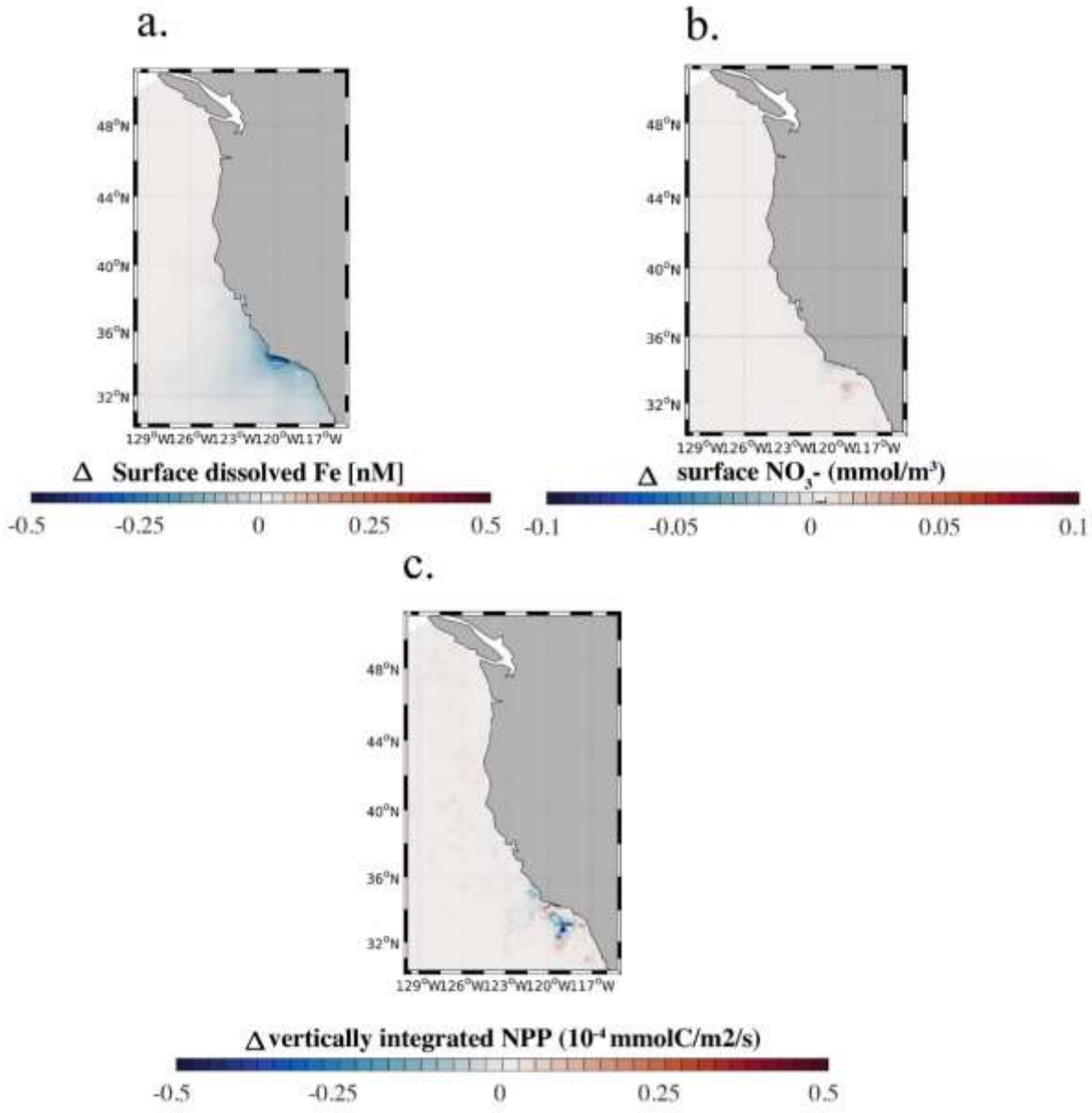


**Figure S2- 6.** (a) Surface dFe anomalies, (b) Surface $NO_3^-$ anomalies, and (c) vertically integrated net primary production (NPP) in the full domain from the Hypoxia-off model run relative to the High flux model run.

## Reference

Aller, R. C., Dwyer, I. P., Perger, D. A. S., Heilbrun, C., Volkenborn, N., and Wehrmann, L. M.: Estimating benthic Fe and reactive solute fluxes, Mar. Chem., 249, 104221, https://doi.org/10.1016/j.marchem.2023.104221, 2023.

Andrews, O. D., Bindoff, N. L., Halloran, P. R., Ilyina, T., and Le Quéré, C.: Detecting an external influence on recent changes in oceanic oxygen using an optimal fingerprinting method, Biogeosciences, 10, 1799–1813, https://doi.org/10.5194/bg-10-1799-2013, 2013.

Aumont, O., Ethé, C., Tagliabue, A., Bopp, L., and Gehlen, M.: PISCES-v2: an ocean biogeochemical model for carbon and ecosystem studies, Geosci. Model Dev., 8, 2465–2513, https://doi.org/10.5194/gmd-8-2465-2015, 2015.

Barbeau, K.: Photochemistry of Organic Iron(III) Complexing Ligands in Oceanic Systems, Photochem. Photobiol., 82, 1505–1516, https://doi.org/10.1111/j.1751-1097.2006.tb09806.x, 2006.

Bates, N. R. and Johnson, R. J.: Acceleration of ocean warming, salinification, deoxygenation and acidification in the surface subtropical North Atlantic Ocean, Commun. Earth Environ., 1, 1–12, https://doi.org/10.1038/s43247-020-00030-5, 2020.

Behl, R. J. and Kennett, J. P.: Brief interstadial events in the Santa Barbara basin, NE Pacific, during the past 60 kyr, Nature, 379, 243–246, https://doi.org/10.1038/379243a0, 1996.

Berg, J. S., Ahmerkamp, S., Pjevac, P., Hausmann, B., Milucka, J., and Kuypers, M. M. M.: How low can they go? Aerobic respiration by microorganisms under apparent anoxia, FEMS Microbiol. Rev., 46, fuac006, https://doi.org/10.1093/femsre/fuac006, 2022.

Bernhard, J. M., Casciotti, K. L., McIlvin, M. R., Beaudoin, D. J., Visscher, P. T., and Edgcomb, V. P.: Potential importance of physiologically diverse benthic foraminifera in sedimentary nitrate storage and respiration, J. Geophys. Res. Biogeosciences, 117, https://doi.org/10.1029/2012JG001949, 2012.

Biller, D. V. and Bruland, K. W.: Sources and distributions of Mn, Fe, Co, Ni, Cu, Zn, and Cd relative to macronutrients along the central California coast during the spring and summer upwelling season, Mar. Chem., 155, 50–70, https://doi.org/10.1016/j.marchem.2013.06.003, 2013.

Biller, D. V., Coale, T. H., Till, R. C., Smith, G. J., and Bruland, K. W.: Coastal iron and nitrate distributions during the spring and summer upwelling season in the central California Current upwelling regime, Cont. Shelf Res., 66, 58–72, https://doi.org/10.1016/j.csr.2013.07.003, 2013.

Bograd, S. J., Schwing, F. B., Castro, C. G., and Timothy, D. A.: Bottom water renewal in the Santa Barbara Basin, J. Geophys. Res. Oceans, 107, 9-1-9–9, https://doi.org/10.1029/2001JC001291, 2002.

Bograd, S. J., Castro, C. G., Di Lorenzo, E., Palacios, D. M., Bailey, H., Gilly, W., and Chavez, F. P.: Oxygen declines and the shoaling of the hypoxic boundary in the California Current, Geophys. Res. Lett., 35, https://doi.org/10.1029/2008GL034185, 2008.

Bograd, S. J., Buil, M. P., Lorenzo, E. D., Castro, C. G., Schroeder, I. D., Goericke, R., Anderson, C. R., Benitez-Nelson, C., and Whitney, F. A.: Changes in source waters to the Southern California Bight, Deep Sea Res. Part II Top. Stud. Oceanogr., 112, 42–52, https://doi.org/10.1016/j.dsr2.2014.04.009, 2015.

Boiteau, R. M., Till, C. P., Coale, T. H., Fitzsimmons, J. N., Bruland, K. W., and Repeta, D. J.: Patterns of iron and siderophore distributions across the California Current System, Limnol. Oceanogr., 64, 376–389, https://doi.org/10.1002/lno.11046, 2019.

Bopp, L., Resplandy, L., Orr, J. C., Doney, S. C., Dunne, J. P., Gehlen, M., Halloran, P., Heinze, C., Ilyina, T., Séférian, R., Tjiputra, J., and Vichi, M.: Multiple stressors of ocean ecosystems in the 21st century: projections with CMIP5 models, Biogeosciences, 10, 6225–6245, https://doi.org/10.5194/bg-10-6225-2013, 2013.

Brander, K., Cochrane, K., Barange, M., and Soto, D.: Climate Change Implications for Fisheries and Aquaculture, in: Climate Change Impacts on Fisheries and Aquaculture, edited by: Phillips, B. F. and Pérez-Ramírez, M., John Wiley & Sons, Ltd, Chichester, UK, 45–62, https://doi.org/10.1002/9781119154051.ch3, 2017.

Bray, N. A., Keyes, A., and Morawitz, W. M. L.: The California Current system in the Southern California Bight and the Santa Barbara Channel, J. Geophys. Res. Oceans, 104, 7695–7714, https://doi.org/10.1029/1998JC900038, 1999.

Breitburg, D., Levin, L. A., Oschlies, A., Grégoire, M., Chavez, F. P., Conley, D. J., Garçon, V., Gilbert, D., Gutiérrez, D., Isensee, K., Jacinto, G. S., Limburg, K. E., Montes, I., Naqvi, S. W. A., Pitcher, G. C., Rabalais, N. N., Roman, M. R., Rose, K. A., Seibel, B. A., Telszewski, M., Yasuhara, M., and Zhang, J.: Declining oxygen in the global ocean and coastal waters, Science, 359, eaam7240, https://doi.org/10.1126/science.aam7240, 2018.

Bruland, K. W., Rue, E. L., and Smith, G. J.: Iron and macronutrients in California coastal upwelling regimes: Implications for diatom blooms, Limnol. Oceanogr., 46, 1661–1674, https://doi.org/10.4319/lo.2001.46.7.1661, 2001.

Bruland, K. W., Middag, R., and Lohan, M. C.: Controls of Trace Metals in Seawater, in: Treatise on Geochemistry, Elsevier, 19–51, https://doi.org/10.1016/B978-0-08-095975-7.00602-1, 2014.

Bundy, R. M., Biller, D. V., Buck, K. N., Bruland, K. W., and Barbeau, K. A.: Distinct pools of dissolved iron-binding ligands in the surface and benthic boundary layer of the California Current, Limnol. Oceanogr., 59, 769–787, https://doi.org/10.4319/lo.2014.59.3.0769, 2014.

Bundy, R. M., Abdulla, H. A. N., Hatcher, P. G., Biller, D. V., Buck, K. N., and Barbeau, K. A.: Iron-binding ligands and humic substances in the San Francisco Bay estuary and estuarine-

influenced shelf regions of coastal California, Mar. Chem., 173, 183–194, https://doi.org/10.1016/j.marchem.2014.11.005, 2015.

Bundy, R. M., Jiang, M., Carter, M., and Barbeau, K. A.: Iron-Binding Ligands in the Southern California Current System: Mechanistic Studies, Front. Mar. Sci., 3, https://doi.org/10.3389/fmars.2016.00027, 2016.

Canfield, D. E. and Kraft, B.: The 'oxygen' in oxygen minimum zones, Environ. Microbiol., 24, 5332–5344, https://doi.org/10.1111/1462-2920.16192, 2022.

Capet, X., Campos, E. J., and Paiva, A. M.: Submesoscale activity over the Argentinian shelf, Geophys. Res. Lett., 35, https://doi.org/10.1029/2008GL034736, 2008.

Carr, M.-E. and Kearns, E. J.: Production regimes in four Eastern Boundary Current systems, Deep Sea Res. Part II Top. Stud. Oceanogr., 50, 3199–3221, https://doi.org/10.1016/j.dsr2.2003.07.015, 2003.

Chanton, J. P., Martens, C. S., and Goldhaber, M. B.: Biogeochemical cycling in an organic-rich coastal marine basin. 7. Sulfur mass balance, oxygen uptake and sulfide retention, Geochim. Cosmochim. Acta, 51, 1187–1199, https://doi.org/10.1016/0016-7037(87)90211-0, 1987.

Chappell, P., Armbrust, E., Barbeau, K., Bundy, R., Moffett, J., Vedamati, J., and Jenkins, B.: Patterns of diatom diversity correlate with dissolved trace metal concentrations and longitudinal position in the northeast Pacific coastal-offshore transition zone, Mar. Ecol. Prog. Ser., 609, 69–86, https://doi.org/10.3354/meps12810, 2019.

Chase, Z.: Iron, nutrient, and phytoplankton distributions in Oregon coastal waters, J. Geophys. Res., 107, 3174, https://doi.org/10.1029/2001JC000987, 2002.

Chase, Z., Johnson, K. S., Elrod, V. A., Plant, J. N., Fitzwater, S. E., Pickell, L., and Sakamoto, C. M.: Manganese and iron distributions off central California influenced by upwelling and shelf width, Mar. Chem., 95, 235–254, https://doi.org/10.1016/j.marchem.2004.09.006, 2005.

Chavez, F. P. and Messié, M.: A comparison of Eastern Boundary Upwelling Ecosystems, Prog. Oceanogr., 83, 80–96, https://doi.org/10.1016/j.pocean.2009.07.032, 2009.

Checkley, D. M. and Barth, J. A.: Patterns and processes in the California Current System, Prog. Oceanogr., 83, 49–64, https://doi.org/10.1016/j.pocean.2009.07.028, 2009.

Chhak, K. and Di Lorenzo, E.: Decadal variations in the California Current upwelling cells, Geophys. Res. Lett., 34, https://doi.org/10.1029/2007GL030203, 2007.

Conley, D. J., Carstensen, J., Aigars, J., Axe, P., Bonsdorff, E., Eremina, T., Haahti, B.-M., Humborg, C., Jonsson, P., Kotta, J., Lännegren, C., Larsson, U., Maximov, A., Medina, M. R., Lysiak-Pastuszak, E., Remeikaité-Nikiené, N., Walve, J., Wilhelms, S., and Zillén, L.: Hypoxia is increasing in the coastal zone of the Baltic Sea, Environ. Sci. Technol., 45, 6777–6783, https://doi.org/10.1021/es201212r, 2011.

Craig, R. K.: The New United Nations High Seas Treaty: A Primer, Nat. Resour. Environ., 34, 48–50, 2020.

Dale, A. W., Nickelsen, L., Scholz, F., Hensen, C., Oschlies, A., and Wallmann, K.: A revised global estimate of dissolved iron fluxes from marine sediments: GLOBAL BENTHIC IRON FLUXES, Glob. Biogeochem. Cycles, 29, 691–707, https://doi.org/10.1002/2014GB005017, 2015.

Damien, P., Bianchi, D., McWilliams, J. C., Kessouri, F., Deutsch, C., Chen, R., and Renault, L.: Enhanced Biogeochemical Cycling Along the U.S. West Coast Shelf, Glob. Biogeochem. Cycles, 37, e2022GB007572, https://doi.org/10.1029/2022GB007572, 2023.

Deutsch, C., Sarmiento, J. L., Sigman, D. M., Gruber, N., and Dunne, J. P.: Spatial coupling of nitrogen inputs and losses in the ocean, Nature, 445, 163–167, https://doi.org/10.1038/nature05392, 2007.

Deutsch, C., Brix, H., Ito, T., Frenzel, H., and Thompson, L.: Climate-Forced Variability of Ocean Hypoxia, Science, 333, 336–339, https://doi.org/10.1126/science.1202422, 2011.

Deutsch, C., Frenzel, H., McWilliams, J. C., Renault, L., Kessouri, F., Howard, E., Liang, J.-H., Bianchi, D., and Yang, S.: Biogeochemical variability in the California Current System, Prog. Oceanogr., 196, 102565, https://doi.org/10.1016/j.pocean.2021.102565, 2021.

Dijkstra, N., Kraal, P., Kuypers, M. M. M., Schnetger, B., and Slomp, C. P.: Are Iron-Phosphate Minerals a Sink for Phosphorus in Anoxic Black Sea Sediments?, PLOS ONE, 9, e101139, https://doi.org/10.1371/journal.pone.0101139, 2014.

Ekau, W., Auel, H., Pörtner, H.-O., and Gilbert, D.: Impacts of hypoxia on the structure and processes in pelagic communities (zooplankton, macro-invertebrates and fish), Biogeosciences, 7, 1669–1699, https://doi.org/10.5194/bg-7-1669-2010, 2010.

Esther, J., Sukla, L. B., Pradhan, N., and Panda, S.: Fe (III) reduction strategies of dissimilatory iron reducing bacteria, Korean J. Chem. Eng., 32, 1–14, https://doi.org/10.1007/s11814-014-0286-x, 2015.

Evans, N., Schroeder, I. D., Pozo Buil, M., Jacox, M. G., and Bograd, S. J.: Drivers of Subsurface Deoxygenation in the Southern California Current System, Geophys. Res. Lett., 47, https://doi.org/10.1029/2020GL089274, 2020a.

Evans, N., Schroeder, I. D., Pozo Buil, M., Jacox, M. G., and Bograd, S. J.: Drivers of Subsurface Deoxygenation in the Southern California Current System, Geophys. Res. Lett., 47, e2020GL089274, https://doi.org/10.1029/2020GL089274, 2020b.

Fennel, K. and Testa, J. M.: Biogeochemical Controls on Coastal Hypoxia, Annu. Rev. Mar. Sci., 11, 105–130, https://doi.org/10.1146/annurev-marine-010318-095138, 2019.

Firme, G. F., Rue, E. L., Weeks, D. A., Bruland, K. W., and Hutchins, D. A.: Spatial and temporal variability in phytoplankton iron limitation along the California coast and consequences

for Si, N, and C biogeochemistry: SPATIAL AND TEMPORAL VARIABILITY IN PHYTOPLANKTON IRON, Glob. Biogeochem. Cycles, 17, https://doi.org/10.1029/2001GB001824, 2003.

Franco, A. C., Kim, H., Frenzel, H., Deutsch, C., Ianson, D., Sumaila, U. R., and Tortell, P. D.: Impact of warming and deoxygenation on the habitat distribution of Pacific halibut in the Northeast Pacific, Fish. Oceanogr., 31, 601–614, https://doi.org/10.1111/fog.12610, 2022.

Fuchsman, C. A., Devol, A. H., Chase, Z., Reimers, C. E., and Hales, B.: Benthic fluxes on the Oregon shelf, Estuar. Coast. Shelf Sci., 163, 156–166, https://doi.org/10.1016/j.ecss.2015.06.001, 2015.

Furrer, G. and Wehrli, B.: Biogeochemical processes at the sediment-water interface: measurements and modeling, Appl. Geochem., 8, 117–119, https://doi.org/10.1016/S0883-2927(09)80021-8, 1993.

García-Reyes, M. and Largier, J.: Observations of increased wind-driven coastal upwelling off central California, J. Geophys. Res., 115, C04011, https://doi.org/10.1029/2009JC005576, 2010.

Gledhill, M.: The organic complexation of iron in the marine environment: a review, Front. Microbiol., 3, https://doi.org/10.3389/fmicb.2012.00069, 2012.

Goericke, R., Bograd, S. J., and Grundle, D. S.: Denitrification and flushing of the Santa Barbara Basin bottom waters, Deep Sea Res. Part II Top. Stud. Oceanogr., 112, 53–60, https://doi.org/10.1016/j.dsr2.2014.07.012, 2015.

Grasshoff, K. and Ehrhardt, M.: Methods of seawater analysis, 3rd, completely rev. and extended ed. ed., Wiley-VCH, Weinheim, New York, xxxii, 600 pp., 1999.

Grégoire, M., Garçon, V., Garcia, H., Breitburg, D., Isensee, K., Oschlies, A., Telszewski, M., Barth, A., Bittig, H. C., Carstensen, J., Carval, T., Chai, F., Chavez, F., Conley, D., Coppola, L., Crowe, S., Currie, K., Dai, M., Deflandre, B., Dewitte, B., Diaz, R., Garcia-Robledo, E., Gilbert, D., Giorgetti, A., Glud, R., Gutierrez, D., Hosoda, S., Ishii, M., Jacinto, G., Langdon, C., Lauvset, S. K., Levin, L. A., Limburg, K. E., Mehrtens, H., Montes, I., Naqvi, W., Paulmier, A., Pfeil, B., Pitcher, G., Pouliquen, S., Rabalais, N., Rabouille, C., Recape, V., Roman, M., Rose, K., Rudnick, D., Rummer, J., Schmechtig, C., Schmidtko, S., Seibel, B., Slomp, C., Sumalia, U. R., Tanhua, T., Thierry, V., Uchida, H., Wanninkhof, R., and Yasuhara, M.: A Global Ocean Oxygen Database and Atlas for Assessing and Predicting Deoxygenation and Ocean Health in the Open and Coastal Ocean, Front. Mar. Sci., 8, 2021.

Hawco, N. J., Barone, B., Church, M. J., Babcock-Adams, L., Repeta, D. J., Wear, E. K., Foreman, R. K., Björkman, K. M., Bent, S., Van Mooy, B. A. S., Sheyn, U., DeLong, E. F., Acker, M., Kelly, R. L., Nelson, A., Ranieri, J., Clemente, T. M., Karl, D. M., and John, S. G.: Iron Depletion in the Deep Chlorophyll Maximum: Mesoscale Eddies as Natural Iron Fertilization Experiments, Glob. Biogeochem. Cycles, 35, https://doi.org/10.1029/2021GB007112, 2021.

Hendershott and Winant: Surface Circulation in the Santa Barbara Channel, Oceanography, 9, 114–121, https://doi.org/10.5670/oceanog.1996.14, 1996.

Hogle, S. L., Dupont, C. L., Hopkinson, B. M., King, A. L., Buck, K. N., Roe, K. L., Stuart, R. K., Allen, A. E., Mann, E. L., Johnson, Z. I., and Barbeau, K. A.: Pervasive iron limitation at subsurface chlorophyll maxima of the California Current, Proc. Natl. Acad. Sci., 115, 13300–13305, https://doi.org/10.1073/pnas.1813192115, 2018.

Homoky, W. B., Conway, T. M., John, S. G., König, D., Deng, F., Tagliabue, A., and Mills, R. A.: Iron colloids dominate sedimentary supply to the ocean interior, Proc. Natl. Acad. Sci., 118, e2016078118, https://doi.org/10.1073/pnas.2016078118, 2021.

Huang, J., Jones, A., Waite, T. D., Chen, Y., Huang, X., Rosso, K. M., Kappler, A., Mansor, M., Tratnyek, P. G., and Zhang, H.: Fe(II) Redox Chemistry in the Environment, Chem. Rev., 121, 8161–8233, https://doi.org/10.1021/acs.chemrev.0c01286, 2021.

Jensen, L. T., Morton, P., Twining, B. S., Heller, M. I., Hatta, M., Measures, C. I., John, S., Zhang, R., Pinedo-Gonzalez, P., Sherrell, R. M., and Fitzsimmons, J. N.: A comparison of marine Fe and Mn cycling: U.S. GEOTRACES GN01 Western Arctic case study, Geochim. Cosmochim. Acta, 288, 138–160, https://doi.org/10.1016/j.gca.2020.08.006, 2020.

John, S. G., Mendez, J., Moffett, J., and Adkins, J.: The flux of iron and iron isotopes from San Pedro Basin sediments, Geochim. Cosmochim. Acta, 93, 14–29, https://doi.org/10.1016/j.gca.2012.06.003, 2012.

Johnson, K. S., Elrod, V. A., Fitzwater, S. E., Plant, J. N., Chavez, F. P., Tanner, S. J., Gordon, R. M., Westphal, D. L., Perry, K. D., Wu, J., and Karl, D. M.: Surface ocean-lower atmosphere interactions in the Northeast Pacific Ocean Gyre: Aerosols, iron, and the ecosystem response, Glob. Biogeochem. Cycles, 17, https://doi.org/10.1029/2002GB002004, 2003.

Jørgensen, B. B. and Nelson, D. C.: Sulfide oxidation in marine sediments: Geochemistry meets microbiology, in: Sulfur Biogeochemistry - Past and Present, Geological Society of America, https://doi.org/10.1130/0-8137-2379-5.63, 2004.

Kämpf, J. and Chapman, P.: The California Current Upwelling System, in: Upwelling Systems of the World: A Scientific Journey to the Most Productive Marine Ecosystems, edited by: Kämpf, J. and Chapman, P., Springer International Publishing, Cham, 97–160, https://doi.org/10.1007/978-3-319-42524-5_4, 2016.

Kappler, A., Bryce, C., Mansor, M., Lueder, U., Byrne, J. M., and Swanner, E. D.: An evolving view on biogeochemical cycling of iron, Nat. Rev. Microbiol., 19, 360–374, https://doi.org/10.1038/s41579-020-00502-7, 2021.

Keeling, R. F., Körtzinger, A., and Gruber, N.: Ocean Deoxygenation in a Warming World, Annu. Rev. Mar. Sci., 2, 199–229, https://doi.org/10.1146/annurev.marine.010908.163855, 2010.

Kessouri, F., Bianchi, D., Renault, L., McWilliams, J. C., Frenzel, H., and Deutsch, C. A.: Submesoscale Currents Modulate the Seasonal Cycle of Nutrients and Productivity in the

California Current System, Glob. Biogeochem. Cycles, 34, e2020GB006578, https://doi.org/10.1029/2020GB006578, 2020.

King, A. L. and Barbeau, K. A.: Dissolved iron and macronutrient distributions in the southern California Current System, J. Geophys. Res., 116, C03018, https://doi.org/10.1029/2010JC006324, 2011.

Kononets, M., Tengberg, A., Nilsson, M., Ekeroth, N., Hylén, A., Robertson, E. K., van de Velde, S., Bonaglia, S., Rütting, T., Blomqvist, S., and Hall, P. O. J.: In situ incubations with the Gothenburg benthic chamber landers: Applications and quality control, J. Mar. Syst., 214, 103475, https://doi.org/10.1016/j.jmarsys.2020.103475, 2021.

Kwiatkowski, L., Torres, O., Bopp, L., Aumont, O., Chamberlain, M., Christian, J. R., Dunne, J. P., Gehlen, M., Ilyina, T., John, J. G., Lenton, A., Li, H., Lovenduski, N. S., Orr, J. C., Palmieri, J., Santana-Falcón, Y., Schwinger, J., Séférian, R., Stock, C. A., Tagliabue, A., Takano, Y., Tjiputra, J., Toyama, K., Tsujino, H., Watanabe, M., Yamamoto, A., Yool, A., and Ziehn, T.: Twenty-first century ocean warming, acidification, deoxygenation, and upper-ocean nutrient and primary production decline from CMIP6 model projections, Biogeosciences, 17, 3439–3470, https://doi.org/10.5194/bg-17-3439-2020, 2020.

Laufkötter, C., John, J. G., Stock, C. A., and Dunne, J. P.: Temperature and oxygen dependence of the remineralization of organic matter, Glob. Biogeochem. Cycles, 31, 1038–1050, https://doi.org/10.1002/2017GB005643, 2017.

Levin, L. A. and Breitburg, D. L.: Linking coasts and seas to address ocean deoxygenation, Nat. Clim. Change, 5, 401–403, https://doi.org/10.1038/nclimate2595, 2015.

Llapapasca, M. A., Pardo, M. A., Grados, D., and Quiñones, J.: The oxygen minimum zone relative depth is a key driver of dolphin habitats in the northern Humboldt Current System, Front. Mar. Sci., 9, 2022.

Long, A. M., Jurgensen, S. K., Petchel, A. R., Savoie, E. R., and Brum, J. R.: Microbial Ecology of Oxygen Minimum Zones Amidst Ocean Deoxygenation, Front. Microbiol., 12, 748961, https://doi.org/10.3389/fmicb.2021.748961, 2021.

Lueder, U., Barker Jørgensen, B., Kappler, A., and Schmidt, C.: Photochemistry of iron in aquatic environments, Environ. Sci. Process. Impacts, 22, 12–24, https://doi.org/10.1039/C9EM00415G, 2020.

Mahowald, N. M., Muhs, D. R., Levis, S., Rasch, P. J., Yoshioka, M., Zender, C. S., and Luo, C.: Change in atmospheric mineral aerosols in response to climate: Last glacial period, preindustrial, modern, and doubled carbon dioxide climates: DUST RESPONSE TO CLIMATE, J. Geophys. Res. Atmospheres, 111, n/a-n/a, https://doi.org/10.1029/2005JD006653, 2006.

McCormick, L. R. and Levin, L. A.: Physiological and ecological implications of ocean deoxygenation for vision in marine organisms, Philos. Transact. A Math. Phys. Eng. Sci., 375, 20160322, https://doi.org/10.1098/rsta.2016.0322, 2017.

McMahon, P. B. and Chapelle, F. H.: Microbial production of organic acids in aquitard sediments and its role in aquifer geochemistry, Nature, 349, 233–235, https://doi.org/10.1038/349233a0, 1991.

Melton, E. D., Swanner, E. D., Behrens, S., Schmidt, C., and Kappler, A.: The interplay of microbially mediated and abiotic reactions in the biogeochemical Fe cycle, Nat. Rev. Microbiol., 12, 797–808, https://doi.org/10.1038/nrmicro3347, 2014.

Middelburg, J. J. and Levin, L. A.: Coastal hypoxia and sediment biogeochemistry, Biogeosciences, 6, 1273–1293, https://doi.org/10.5194/bg-6-1273-2009, 2009a.

Middelburg, J. J. and Levin, L. A.: Coastal hypoxia and sediment biogeochemistry, 1273–1293, 2009b.

Mills, M. M., Ridame, C., Davey, M., La Roche, J., and Geider, R. J.: Iron and phosphorus co-limit nitrogen fixation in the eastern tropical North Atlantic, Nature, 429, 292–294, https://doi.org/10.1038/nature02550, 2004.

Moore, J. K. and Braucher, O.: Sedimentary and mineral dust sources of dissolved iron to the world ocean, Biogeosciences, 5, 631–656, https://doi.org/10.5194/bg-5-631, 2008.

Moore, J. K., Doney, S. C., Kleypas, J. A., Glover, D. M., and Fung, I. Y.: An intermediate complexity marine ecosystem model for the global domain, Deep Sea Res. Part II Top. Stud. Oceanogr., 49, 403–462, https://doi.org/10.1016/S0967-0645(01)00108-4, 2001.

Moore, J. K., Doney, S. C., and Lindsay, K.: Upper ocean ecosystem dynamics and iron cycling in a global three-dimensional model: GLOBAL ECOSYSTEM-BIOGEOCHEMICAL MODEL, Glob. Biogeochem. Cycles, 18, n/a-n/a, https://doi.org/10.1029/2004GB002220, 2004.

Morée, A. L., Clarke, T. M., Cheung, W. W. L., and Frölicher, T. L.: Impact of deoxygenation and warming on global marine species in the 21st century, Biogeosciences, 20, 2425–2454, https://doi.org/10.5194/bg-20-2425-2023, 2023.

Moreno, A. R., Anderson, C., Kudela, R. M., Sutula, M., Edwards, C., and Bianchi, D.: Development, calibration, and evaluation of a model of *Pseudo-nitzschia* and domoic acid production for regional ocean modeling studies, Harmful Algae, 118, 102296, https://doi.org/10.1016/j.hal.2022.102296, 2022.

Morgan, B. and Lahav, O.: The effect of pH on the kinetics of spontaneous Fe(II) oxidation by O2 in aqueous solution – basic principles and a simple heuristic description, Chemosphere, 68, 2080–2084, https://doi.org/10.1016/j.chemosphere.2007.02.015, 2007.

Morison, J., Kwok, R., Peralta-Ferriz, C., Alkire, M., Rigor, I., Andersen, R., and Steele, M.: Changing Arctic Ocean freshwater pathways, Nature, 481, 66–70, https://doi.org/10.1038/nature10705, 2012.

Myhre, S. E., Pak, D., Borreggine, M., Kennett, J. P., Nicholson, C., Hill, T. M., and Deutsch, C.: Oxygen minimum zone biotic baseline transects for paleoceanographic reconstructions in

Santa Barbara Basin, CA, Deep Sea Res. Part II Top. Stud. Oceanogr., 150, 118–131, https://doi.org/10.1016/j.dsr2.2017.12.009, 2018.

Noffke, A., Hensen, C., Sommer, S., Scholz, F., Bohlen, L., Mosch, T., Graco, M., and Wallmann, K.: Benthic iron and phosphorus fluxes across the Peruvian oxygen minimum zone, Limnol. Oceanogr., 57, 851–867, https://doi.org/10.4319/lo.2012.57.3.0851, 2012.

Oschlies, A., Brandt, P., Stramma, L., and Schmidtko, S.: Drivers and mechanisms of ocean deoxygenation, Nat. Geosci., 11, 467–473, https://doi.org/10.1038/s41561-018-0152-2, 2018.

Pham, A. L. D. and Ito, T.: Formation and Maintenance of the GEOTRACES Subsurface-Dissolved Iron Maxima in an Ocean Biogeochemistry Model, Glob. Biogeochem. Cycles, 32, 932–953, https://doi.org/10.1029/2017GB005852, 2018.

Pham, A. L. D. and Ito, T.: Ligand Binding Strength Explains the Distribution of Iron in the North Atlantic Ocean, Geophys. Res. Lett., 46, 7500–7508, https://doi.org/10.1029/2019GL083319, 2019.

Pitcher, G. C., Aguirre-Velarde, A., Breitburg, D., Cardich, J., Carstensen, J., Conley, D. J., Dewitte, B., Engel, A., Espinoza-Morriberón, D., Flores, G., Garçon, V., Graco, M., Grégoire, M., Gutiérrez, D., Hernandez-Ayon, J. M., Huang, H.-H. M., Isensee, K., Jacinto, M. E., Levin, L., Lorenzo, A., Machu, E., Merma, L., Montes, I., Swa, N., Paulmier, A., Roman, M., Rose, K., Hood, R., Rabalais, N. N., Salvanes, A. G. V., Salvatteci, R., Sánchez, S., Sifeddine, A., Tall, A. W., Plas, A. K. van der, Yasuhara, M., Zhang, J., and Zhu, Z.: System controls of coastal and open ocean oxygen depletion, Prog. Oceanogr., 197, 102613, https://doi.org/10.1016/j.pocean.2021.102613, 2021.

Pozo Buil, M. and Di Lorenzo, E.: Decadal dynamics and predictability of oxygen and subsurface tracers in the California Current System, Geophys. Res. Lett., 44, 4204–4213, https://doi.org/10.1002/2017GL072931, 2017.

Qin, Q., Kinnaman, F. S., Gosselin, K. M., Liu, N., Treude, T., and Valentine, D. L.: Seasonality of water column methane oxidation and deoxygenation in a dynamic marine environment, Geochim. Cosmochim. Acta, 336, 219–230, https://doi.org/10.1016/j.gca.2022.09.017, 2022.

Reimers, C. E., Lange, C. B., Tabak, M., and Bernhard, J. M.: Seasonal spillover and varve formation in the Santa Barbara Basin, California, Limnol. Oceanogr., 35, 1577–1585, https://doi.org/10.4319/lo.1990.35.7.1577, 1990.

Reissmann, J. H., Burchard, H., Feistel, R., Hagen, E., Lass, H. U., Mohrholz, V., Nausch, G., Umlauf, L., and Wieczorek, G.: Vertical mixing in the Baltic Sea and consequences for eutrophication – A review, Prog. Oceanogr., 82, 47–80, https://doi.org/10.1016/j.pocean.2007.10.004, 2009.

Renault, L., Deutsch, C., McWilliams, J. C., Frenzel, H., Liang, J.-H., and Colas, F.: Partial decoupling of primary productivity from upwelling in the California Current system, Nat. Geosci., 9, 505–508, https://doi.org/10.1038/ngeo2722, 2016.

Renault, L., McWilliams, J. C., Kessouri, F., Jousse, A., Frenzel, H., Chen, R., and Deutsch, C.: Evaluation of high-resolution atmospheric and oceanic simulations of the California Current System, Prog. Oceanogr., 195, 102564, https://doi.org/10.1016/j.pocean.2021.102564, 2021.

Robinson, C.: Microbial Respiration, the Engine of Ocean Deoxygenation, Front. Mar. Sci., 5, 2019.

Robinson, D., Pham, A. L. D., Yousavich, D. J., Janssen, F., Wenzhöfer, F., Arrington, E. C., Gosselin, K. M., Sandoval-Belmar, M., Mar, M., Valentine, D. L., Bianchi, D., and Treude, T.: Iron “Ore” Nothing: Benthic iron fluxes from the oxygen-deficient Santa Barbara Basin enhance phytoplankton productivity in surface waters, Biogeosciences Discuss., 1–36, https://doi.org/10.5194/bg-2022-237, 2022.

Sánchez-Velasco, L., Godínez, V. M., Ruvalcaba-Aroche, E. D., Márquez-Artavia, A., Beier, E., Barton, E. D., and Jiménez-Rosenberg, S. P. A.: Larval Fish Habitats and Deoxygenation in the Northern Limit of the Oxygen Minimum Zone off Mexico, J. Geophys. Res. Oceans, 124, 9690–9705, https://doi.org/10.1029/2019JC015414, 2019.

Sañudo-Wilhelmy, S., Kustka, A., Gobler, C., Hutchins, D., Yang, M., Lwiza, K., Burns, J., Raven, J., and Carpenter, E.: Phosphorus limitation of nitrogen fixation by Trichodesmium in the central Atlantic Ocean, Nature, 411, 66–9, https://doi.org/10.1038/35075041, 2001.

Schmidtko, S., Stramma, L., and Visbeck, M.: Decline in global oceanic oxygen content during the past five decades, Nature, 542, 335–339, https://doi.org/10.1038/nature21399, 2017.

Severmann, S., McManus, J., Berelson, W. M., and Hammond, D. E.: The continental shelf benthic iron flux and its isotope composition, Geochim. Cosmochim. Acta, 74, 3984–4004, https://doi.org/10.1016/j.gca.2010.04.022, 2010a.

Severmann, S., McManus, J., Berelson, W. M., and Hammond, D. E.: The continental shelf benthic iron flux and its isotope composition, Geochim. Cosmochim. Acta, 74, 3984–4004, https://doi.org/10.1016/j.gca.2010.04.022, 2010b.

Shchepetkin, A. F.: An adaptive, Courant-number-dependent implicit scheme for vertical advection in oceanic modeling, Ocean Model., 91, 38–69, https://doi.org/10.1016/j.ocemod.2015.03.006, 2015.

Shchepetkin, A. F. and McWilliams, J. C.: The regional oceanic modeling system (ROMS): a split-explicit, free-surface, topography-following-coordinate oceanic model, Ocean Model., 9, 347–404, https://doi.org/10.1016/j.ocemod.2004.08.002, 2005.

Shepherd, J. G., Brewer, P. G., Oschlies, A., and Watson, A. J.: Ocean ventilation and deoxygenation in a warming world: introduction and overview, Philos. Trans. R. Soc. Math. Phys. Eng. Sci., 375, 20170240, https://doi.org/10.1098/rsta.2017.0240, 2017.

Shiller, A. M., Gieskes, J. M., and Brian Price, N.: Particulate iron and manganese in the Santa Barbara Basin, California, Geochim. Cosmochim. Acta, 49, 1239–1249, https://doi.org/10.1016/0016-7037(85)90013-4, 1985.

Sholkovitz, E. and Soutar, A.: Changes in the composition of the bottom water of the Santa Barbara Basin: effect of turbidity currents, Deep Sea Res. Oceanogr. Abstr., 22, 13–21, https://doi.org/10.1016/0011-7471(75)90014-5, 1975.

Sholkovitz, E. R. and Gieskes, J. M.: A PHYSICAL-CHEMICAL STUDY OF THE FLUSHING OF THE SANTA BARBARA BASIN1: FLUSHING OF THE SANTA BARBARA BASIN, Limnol. Oceanogr., 16, 479–489, https://doi.org/10.4319/lo.1971.16.3.0479, 1971.

Sigman, D. M., Robinson, R., Knapp, A. N., van Geen, A., McCorkle, D. C., Brandes, J. A., and Thunell, R. C.: Distinguishing between water column and sedimentary denitrification in the Santa Barbara Basin using the stable isotopes of nitrate, Geochem. Geophys. Geosystems, 4, https://doi.org/10.1029/2002GC000384, 2003.

Soetaert, K., Middelburg, J. J., Herman, P. M. J., and Buis, K.: On the coupling of benthic and pelagic biogeochemical models, Earth-Sci. Rev., 51, 173–201, https://doi.org/10.1016/S0012-8252(00)00004-0, 2000.

Sommer, S., Gier, J., Treude, T., Lomnitz, U., Dengler, M., Cardich, J., and Dale, A. W.: Depletion of oxygen, nitrate and nitrite in the Peruvian oxygen minimum zone cause an imbalance of benthic nitrogen fluxes, Deep Sea Res. Part Oceanogr. Res. Pap., 112, 113–122, https://doi.org/10.1016/j.dsr.2016.03.001, 2016.

Stramma, L., Schmidtko, S., Levin, L. A., and Johnson, G. C.: Ocean oxygen minima expansions and their biological impacts, Deep Sea Res. Part Oceanogr. Res. Pap., 57, 587–595, https://doi.org/10.1016/j.dsr.2010.01.005, 2010.

Stramma, L., Prince, E. D., Schmidtko, S., Luo, J., Hoolihan, J. P., Visbeck, M., Wallace, D. W. R., Brandt, P., and Körtzinger, A.: Expansion of oxygen minimum zones may reduce available habitat for tropical pelagic fishes, Nat. Clim. Change, 2, 33–37, https://doi.org/10.1038/nclimate1304, 2012.

Tagliabue, A., Sallée, J.-B., Bowie, A. R., Lévy, M., Swart, S., and Boyd, P. W.: Surface-water iron supplies in the Southern Ocean sustained by deep winter mixing, Nat. Geosci., 7, 314–320, https://doi.org/10.1038/ngeo2101, 2014.

Tagliabue, A., Aumont, O., DeAth, R., Dunne, J. P., Dutkiewicz, S., Galbraith, E., Misumi, K., Moore, J. K., Ridgwell, A., Sherman, E., Stock, C., Vichi, M., Völker, C., and Yool, A.: How well do global ocean biogeochemistry models simulate dissolved iron distributions?: GLOBAL IRON MODELS, Glob. Biogeochem. Cycles, 30, 149–174, https://doi.org/10.1002/2015GB005289, 2016.

Tagliabue, A., Bowie, A. R., Boyd, P. W., Buck, K. N., Johnson, K. S., and Saito, M. A.: The integral role of iron in ocean biogeochemistry, Nature, 543, 51–59, https://doi.org/10.1038/nature21058, 2017.

Testa, J. M., Brady, D. C., Di Toro, D. M., Boynton, W. R., Cornwell, J. C., and Kemp, W. M.: Sediment flux modeling: Simulating nitrogen, phosphorus, and silica cycles, Estuar. Coast. Shelf Sci., 131, 245–263, https://doi.org/10.1016/j.ecss.2013.06.014, 2013.

Tiano, L., Garcia-Robledo, E., Dalsgaard, T., Devol, A. H., Ward, B. B., Ulloa, O., Canfield, D. E., and Peter Revsbech, N.: Oxygen distribution and aerobic respiration in the north and south eastern tropical Pacific oxygen minimum zones, Deep Sea Res. Part Oceanogr. Res. Pap., 94, 173–183, https://doi.org/10.1016/j.dsr.2014.10.001, 2014.

Till, C. P., Solomon, J. R., Cohen, N. R., Lampe, R. H., Marchetti, A., Coale, T. H., and Bruland, K. W.: The iron limitation mosaic in the California Current System: Factors governing Fe availability in the shelf/near-shelf region, Limnol. Oceanogr., 64, 109–123, https://doi.org/10.1002/lno.11022, 2019.

Treude, T., Smith, C. R., Wenzhöfer, F., Carney, E., Bernardino, A. F., Hannides, A. K., Krüger, M., and Boetius, A.: Biogeochemistry of a deep-sea whale fall: sulfate reduction, sulfide efflux and methanogenesis, Mar. Ecol. Prog. Ser., 382, 1–21, 2009.

Treude, T., Hamdan, L. J., Lemieux, S., Dale, A. W., and Sommer, S.: Rapid sulfur cycling in sediments from the Peruvian oxygen minimum zone featuring simultaneous sulfate reduction and sulfide oxidation, Limnol. Oceanogr., 66, 2661–2671, https://doi.org/10.1002/lno.11779, 2021.

Ulloa, O., Canfield, D. E., DeLong, E. F., Letelier, R. M., and Stewart, F. J.: Microbial oceanography of anoxic oxygen minimum zones, Proc. Natl. Acad. Sci. U. S. A., 109, 15996–16003, https://doi.org/10.1073/pnas.1205009109, 2012.

Valentine, D. L., Fisher, G. B., Pizarro, O., Kaiser, C. L., Yoerger, D., Breier, J. A., and Tarn, J.: Autonomous Marine Robotic Technology Reveals an Expansive Benthic Bacterial Community Relevant to Regional Nitrogen Biogeochemistry, Environ. Sci. Technol., 50, 11057–11065, https://doi.org/10.1021/acs.est.6b03584, 2016.

Wallmann, K., José, Y. S., Hopwood, M. J., Somes, C. J., Dale, A. W., Scholz, F., Achterberg, E. P., and Oschlies, A.: Biogeochemical feedbacks may amplify ongoing and future ocean deoxygenation: a case study from the Peruvian oxygen minimum zone, Biogeochemistry, 159, 45–67, https://doi.org/10.1007/s10533-022-00908-w, 2022.

White, M. E., Rafter, P. A., Stephens, B. M., Wankel, S. D., and Aluwihare, L. I.: Recent Increases in Water Column Denitrification in the Seasonally Suboxic Bottom Waters of the Santa Barbara Basin, Geophys. Res. Lett., 46, 6786–6795, https://doi.org/10.1029/2019GL082075, 2019.

Widdows, J. and Brinsley, M.: Impact of biotic and abiotic processes on sediment dynamics and the consequences to the structure and functioning of the intertidal zone, J. Sea Res., 48, 143–156, https://doi.org/10.1016/S1385-1101(02)00148-X, 2002.

Yamamoto, A., Hajima, T., Yamazaki, D., Noguchi Aita, M., Ito, A., and Kawamiya, M.: Competing and accelerating effects of anthropogenic nutrient inputs on climate-driven changes in ocean carbon and oxygen cycles, Sci. Adv., 8, eabl9207, https://doi.org/10.1126/sciadv.abl9207, 2022.

Yao, M., Henny, C., and Maresca, J. A.: Freshwater Bacteria Release Methane as a By-Product of Phosphorus Acquisition, Appl. Environ. Microbiol., 82, 6994–7003, https://doi.org/10.1128/AEM.02399-16, 2016.

Yousavich, D. J., Robinson, D., Peng, X., Krause, S. J. E., Wenzhoefer, F., Janßen, F., Liu, N., Tarn, J., Kinnaman, F., Valentine, D. L., and Treude, T.: Marine anoxia initiates giant sulfur-bacteria mat proliferation and associated changes in benthic nitrogen, sulfur, and iron cycling in the Santa Barbara Basin, California Borderland, EGUsphere, 1–48, https://doi.org/10.5194/egusphere-2023-1198, 2023.

Zhou, Y., Gong, H., and Zhou, F.: Responses of Horizontally Expanding Oceanic Oxygen Minimum Zones to Climate Change Based on Observations, Geophys. Res. Lett., 49, e2022GL097724, https://doi.org/10.1029/2022GL097724, 2022.

# Chapter 3: Spatial distribution and temporal variability of dissolved oxygen in the Santa Barbara Basin, California

**De'Marcus Robinson**[1*], Daniele Bianchi[1], Na Liu[3,4], David L. Valentine[3,4], Tina Treude [1,2]

[1]Department of Atmospheric and Oceanic Sciences, University of California Los Angeles, Los Angeles, CA, USA

[2]Department of Earth, Planetary, and Space Sciences, University of California Los Angeles, Los Angeles, CA, USA

[4]Department of Earth Science and Marine Science Institute, University of California, Santa Barbara, CA 93106, USA

[4]Interepartment Graduate Program in Marine Science, University of California, Santa Barbara, CA 93106, USA

**Abstract**

Dissolved oxygen has been declining along the coast and open ocean for decades, including within the Santa Barbara Chanel (SBC), a low-oxygen channel in the Southern California borderland. Declining oxygen in the SBC can be attributed to changes in surface and deep-water circulation, and intensification of seasonal coastal upwelling supporting high rates of primary productivity, subsurface remineralization and nutrient cycling. While numerous studies have investigated the influence of hypoxia and anoxia on nutrient cycling and microbial activity in the sediment, and water column of the SBC, studies that characterize the spatial distribution of dissolved oxygen in the channel, and its full temporal water column variability, remain limited. We explore the spatial extent and temporal variability of dissolved oxygen in the SBC, with the goal of increasing our understanding of oxygen dynamics and the consequences for ocean biogeochemistry. To this end, we integrated historical observations of dissolved oxygen from California Cooperative Oceanic Fisheries Investigation (CalCOFI) and other hydrographic programs, with two highly spatially resolved oxygen surveys from recent cruises (AT42-19/2019 and AT50-11/2023) that deployed the Autonomous Underwater Vehicle (AUV) Sentry and the Remotely Operated Vehicle (ROV) Jason, equipped with oxygen sensors. This new data compilation provides the first spatially resolved characterization of dissolved oxygen across the SBC, and in the basin's bottom boundary layer. We reconstructed oxygen in the bottom boundary layer and applied this reconstruction to an updated Fe parametrization from new benthic flux measurements from the SBC. We estimate that the benthic Fe flux from the reconstructed bottom layer oxygen contributes to approximately 24,000 ton $y^{-1}$.

## Introduction

Dissolved oxygen is essential for aerobic respiration that influences the cycling of carbon, sulfur, iron, and nitrogen in the ocean (Wallmann et al., 2022; Chanton et al., 1987; Tiano et al., 2014). Dissolved oxygen concentrations have been declining along the coast and open ocean for decades (Keeling et al., 2010; Levin and Breitburg, 2015; Schmidtko et al., 2017; Stramma et al., 2010), with potentially negative consequences for marine ecosystems that can cause habitat compression and loss, increase stress on benthic and pelagic organisms, negatively affect local fisheries, and alter patterns of marine mammal migrations (Franco et al., 2022; Llapapasca et al., 2022; McCormick and Levin, 2017; Sánchez-Velasco et al., 2019; Shepherd et al., 2017; Stramma et al., 2012). The causes for oxygen decline, or deoxygenation, are multifaceted, and can be attributed to a combination of physical and biological changes associated with both natural and anthropogenic climate change (Oschlies et al., 2018).

The anthropogenic effect of climate change and carbon dioxide causes a progressive increase in ocean surface temperature (Keeling et al., 2010; Morée et al., 2023; Shepherd et al., 2017). The increase in ocean surface temperature causes a decrease in oxygen solubility and ventilation within the thermocline, while enhancing microbial respiration rates in the surface and subsurface. Simultaneously, the increase in anthropogenic carbon dioxide stimulates primary productivity causing an increase in organic matter production, due to the decay of phytoplankton, influencing increases in microbial respiration and a decline in dissolved oxygen (Berg et al., 2022; Laufkötter et al., 2017; Robinson, 2019; Shepherd et al., 2017; Yamamoto et al., 2022). Along continental shelves, the input in nutrients by freshwater run-off also increases primary production and phytoplankton blooms, and therefore increases subsurface microbial respiration causing a decline in dissolved oxygen (Robinson, 2019; Fennel and Testa, 2019). The intensification of

natural wind-driven upwelling along Eastern boundary upwelling systems and changes in ocean circulation, have contributed to the transport of oxygen-poor, nutrient-rich waters in both coastal and open-ocean (Chhak and Di Lorenzo, 2007; Evans et al., 2020; Pozo Buil and Di Lorenzo, 2017; Robinson, 2019). Both upwelling and changes in circulation can be associated with both multi-decadal natural variability and climate change (Bakun 1990; Rykacewski et al,.2023 ; Wang et al 2015

Eastern boundary upwelling system, such as the California Current System (CCS) along the West Coast of the United States, Mexico and Canada, are particularly susceptible to oxygen loss. In these regions, wind-driven coastal upwelling transports cold, salty, nutrient-rich water from deep ocean depths to the surface ocean (Checkley and Barth, 2009; García-Reyes and Largier, 2010). Along the CCS, coastal upwelling sustain high primary productivity and a diverse ecosystems (Checkley and Barth, 2009), but also undergoes oxygen loss. The loss of oxygen can create hypoxic conditions in the ocean from upwelling, fueling phytoplankton blooms that support high rates of microbial respiration consuming dissolving oxygen at depth. Additionally, hypoxic conditions in the CCS are sustained by transport of low-oxygen tropical waters by the poleward undercurrent, flowing between the surface and sub-surface along the continental shelf and slope (Evans et al., 2020).

Changes in upwelling patterns and deoxygenation in the CCS also impacts SBC and the deep basin (Bograd et al., 2002; Bray et al., 1999; Qin et al., 2022), one of fourteen sub-basins within the Southern California Borderland, located between the Channel Islands and the continental California coast. The SBC frequently experiences seasonal anoxia in the deep basin bottom waters during fall, with irregular flushing and re-oxygenation of dense, hypoxic water below the western sill depth (475 m), during winter and spring (Goericke et al., 2015; Sholkovitz

and Soutar, 1975; White et al., 2019). This seasonal flushing in the basin and channel reflect either change in upwelling strength and frequency, or change in stratification at the sill depth and deep circulation, although the exact cause of flushing events is still unclear (Goericke et al., 2015; Sholkovitz and Gieskes, 1971; White et al., 2019).

Previous studies have examined the influence of low oxygen on the cycle of nutrients in the SBC (Bograd et al., 2002; Bray et al., 1999; Goericke et al., 2015; Robinson et al., 2024; Yousavich et al., 2024). Hypoxic (< 65 μM) and anoxic ( 0 μM) conditions below the sill depth are associated with the decline of nitrate via denitrification, which occurs both in the water column and sediment, as well as benthic dissimilatory nitrate reduction to ammonium, caused in part by, large benthic sulfur-oxidizing bacteria and other benthic microorganisms (Bernhard et al., 2012; Goericke et al., 2015; Peng et al., 2023; Valentine et al., 2016a; White et al., 2019; Yousavich et al., 2024). Low oxygen concentrations (<65 μM ) in the bottom water of the SBC, stimulate the release of dissolved iron and other nutrients from the sediment (Robinson et al., 2024) due to the degradation of organic matter by benthic microbes, along with production and consumption of methane by methanogenesis and anaerobic methane oxidation, observed in the water column and deep sediment (Krause et al., 2023; Qin et al., 2022).

A record of the variability of hypoxia and anoxia between 1986-2020 in the bottom water of the SBC, shows evidence of a decline in flushing frequency, persistent oxygen depletion, reduction in nitrate concentrations, and complete nitrate deficiency (0 μM) events near the bottom in 2005, 2010, 2012, and 2013 (Goericke et al., 2015; Qin et al., 2022; Valentine et al., 2016a). Since 2000, the frequency of low oxygen (<0.5 μM) events outside the springtime upwelling season has increased significantly ($p<0.05$) below 520 m (Goericke et al., 2015). During springtime upwelling, when flushing events occur, deep oxygen concentrations increase up to 20

μM, before returning to values around 1 μM or less following remineralization (Goericke et al., 2015).

While previous studies provided insight on the nutrient cycling, microbial activity, and oxygen dynamics in the SBC, most were limited to analysis in deeper depths of the basin (below the sill depth at 475 m) with less emphasis on the shallower shelf and the sill depth perimeter. A specific emphasis on conditions found at the basin depocenter reflects palaeoceanographic and palaeoecological studies that exploit varve formation in the deep sediment to investigate the decline of oxygen in the basin over centennial and longer timescales (Reimers et al., 1990; Sholkovitz and Gieskes, 1971).

Despite extensive prior works, the connection between oxygen variability from deeper depths of the SBC to the water column interior and surface ocean has not been fully evaluated. Furthermore, the spatial distribution of bottom oxygen across the basin and channel remains poorly characterized due to the scarcity of observations and their typical localization near the depocenter. A better understanding of the spatial distribution and temporal variability of oxygen in the channel is critical to provide a comprehensive picture of nutrient cycling in the deep basin, and their potential connection to conditions found in the shallower surface ocean in the channel (Robinson et al., 2024; McWilliams et al., 2024)). It is also important to establish a baseline to investigate the effects of oxygen loss on benthic ecosystems, ranging from benthic microbial mats, often found below the sill depth, to more oxygenated sediment above the sill; and to explore how expanding hypoxic conditions may contribute to habitat compression and loss in the basin.

The goal of this study is to characterize the spatial distribution and temporal variability of oxygen in the SBC and deep basin, over the recent decades. We base this study on a new dataset

of oxygen measurements that combine recent high-resolution observations from the Autonomous Underwater Vehicle (AUV) *Sentry* and the Remotely Operated Vehicles (ROV) *Jason* and *Hercules*, and historical hydrographic surveys from the California Cooperative Oceanic Fisheries Investigation (CalCOFI) program and other hydrographic surveys and programs, to understand more about the oxygen dynamics in the SBC. This rich dataset provided the first spatially-resolved characterization of oxygen in the SBC and in the deep basin, and full water column oxygen variability from 1985-2023. Furthermore, to expanding on previous benthic iron (Fe) flux results from Robinson et al. (2024), we reconstructed near bottom water oxygen concentrations using this data-set to investigate the spatial distribution and temporal variability of benthic iron (Fe) flux from the basin as an application of this new data-set. Lastly, we discuss the implications of our study in the broader context of global oxygen loss in the coastal ocean.

## 2. Methods & Data Analysis

### 2.1 Hydrographic and oxygen observations in the Santa Barbara Basin

We compiled measurements from existing time-series and high-resolution surveys with autonomous and remotely operated underwater vehicles (including oxygen, temperature, salinity, and pressure/depth) to analyze the temporal variability and spatial distribution of oxygen in the SBC. Hydrographic data consisted of quarterly profiles from the CalCOFI program for the SBC region (33.9-34.5°N and 239–240.8°) that was conducted between 1985-2023, and was integrated with additional hydrographic profiles from programs such as Long Term Ecological Research (LTER), Plumes and Blooms, California Current Ecosystem- LTER, and other regional and local studies. We integrated these profiles with new high-resolution measurements from AUV Sentry (cruises AT42-19/2019 and AT50-11/2023) and ROV Jason (cruise AT42-19/2019) conducted

mostly along the north-south direction of the basin, and from ROV *Hercules* in the northwest side of the basin, between 300-500 m depth (*Nautilus* 2015 and 2016 cruises) (Myhre et al., 2018). In the following, we refer to both ROV and AUV as underwater vehicles (UV).

AUV *Sentry* and ROV *Jason*, operated by the National Deep Submergence Facility at Woods Hole Oceanographic Institution, were deployed as part of two research expeditions carried out in 2019 and 2023 with the R/V *Atlantis*. Oxygen concentrations were measured using Aanderaa 4831 optode sensors (Aanderaa Instruments, Bergen, Norway) connected to ROV *Jason* and AUV *Sentry* between 30 October to 11 November 2019, and by AUV *Sentry* between 1 July to 12 July 2023. ROV *Hercules,* also using Aandraa 4831 optode sensors, was deployed from the R/V *Nautilus* to sample the SBC on the 6th and 17th of August 2015 (Dive H1462) and the 24th and 26th of June 2016 (Dives H1525 and H1527), as part of the Nautilus Exploration Program. *Hercules* dives established two adjacent transects along the seafloor in the northern slope of the basin and a third transect along the southern basin slope (Myhre et al., 2018).

In 2019, AUV *Sentry's* transect had an average altitude of 33 m with the shallowest seafloor depth of 98 m and maximum seafloor depth at 586 m, while ROV *Jason's* transect had a minimum altitude of 0 m while settled on the seafloor, and the shallowest seafloor depth 125 m, and maximum depth of 586. Both AUV and ROV in 2019 had a north-south transect with majority overlapping depths and transect between 350-586 m. The Aanderaa 4831 optode was used to measure oxygen concentration in three-second intervals for AUV *Sentry* and five-second intervals for ROV *Jason*. In 2023, AUV *Sentry* was used again, and followed a similar north-south transect with the minimum depth of 350 m and average altitude of 30 m, and a maximum depth of 585 m. Oxygen was measured at a one-second interval.

Hydrographic data from CalCOFI and other cruises were merged with UV data into a single compilation used for the spatial analysis of oxygen in the basin. Because of the high frequency of oxygen measurement sampled by the UVs, oxygen and other parameters were subsampled to retain one measurement every 10 meters along the track of each UV.

### 2.2 Bathymetry reconstruction

To reconstruct the SBC bathymetry for analysis of the spatial and temporal distribution of oxygen, bathymetric data for the Southern California Bight were downloaded from the Earth Topographic (ETOPO) Global Relief Model database at a resolution of 15-arc sec (>1 km) resolution.

### 2.3 Three-dimensional oxygen data mapping and spatial distribution

A spatial mapping algorithm was applied to the new SBC oxygen compilation to reconstruct the three-dimensional mean climatological oxygen distribution in the channel. Spatial mapping of sparse oceanographic data has a long history in oceanography (World Ocean Atlas, 2024; Levitus, 1983) and has long been used to provide detailed descriptions of the physical and chemical characteristics of the ocean. Here, we followed a mapping approach similar to previous studies of the three-dimensional oxygen distribution at both global and regional scales (Bianchi et al., 2012; Sandoval-Belmar et al., 2023). We applied our mapping method to oxygen data in the SBC and adjacent waters around the channel, opting for a simple algorithm that is adequate for the relatively uncomplicated topography of the region.

The gridding approach utilized MATLAB's gridfit tool, a surface modeling algorithm that fits a smooth surface to data that is irregularly distributed in two-dimensions (D'Errico, 2024). We

chose gridfit because of the ability to include duplicate data and extrapolate without overestimating beyond the input data. In our application, we used gridfit to estimate oxygen concentration at specific grid-points on a regular longitude-latitude grid for the SBC, here taken at the same resolution of the bathymetric data (15 arc-sec). We fit individual surfaces to observed oxygen data at a series of discrete depth levels, selecting all observations that fall within a given depth range that identifies each level. The resulting gridded surfaces are then "stacked" for every depth level to generate a three-dimensional (3-D) gridded reconstruction of oxygen in a selected spatial domain. We subdivided the basin in 45 depth levels between 0 and 1000 m depth, with variable vertical thickness, ranging from 5 m near the surface to 20 m near 600 m depth (the approximate maximum depth of the SBC) to 50 m at 1000 m depth (corresponding to data points outside the SBC).

Prior to horizontal interpolation at each depth level, we introduced a vertical interpolation step to maximize the number of oxygen data points available in each depth layer. To this end, we interpolated vertical oxygen profiles from hydrographic observations onto each level's depth, using a least-square spline approach based on the Shape Language Modeling (D'Errico, 2024). This vertical interpolation step fits a least-square spline to each vertical profile, subdividing the vertical depth range into separate nodes, the number of which is defined in such a way to include at least 4 individual oxygen measurements per vertical interval. We removed results from the vertical interpolation if they belong to a layer that contains no observations and is thicker than 70 m, to avoid interpolation artifacts when the data is too sparse in the vertical direction.

The gridfit algorithm, similar to other mapping procedures, requires specification of parameters that control the smoothness of the surface that fits the data. These parameters in turn depend on the spatial scale of the problem considered. Accurate gridding of oxygen data in the

SBC requires capturing fine-scale gradients that develop within the channel (on scales of the order of 10 km), in particular at depths below the sill, while also preserving relatively smooth large-scale gradients outside the deep channel (on the order of 100 km). To capture both scales, we performed two 3-D oxygen reconstructions. The first reconstructed uses only observations within the SBC and adopts a small smoothness parameter appropriate for the deep SBC. The second reconstruction uses observations across a broader domain that extends well outside the SBC, and adopts a larger smoothness parameter appropriate for the more expansive coastal ocean. We then merged the two resulting gridded datasets by using a spatially dependent weighted mean. We defined the weights by building a 3-D gaussian mask centered in the deep SBC (239.95°, 34.25° N, 560 m depth), with spatial scales of 0.5 degrees longitude, 0.25 degrees latitude, and 250 m depth. This weighting mask transitions from values close to 1 within the deep basin, where higher weights are given to the local gridding, to values of 0 outside it, where higher weights are given to the broader coastal gridding. The resulted merged dataset preserves high-resolution information on the oxygen distribution within the basin, while capturing large scale gradients outside the SBC without overfitting local clusters of data associated with individual sampling stations from CalCOFI and other programs mention previously (Section 2.1).

To validate the results of the 3-D gridding process, we extracted gridded data at the same locations of observations, and calculated statistics such as correlation coefficient, mean bias, and root mean square error between the gridded data and the observations.

### 2.3 Analysis of the temporal variability of oxygen in the SBC

We took advantage of the long series of quarterly hydrographic measurements in the SBC from CalCOFI and other programs to investigate the temporal variability of oxygen in the basin.

To this end, we took all oxygen observations within the SBC and gridded them onto a 2-D grid with time and depth as dimensions. For the time dimension, we used grid points at 3-month intervals; for the depth dimension, we used the same vertical intervals used for the 3-D spatial analysis of oxygen. We then considered all oxygen observations within each time and depth interval to calculate statistics that include the number of observations, the mean, median, and standard deviation of dissolved oxygen and other hydrographic variables. We found that a temporal interval of three months is sufficient to provide a nearly continuous representation of oxygen variability with depth and time within the basin.

We further estimated the climatological seasonal cycle of oxygen at each depth by fitting a cyclical least square spline through the oxygen data as a function of the month of the observation, using the Shape Language Modeling tool (D'Errico, 2024), following the approach developed by (Sandoval-Belmar et al., 2023). With this method, each climatological year is approximated by a periodic least square spline with seven regular nodes, corresponding to a temporal resolution of two months, which is sufficient to reconstruct the seasonal cycle in oxygen at all depths. We then evaluated the least-square spline at each month, taking the middle of the month as representative date, to obtain the climatological seasonal cycle of oxygen at each depth.

We used the resulting monthly climatology to calculate de-seasonalized oxygen anomaly timeseries. Anomalies are obtained by subtracting the monthly climatological oxygen from each gridded oxygen value from the oxygen timeseries at each depth. The results provide a representation of anomalous oxygen concentrations as a function of depth and time, after removal of seasonal variability (Sandoval-Belmar et al., 2023).

### 2.5 Spatial reconstruction of near bottom oxygen and benthic Fe flux

We reconstructed a 2-D map of near bottom water oxygen concentrations in the SBC by taking the deepest oxygen values in the 3-D dataset. Using this near-bottom water reconstruction, we assumed that the oxygen concentration from the deepest layer is representative of oxygen concentrations in the bottom boundary layer. We evaluated this assumption by comparing the reconstructed bottom oxygen with observations that are close (within 100m) of the local bottom. We used the reconstructed bottom water oxygen together with the benthic Fe flux parameterization by (Robinson et al., 2024) to provide an estimate of benthic Fe flux in the basin. For this calculation, we included a representation of temporal variability by adding the seasonal cycle and interannual anomalies to the 2-D map of the mean oxygen at each bottom depth, assuming that these temporally variable components are horizontally homogenous across the basin over monthly timescales (Fig. S3-1).

The benthic Fe release follows the equation:

$$Log_{10}(\varphi_{Fe}) = 2.86 - 0.01 \cdot O_2,$$

Where $\varphi_{Fe}$ is the benthic Fe flux in units of mmol $m^{-3}$, and $O_2$ the bottom water oxygen in units of μmol $m^{-2}$ $d^{-1}$. This parametrization is based on a combination of Fe flux measurements for the California coast from (Severmann et al., 2010), updated to reflect recent observations from the SBC, where high benthic Fe fluxes were measured in the basin, well in excess of previous measurements in this region and other oxygen minimum zones (Robinson et al., 2024)

## 3. Results

### 3.1 Oxygen data compilation for the Santa Barbara Basin

Fig. 3-1 and S3-2 illustrate the distribution of oxygen measurements throughout the SBC. A cluster of measurements are observed near the center of the SBC and the adjacent California borderland. The UV surveys complement the hydrographic data, providing high-resolution sampling along a north-south axis crossing the basin center, with multiple additional hydrographic data near the east-west transects. In contrast, hydrographic measurements are scattered throughout the channel, and are more numerous in the north-west side of the channel, toward the Arguello canyon (34.4-34.5 °N) and north of Santa Rosa Island (240°). Outside the SBC, oxygen profiles are sparse compared to more numerous oxygen profiles within the SBC, but extend to depths greater than ~ 1000 m.

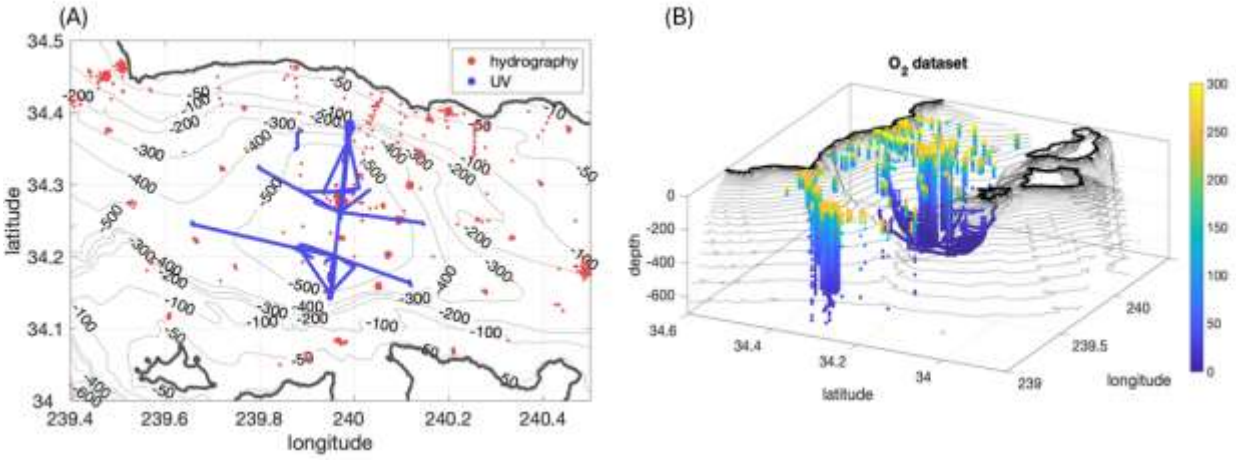


**Figure 3- 1.** The location of compiled individual oxygen profiles and measurements throughout the SBC. (A) Illustration the 2-D distribution of observation types with a combination of Underwater Vehicle (UV) (blue) and hydrographic profiles from CalCOFI and other hydrographic programs (red) with grey contours show isobaths in meters (m). (B) 3-D distribution of individual oxygen measurements (μmol $L^{-1}$) from the data compilation.

We further evaluated the distribution of measurements in the SBC by taking into account the denser sampling of the UV relative to the sparser sampling by the hydrographic profiles. To this end, we subdivided the SBC into individual volumes of approximately 1km by 1km area (0.01 x 0.01 degrees) and 50 m thickness, and recorded the number of distinct months sampled by hydrographic and UV data in each of these volumes. The resulting "data counts" were used as a measure of the ability of the hydrographic and UV dataset to provide relatively independent spatial and temporal information on the oxygen distribution in the SBC (Fig. 3-2).

Most of the data counts are concentrated near the center of the channel, reflecting a high number of profiles from CalCOFI and other hydrographic programs, integrated by the UV data. UVs provide great spatial distribution and resolution near the basin's center by covering the north-south direction in great detail (Fig. 3-2), while observations flanking the basin are scarcer in comparison. Most hydrographic data are within the surface and subsurface layers (< 200 m), while the UV provides higher resolution towards the deeper part of the basin (< 300 m), in particular near and below the sill depth.

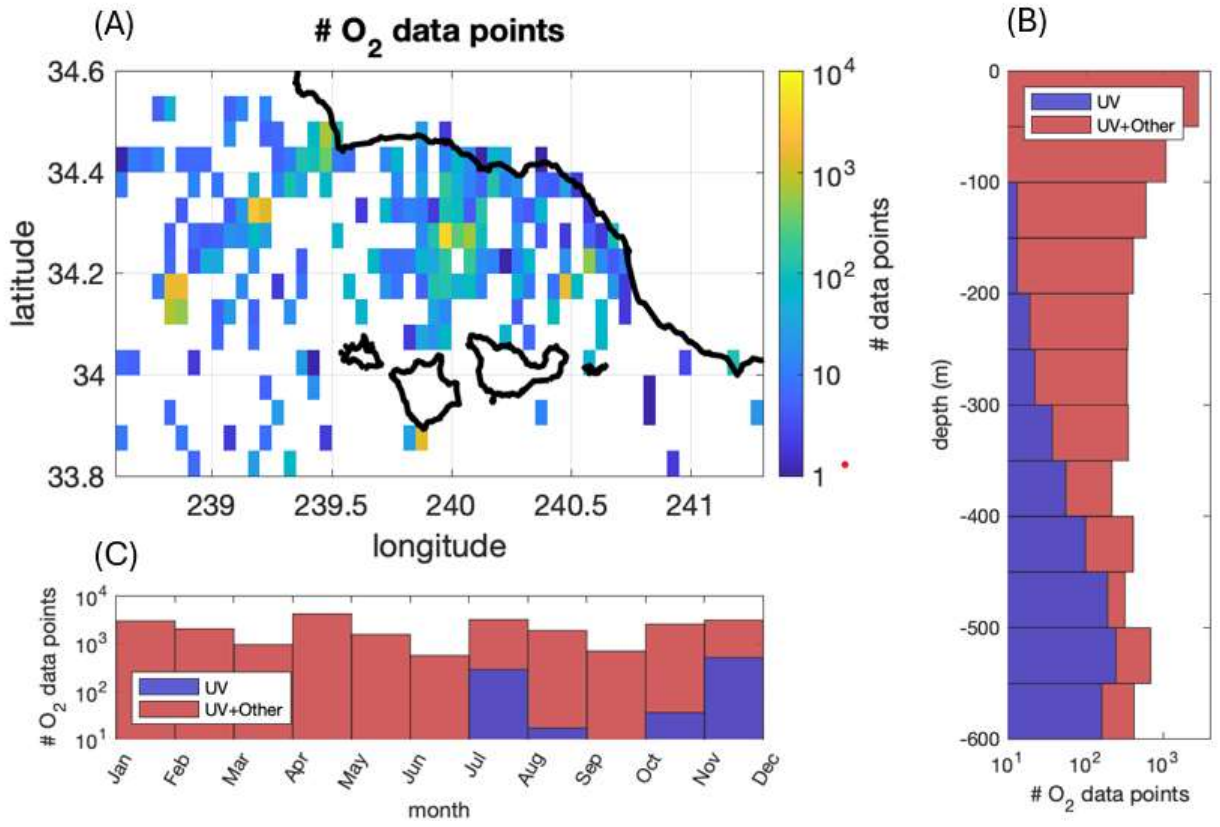


**Figure 3- 2.** Distribution of oxygen observations in the SBC and basin. (A) Data counts as a function of latitude and longitude, where yellow represents a high density of data counts and blue a low density of data counts. Data counts are binned on 0.05 degree boxes (~5 km), and summed in the vertical direction. (B) Data counts as a function of depth, in 50-m thick vertical layers, illustrating UV (blue) and UV + Other (combination of UV + Hydrographic data), (red) separately. (C) Data counts as a function of the observation months showing UV (blue) and UV + Other (combination of UV +Hydrographic data) (red) separately. Here, to account for the high data density of individual UV $O_2$ observations relative to more sparse hydrographic observations, we consider as individual data count any given number of observations in a 0.01 degrees x 0.01 degrees x 10 m volume of water (approximately 1km x 1km x 10 m), taken on the same month.

While hydrographic data span all months of the year with high data count densities, UV data is only represented in July-August and October-December. Overall, after considering all the data in our compilation, UV measurements provide a much better resolved picture of the deep basin than the hydrographic data alone, although they only provide information for limited period in summer and fall.

### 3.2 Spatial distribution of oxygen in the water column and deep basin

Fig. 3 and S3 illustrate the horizontal oxygen distribution in the SBC based on the 3-D gridded dataset, for selected surface, sub-surface, and deep layers. Overall, the 3-D gridded dataset captures the spatial patterns of individual oxygen measurements (shown by the circles in Fig. 3-3 and S3-3) in the SBC. Between 0-50 m, i.e., roughly within the surface mixed layer, oxygen concentrations are relatively high (>250 μM), with gridded oxygen concentrations in good agreement with observations (Fig. 3-2 (A)), despite significant variability in the individual data points, likely reflecting seasonal and interannual fluctuations.

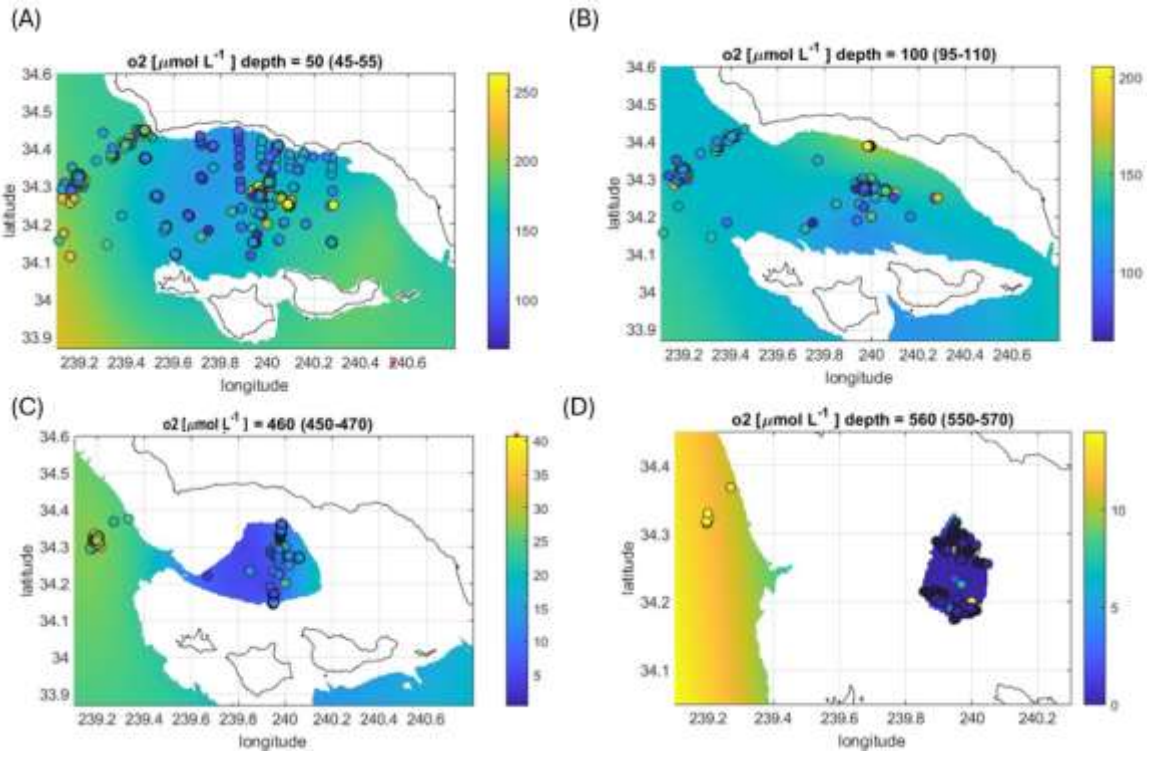


**Figure 3- 3**. Oxygen (μmol $L^{-1}$) distributions from the gridded dataset (color gradient) at 50 m (A), 100 m (B), 480 m (C), and 560 m (D). Circles show observed oxygen concentrations. Note the change in the range of oxygen values between different panels.

Subsurface (~100 m) oxygen concentrations decrease from the surface ocean and become more uniform with depth (Fig. 3-3B); note the smaller number of measurements as depth increases). Below 300 m (Fig. S3-3), oxygen concentrations begin to transition into hypoxic conditions falling below <80 μmol $L^{-1}$ near the center of the SBC, and reaching anoxic or near-anoxic conditions between 500-560 m (Fig. 3-3D). Oxygen measurements west of the SBC (239.0-239.4°) are relatively sparse below depths greater than 500 m, although they appear sufficient to capture the main gradients in oxygen in the region. Within the SBC, most observations are found near the surface (< 100 m) close to the depocenter (34.2-34.3°N), and along the bottom (following the bathymetry in the case of the UV surveys), with a dearth of measurements in the sub-surface layer (100-350 m) of the basin (Fig. 3-4). Despite the decrease in the area of the basin below the sill, the number of combined hydrographic and UV measurements appear adequate to reconstruct the spatial distribution of oxygen and the volume of low-oxygen water.

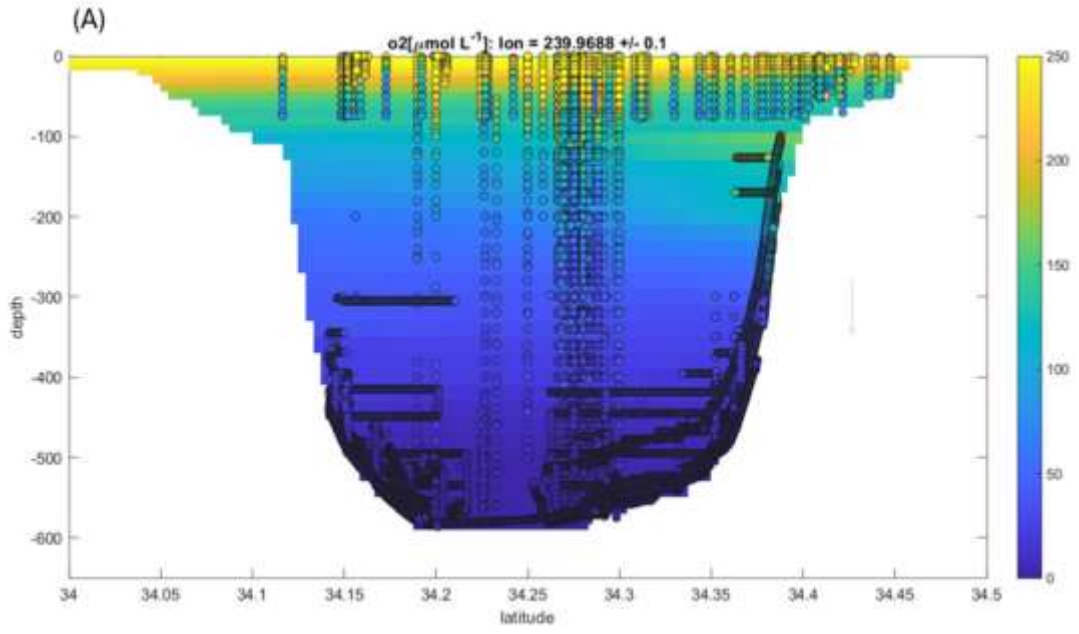

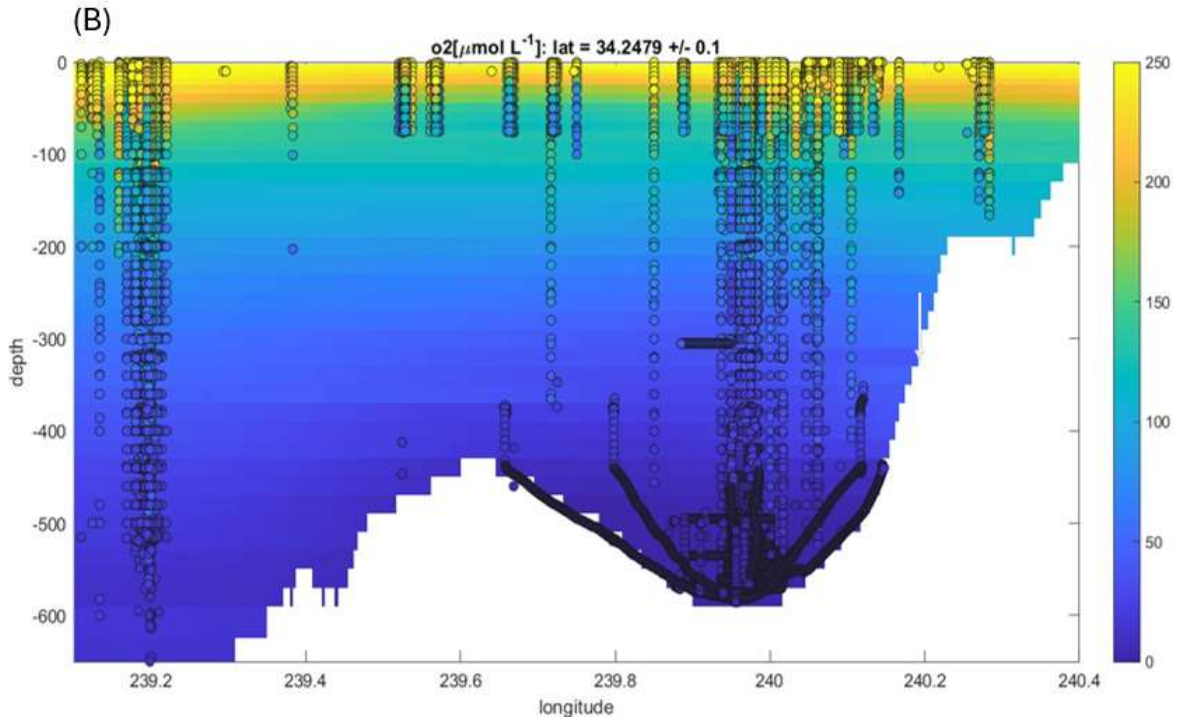


**Figure 3- 4.** Cross section distribution of oxygen in the SBC and outside of the SBC. (A) Longitudinal and (B) Latitudinal cross section covering oxygen distribution (0-250 µM) in the SBC and the open ocean beyond the western sill (white arrow). Oxygen profiles (circles) are superimposed onto the gridded oxygen data.

### 3.3 Temporal variability of oxygen in the Santa Barbara Channel

We investigated the temporal variability of oxygen in the SBC based on the vertically resolved time-series of hydrographic measurements collected between 1985-2023 (Fig. 3-5). At the surface and in the sub-surface (<200 m), oxygen concentrations are highly dynamic and show rapid fluctuations, mostly on seasonal timescales, possibly reflecting a combination of upwelling of low-oxygen water, high oxygen production during phytoplankton blooms phases followed by enhanced subsurface respiration, and increases in air-sea gas exchange and turbulent mixing that replenish oxygen at the surface in wintertime. Conversely, oxygen concentrations below 300 m were relatively more stable than the surface and subsurface (Fig 3-5).

A closer inspection of the seasonal cycle in the water column interior (200-400 m) and deep layers (>400 m) reveal contrasting behavior with muted variability and a transition near the sill depth (475 m) (Fig. 3-5 (C-D)). In the interior, oxygen concentrations show maxima during late winter and late summer, and minima in the spring and early fall. These changes likely reflect the cycle of interior upwelling and relaxation, as well as the enhanced remineralization of freshly produced organic matter following upwelling. (Fig 3-5 (C)). Below the sill, the seasonal cycle of oxygen is relatively weaker, and shows an opposite phasing compared to the interior, with more oxygenated conditions during times of relaxation in late spring and upwelling early summer, followed by a depletion in late summer and fall.

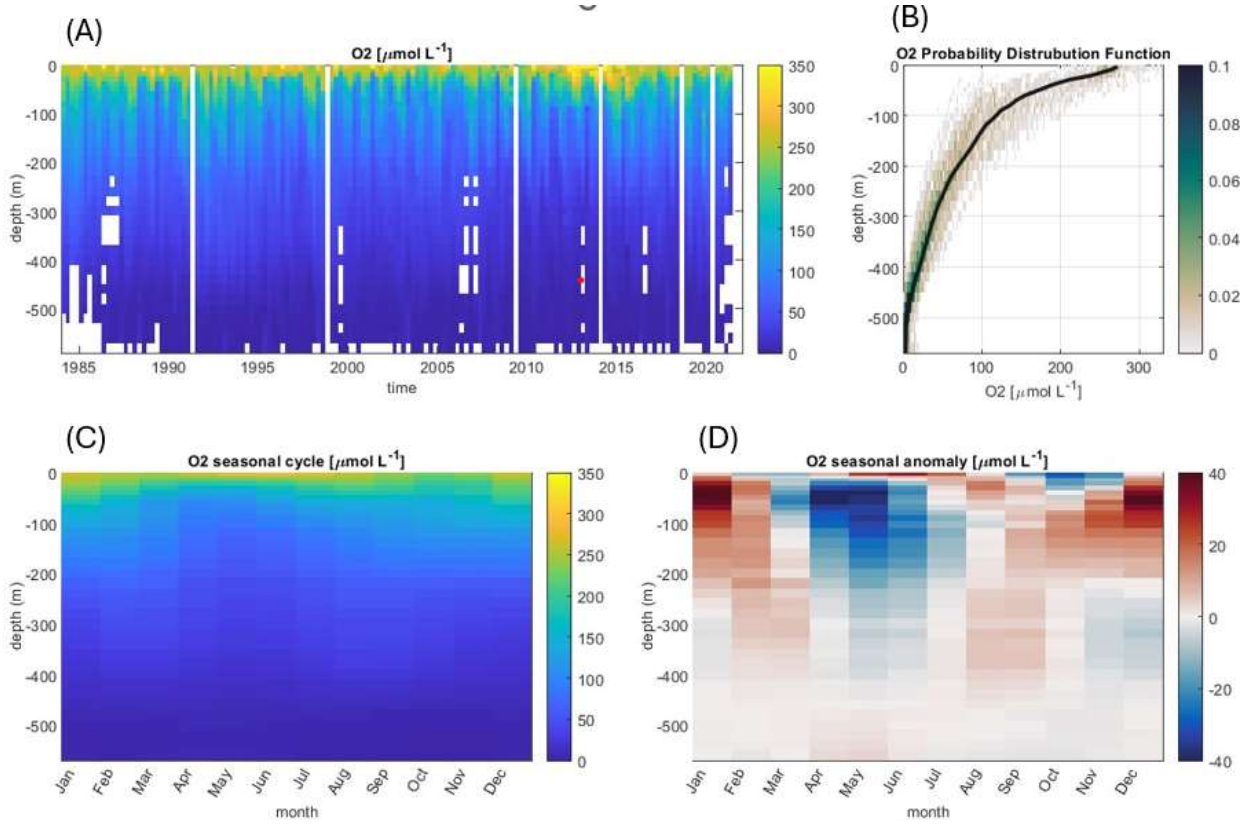


**Figure 3- 5.** Temporal variability of oxygen (µmol $L^{-1}$) the for the SBC only. (A) Hovmöller diagram of $O_2$ at 4-month (seasonal) intervals. Note the uneven vertical bin width. (B) profile showing the probability distribution function of $O_2$ as a function of depth, essentially the variability, and the mean. (C) The seasonal cycle at 2 months resolution, and (D) the seasonal anomalies relative to the mean.

Removing the seasonal variability reveals the detail of the non-stationary oxygen dynamics, with generally positive anomalies dominating before 1995, and mostly negative anomalies thereafter (Fig. 3-6 (A)). In particular, the 2005-2015 period shows the development of negative anomalies within the interior (100-450 m), with a decadal progression from surface to deeper layers, and lowest interior oxygen concentrations between 2010-2015. After 2015, oxygen anomalies begin to show irregular oscillations between negative and positive phases. Overall, during the entire period of analysis, the interior (100-300 m) is characterized by a negative oxygen trend corresponding to a decline by slightly less than 0.2 $\mu$mol $L^{-1}$ per decade (Fig 6 (B)). In contrast, we observe a very weak to negligible negative trend below the sill depth, in particular,

near the bottom, suggesting that dynamics other than seasonality have more influence in the semi-enclosed deep basin (Fig 6 (C)). Despite the lack of clear long-term trends, near-bottom oxygen anomalies indicate the presence of flushing events in the deep basin. These appear mostly episodes with an increase in bottom oxygen concentrations around 10 $\mu$mol $L^{-1}$ resulting in an oxygen variability of 3.2 $\mu$mol $L^{-1}$ (the standard deviation of the oxygen anomalies) at a depth of 560 m. However, flushing events in the deep basin show an irregular interannual distribution that does not appear to be clearly connected to variations observed in the surface and subsurface layers of the water column.

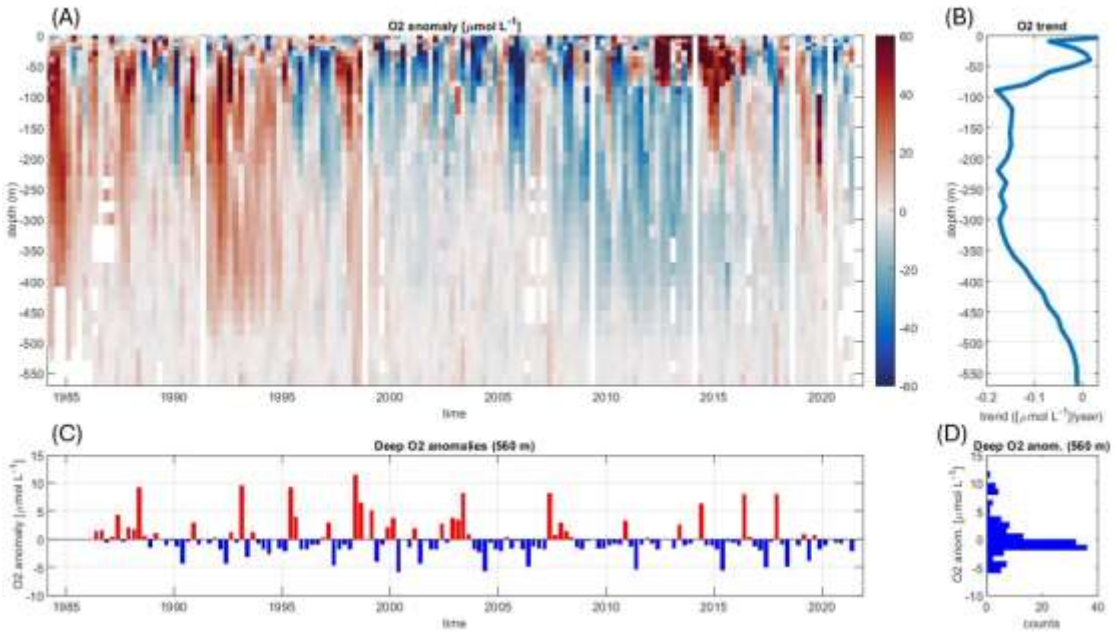


**Figure 3- 6.** (A) Hovmöller diagram of $O_2$ anomalies after removing the seasonal cycle. Note uneven vertical bin width. (B) Profile showing $O_2$ trend over time as a function of depth, also visible in (C). Deep $O_2$ anomalies at 560 m (core of the basin) (D) showing a relatively small amplitude, punctuated by oxygenation events.

### 3.4 Bottom water oxygen reconstructions and benthic iron flux estimates in the deep basin

Reconstructed bottom water oxygen distribution exhibit declining oxygen concentrations throughout deeper depths (>300 m) towards the western sill, and increasing oxygen concentrations towards the shallower eastern sill (Fig. 3-7). In shallow depths of the continental shelf and upper slope (<100 m), oxygen remains relatively high (>150 $\mu$mol $L^{-1}$) compared to deep depths. A comparison of mapped and in-situ bottom oxygen data shows a good agreement, with anomalies generally below 10 $\mu$mol $L^{-1}$, with negligible mean bias (Fig. S3-4). However, we note a tendence of our gridded dataset to slightly overestimate bottom oxygen at very low oxygen concentrations, with a mean bias of approximately 1.1 $\mu$mol $L^{-1}$ for observed bottom oxygen concentrations less than 5 $\mu$mol $L^{-1}$.

By reconstructing bottom water oxygen in the deep basin, we can provide an estimate of benthic iron (Fe) flux, using an empirical relationship that relates bottom water oxygen and benthic Fe flux (Severmann et al., 2010; Deutsch et al., 2021) that is recalibrated with recent observations from the basin (Robinson et al., 2024). Accordingly, benthic Fe flux rapidly increases with declining bottom water oxygen and increasing depth (Fig. 3-7). Integrated across the deep basin, our bottom oxygen and benthic Fe flux reconstructions suggest that 13.5 mol $s^{-1}$ Fe are released from the sediment, equivalent to approximately 24,000 ton $yr^{-1}$.

The highest benthic Fe fluxes are confined within the deeper depths (>450 m) of the basin that overlap with hypoxic and anoxic conditions. Approximately half of the deep basin's benthic Fe flux is released by sediment below the basin sill (Fig. 3-7C), where oxygen concentrations are persistently low, despite this deep part of the basin occupying less than 20% of the basin's surface area (Fig. 3-7D).

Because of the seasonal and interannual variability in oxygen concentrations, estimated benthic Fe fluxes likely varied with time (1985-2023), as the average oxygen concentration that overlaps with benthic Fe flux decreases along the same time interval (Fig. 3-7).

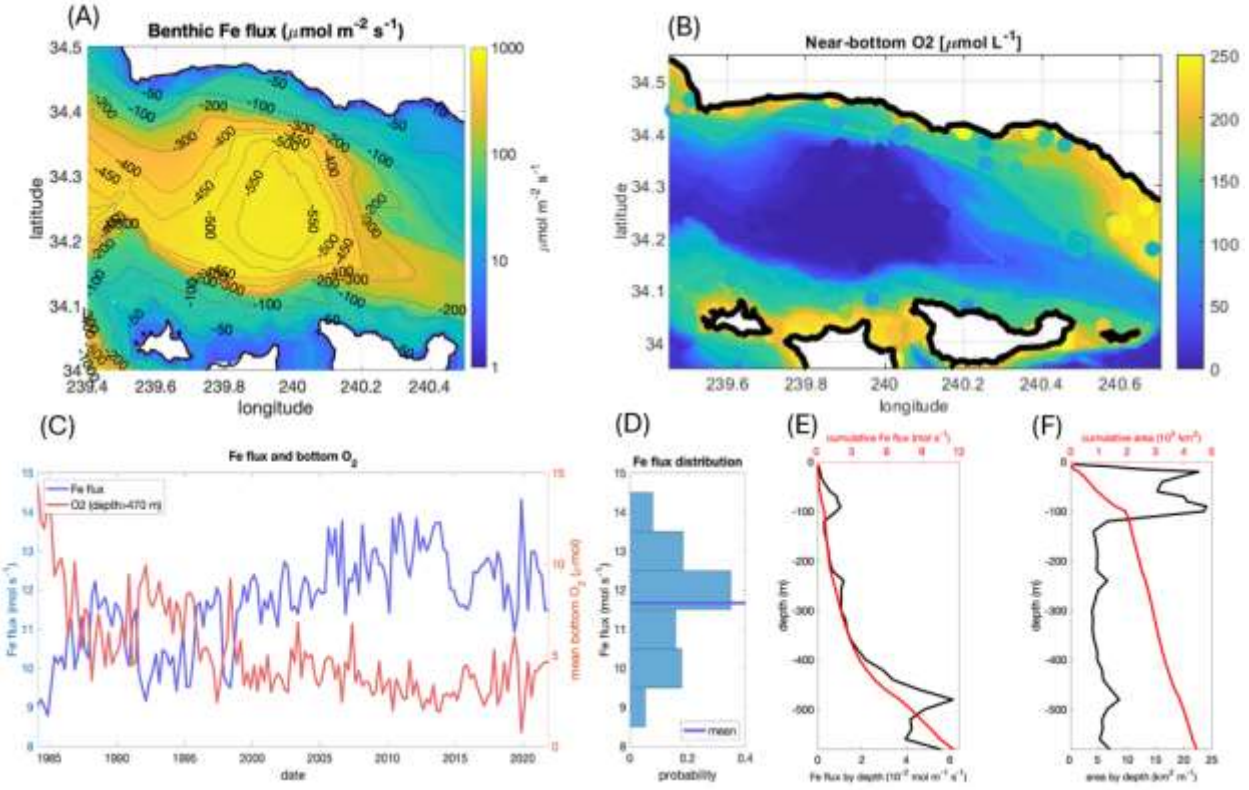


**Figure 3- 7.** Reconstruction of bottom water oxygen concentration and benthic Fe flux. (A) Reconstructed benthic Fe flux extrapolated from near-bottom oxygen. (B) Near-bottom $O_2$ from the 3-D gridded data in the background. Circles show near-bottom observations. (C), (D) mean and cumulative bottom surface area and flux as a function of depth. (E) Timeseries of bottom oxygen in the deep SBC basin (red, depth >470m) and total benthic Fe flux for the basin (red) as a function of time. (F) Histogram and mean Fe flux in the SBC.

## 4. Discussion

### 4.2 High-resolution oxygen observations illuminate the distribution of oxygen in the Santa Barbara Channel

The integration of hydrographic data with a series of new surveys from UV in the SBC reveals the spatial and temporal variability of oxygen in the SBC, expanding the results from previous studies (Goericke et al., 2015; Reimers et al., 1990; Robinson et al., 2024; Sholkovitz and Gieskes, 1971). Just below the surface ocean (45-50 m), oxygen concentrations are characterized by high spatial variability, with relatively high (>200 $\mu$mol $L^{-1}$) and low (200-100 $\mu$mol $L^{-1}$) concentrations, with lower oxygen concentrations within the western side of the basin, relative to oxygen concentrations outside the basin (Fig. 3-3**)**. Low oxygen concentrations at shallow depths can be explained by upwelling and mixing that transport low-oxygen waters and nutrients from the water column interior to the surface (Brzezinski and Washburn, 2011; Hendershott and Winant, 1996; Kessouri et al., 2022). In particular, the characteristic cyclonic circulation that characterize the SBC can lift isopycnal surfaces and shoal lower oxygen concentrations closer to the surface (Bograd et al., 2008; Brzezinski and Washburn, 2011). This process can be exacerbated by submesoscale cyclonic eddies formed by interactions between large-scale currents and the Channel Islands and wind forcings (Kessouri et al., 2022). Low oxygen conditions may also reflect transport by the poleward California Under Current (CUC) into the SBC, followed by mixing with the CCS by eddies (Chhak and Di Lorenzo, 2007; Evans et al., 2020). Upwelling of CUC waters is plausible, although knowledge of transport and fate of low-oxygen waters carried by the CUC directly into the SBC is limited.

The subsurface and interior oxygen concentrations of the SBC are more homogenous and become predominantly hypoxic below a depth of around 250 m (Fig. 3-3). Subsurface waters are characteristically lower in oxygen in the channel compared to the broader CCS to the west (Fig. 3). Thus, while low subsurface oxygen may reflect transport and exchange of waters between the broader CCS and the SBC, local physical and biogeochemical processes, including increased remineralization appear to be important. Because of the interaction between wind-driven upwelling and the predominantly anticyclonic circulation in the SBC, this region is characterized by upward movement of isopycnals that enhance nutrient supply to surface waters, fueling high primary production and export, and higher remineralization at depth (Brzezinski and Washburn, 2011; Kessouri et al., 2022; Renault et al., 2016). These processes likely contribute to lowering subsurface oxygen in the SBC relative to CCS, and are likely enhanced by reduced ventilation and exchange with open-ocean waters, which would increase water residence time in this semi-enclosed basin (McWilliams et al., 2024).

Between depths of 400-500 m, oxygen concentration inside and outside the basin begin to differ significantly, with oxygen concentrations in the basin 10 $\mu$mol $L^{-1}$ lower than outside the basin, reflecting higher remineralization rates in deep waters and the sediment, and increasingly reduced ventilations by CCS waters (Fig. 3-3 and S3-3). Below the sill depth and near the depocenter, oxygen concentrations in the basin become increasingly disconnected from those outside of the basin, due to limited flushing and reoxygenation below the sill depth, along with continuing remineralization in bottom waters and the sediment. Below the sill depth, oxygen often reaches anoxic conditions, although some variability is observed in both space and time, reflecting the episodic nature of flushing events followed by quiescent phases of declining oxygen, but also the deep circulation forced by near-bottom currents and flushing events, which alter the spatial

distribution of older and newly ventilated waters across the basin (Goericke et al., 2015; Krause et al., 2023; McWilliams et al., 2024). The widespread hypoxia and anoxia observed below the sill are consistent with observations of widespread formation of microbial mats of sulfur-oxidizing bacteria and marine biota that can tolerate low oxygen conditions (Valentine et al., 2016a; Yousavich et al., 2024).

### 4.1 Temporal Variability: The Santa Barbara Channel and the California Current

Oxygen variability in the surface and interior of the water column in the SBC is the result of the seasonal dynamics of upwelling and transport from the CCS, with the additional influence of mesoscale and submesoscale eddies along the CCS and SBC. At the bottom of the deep basin below the sill, an “out of sync” seasonal transport of oxygen is influenced by topography, flushing events and remineralization. Recently, it has been shown that physical transport by the horizontal and vertical mean current, and anticyclonic circulation at the sill depth, support the seasonal oxygen anomaly dynamics and lag between oxygen flushing into the depocenter from waters originating in the CCS outside the basin (McWilliams et al., 2024)

Examining a long timeseries of oxygen observations below 475 m show strongly hypoxic or anoxic deep waters year around, punctuated flushing events that tend to occur during the spring upwelling season (Fig. 3-6). Flushing events reflect episodic intrusion of relatively hypoxic oxygenated and low-temperature Pacific waters that reach the depocenter and mix with old, warmer, low oxygen water, causing periodic oxygenation of bottom waters in the basin. After individual flushing events, which can be rapid, occurring at sub-seasonal timescales (McWilliams et al., 2024) high remineralization rates in the deep basin provide a steady removal of oxygen (Burdige et al., 2016; Goericke et al., 2015; Thunell, 1998; White et al., 2019). Because flushing

events do not necessarily occur every upwelling season, the climatological seasonal cycle of the deep basin remains relatively "out of sync" compared variability outside the basin (Fig 3-5. and 3-6). Even when flushing events occur, they appear to increase oxygen by only up to approximately 10 $\mu$mol $L^{-1}$, reflecting hypoxic conditions outside the sill, and thus the basin may not undergo full oxygenation of relatively oxic water. While oxygen has an "out of sync" seasonal cycle between the interior and deep, this sync is less apparent for salinity and temperature (Fig. S3-5 and S3-6), which suggest some degree of decoupling between oxygen and physical properties transported by water intrusions from the CCS, e.g., reflecting the fact that oxygen is removed quickly by remineralization.

Above the sill depth (> 475 m), oxygen dynamics in the water column interior and surface are relatively coherent. After 1997, the overall trend of oxygen in both the surface and interior of the SBC is negative (Fig. 3-6). This oxygen decline can result from a combination of factors: increases in sea-surface temperature and remineralization in the broad CCS from climate change (Evans et al., 2020; Low et al., 2021), with the resulting transport of low-oxygen water into the basin from the west; or increases in subsurface remineralization rates in the SBC, as reflected by the decline of oxygen from the surface to the interior of the basin (Burdige et al., 2016; Goericke et al., 2015; Sholkovitz and Gieskes, 1971; Thunell, 1998). The exact dominating physical or biogeochemical control of interannual oxygen decline in the basin deserves further study

### 4.3 Implications for sediment biogeochemistry and Fe release in the Santa Barbara Channel

Anoxic and nearly anoxic bottom waters in the basin influence the release of nutrients and reduced compounds from the sediment. Using our 2-D reconstructions of near-bottom oxygen and an empirical relationship for benthic Fe release, we provided a spatially-resolved extrapolation of the benthic Fe flux in the basin (Fig. 3-7). High benthic Fe fluxes (several 100 $\mu$mol $m^{-2}$ $d^{-1}$) are located closer to the depocenter, at depths greater than 500 m, where extreme hypoxia and anoxia occur. This are consistent with recent observations showing that benthic Fe flux is highest at the depocenter (Robinson et al., 2024). At shallower depths, oxygen concentrations increase and benthic Fe flux decreases following the inverse relationship between oxygen and Fe flux.

Note that our reconstructions are based on a climatological approximation of bottom oxygen based on all measurements available, with superposed temporal variability from hydrographic timeseries. Thus, it is likely to severely underestimate the complexity of oxic/anoxic cycles in the deep basin and sediment. This oxygen and benthic Fe flux reconstruction may provide more inference on microbial dynamics, which are altered by seasonal variability of oxygen in the deep basin and in the organic carbon flux sinking from shallower depths (Burdige et al., 2016; Thunell, 1998; Valentine et al., 2016).

Our oxygen reconstructions can provide useful information to develop and constrain ocean biogeochemical models (Deutsch et al., 2021; Robinson et al., 2024), for example by tightening local estimates on the cycling of Fe in the basin and the CCS. Further work should focus on other aspects of ocean biogeochemical processes affecting nutrient cycles and ultimately primary production, including denitrification, phosphate flux, sedimentary sulfate reduction or organic carbon respiration that can be extrapolated similarly as that oxygen reconstruction.

### 4.4 Future studies on oxygen and nitrogen dynamics in Santa Barbara Channel and outlook on microbial mat assemblage

The SBC is characterized by a unique biogeochemical environment because of the presence of anoxia and hypoxia in the basin, and the intermittent seasonal flushing with more oxygenated water. These conditions contribute to the particular biogeochemical system in the basin. Because of the basin's low-oxygen environment, studies relating low-oxygen to microbial assemblage, ocean biogeochemistry, and metabolic activity are becoming increasingly valuable in light of global and coastal oxygen loss (Evans et al., 2020; Krause et al., 2023; Robinson et al., 2024; Schmidtko et al., 2017; Valentine et al., 2016b; Yousavich et al., 2024). Building on our high-resolution dataset and the resulting spatial reconstructions of oxygen variability in the basin, future studies could target aspects such as co-occurring spatial and temporal variations in oxygen, the detailed dynamics of flushing events, and their ecological, biological and biogeochemical ramifications in the SBC.

Furthermore, future studies relating the spatial distribution of anoxia and hypoxia in this study could focus on quantifying the benthic microbial assemblage, sediment geochemistry, denitrification and methane oxidation dynamics in the basin including the influence of foraminifera and sulfur-oxidizing bacteria on the nitrogen cycle. Previous studies focusing on characterizing microbial mats, their distribution in relation to oxygen, and their geochemistry have been mostly confined within the depocenter of the basin, where anoxic conditions tend to be more common and persistent (Goericke et al., 2015; Krause et al., 2023; Peng et al., 2023; Reimers et al., 1990; Robinson et al., 2024; Valentine et al., 2016; Yousavich et al., 2024). The widespread distribution of nearly anoxic conditions inferred by our study could suggest a correlation with that expansion of microbial mats in the basin (Valentine et al., 2016a; Yousavich et al., 2024) and the

cumulative rate of sedimentary sulfate reduction occurring in the basin (Yousavich et al., 2024). Previous observations showed that nitrate has a seasonal and metabolic dynamic to that of oxygen, whereby nitrate concentrations decrease during anoxic periods (Goericke et al., 2015; Peng et al., 2023; Sigman et al., 2003). Correlating spatial distribution of oxygen to benthic microbial mat assemblage can provide further insight into the nitrogen dynamics in the basin, and help identifying if dissimilatory nitrate reduction to ammonium is occurring at the transition between anoxic and hypoxic waters, expanding on previous studies between nitrogen and benthic microbes in the basin (Peng et al., 2023; Sigman et al., 2003; Valentine et al., 2016; Yousavich et al., 2024).

**Conclusion**

Using a new compilation of oxygen measurements in the SBC that combines historical hydrographic profiles and new, highly spatially resolved UV observations, we reconstructed a 3-D spatial distribution and temporal variability of oxygen in the basin. Our mapped dataset indicates that hypoxia is pervasive throughout the basin, in particular near the bottom, with hypoxic to anoxic conditions prevalent towards the western sill, and slightly more oxygenated condition towards the eastern sill. We also characterized the intense seasonal cycle and interannual to decadal variability of the surface and subsurface oxygen distribution, which we attribute to upwelling dynamics and exchanges with the surrounding CCS in the west. The subsurface seasonal cycle contrasts with the "out-of-sync" cycle and variability near and below the sill, which are mostly influenced by episodic events, with more common oxygenation in spring, and local remineralization. Our results also suggest a large release of Fe from the deep sediment, with potential for significant changes related to the overall oxygenation state of the deep basin. However, the extent to which this Fe is able to escape the deep basin to potentially affect the

biogeochemistry of surface water, rather than re-precipitating into the basin sediment, remains to be experimentally determined.

**Supplementary Material**

**Spatial Distribution and Temporal Variability of oxygen in the Santa Barbara Basin**

**De'Marcus Robinson[1],** Daniele Bianchi[1], Na Liu[3,4], David L. Valentine[3,4], Tina Treude [1,2],

[1]Department of Atmospheric and Oceanic Sciences, University of California Los Angeles, Los Angeles, CA, USA

[2]Department of Earth, Planetary, and Space Sciences, University of California Los Angeles, Los Angeles, CA, USA

[4]Department of Earth Science and Marine Science Institute, University of California, Santa Barbara, CA 93106, USA

[4]Interepartment Graduate Program in Marine Science, University of California, Santa Barbara, CA 93106, USA

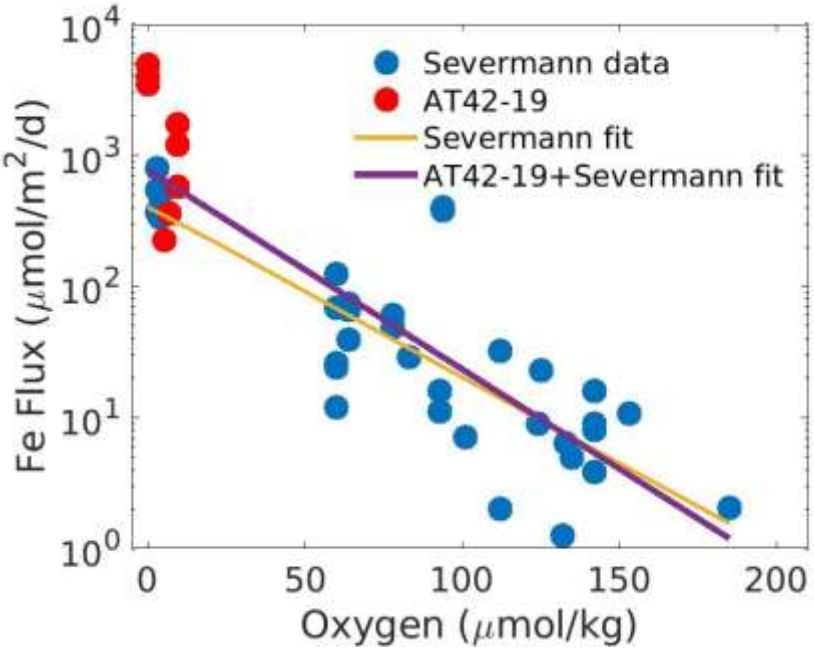


**Figure S3- 1.** Combined benthic Fe flux data as a function of bottom oxygen from Robinson et al. (2024). Blue dots show benthic Fe flux data compiled by Severmann et al. (2010); red dots represent benthic Fe flux data from Robinson et al . (2024). The yellow line shows an exponential fits to the dataset by Severmann et al. (2010) while the purple line illustrates the updated exponential fit from combined benthic Fe flux (red and blue).

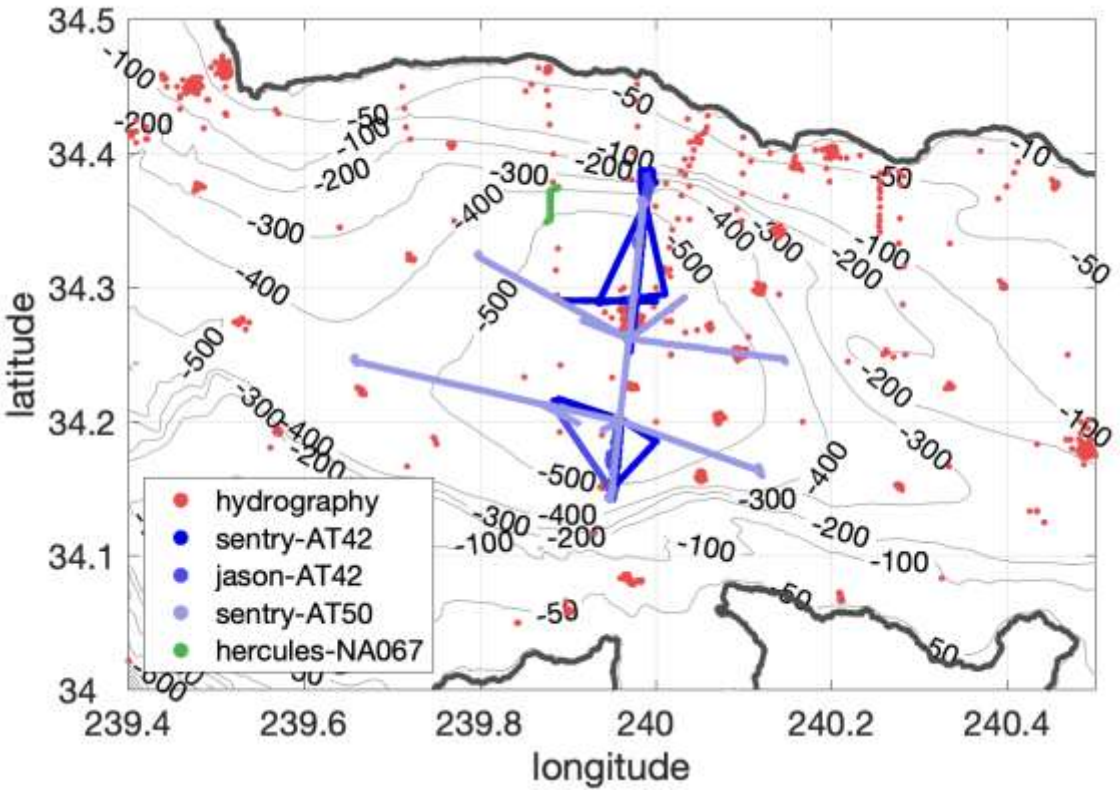


**Figure S3- 2.** The distribution of oxygen profiles and transects throughout the channel. The variations in blue represent the transect for Remotely Operated Vehicle (ROV) Jason and Autonomous Underwater Vehicle (AUV) Sentry, while ROV Hercules is in green. The points in red represent oxygen profiles California Cooperative Oceanic Fisheries (CalCOFI) and other hydrographic data. Isolines show the water depth in m.

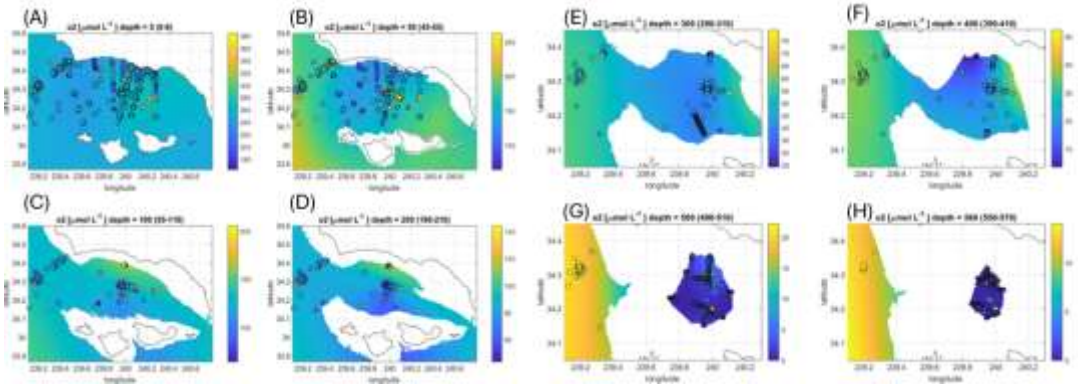


**Figure S3- 3.** Spatial oxygen distribution. Oxygen (μmol $L^{-1}$) distributions from the gridded dataset (color gradient) at 5 m (A), 50 m (B), 100 m (C), 200 m (D), 300 m (E), 400 m (F), 500 m (G), and 560 m (H). Circles show observed oxygen concentrations. Note the change in the range of oxygen values between different panels.

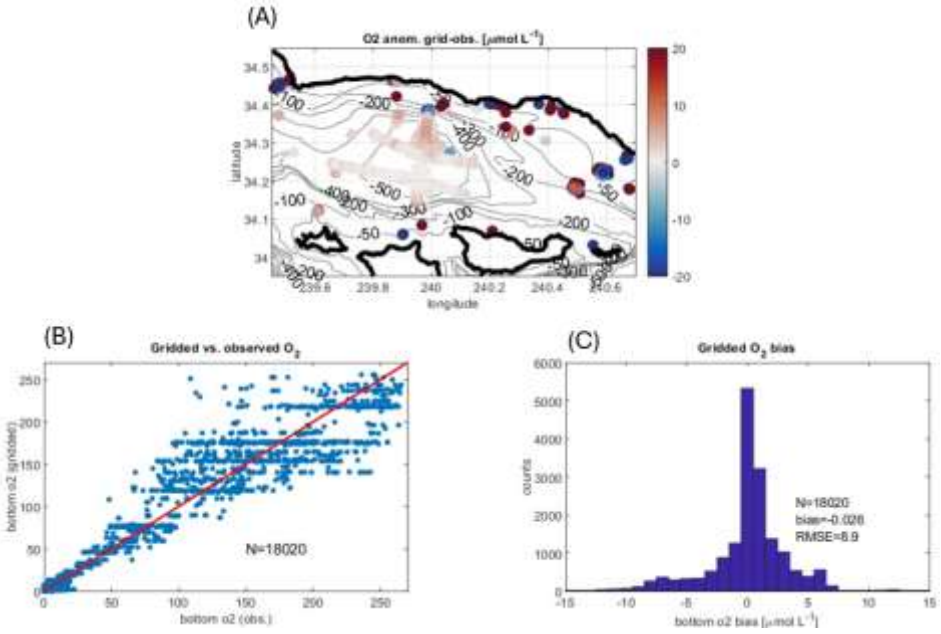


**Figure S3- 4.** Statistics of oxygen distribution for near bottom oxygen reconstruction. (A) shows the oxygen anomalies that tend to be < 10 $\mu$mol $L^{-1}$ and centered around zero. (B) illustrates the correlation between observed and gridded oxygen with a scatter-plot (C) illustrates the correlation between observed and gridded oxygen with a histogram.

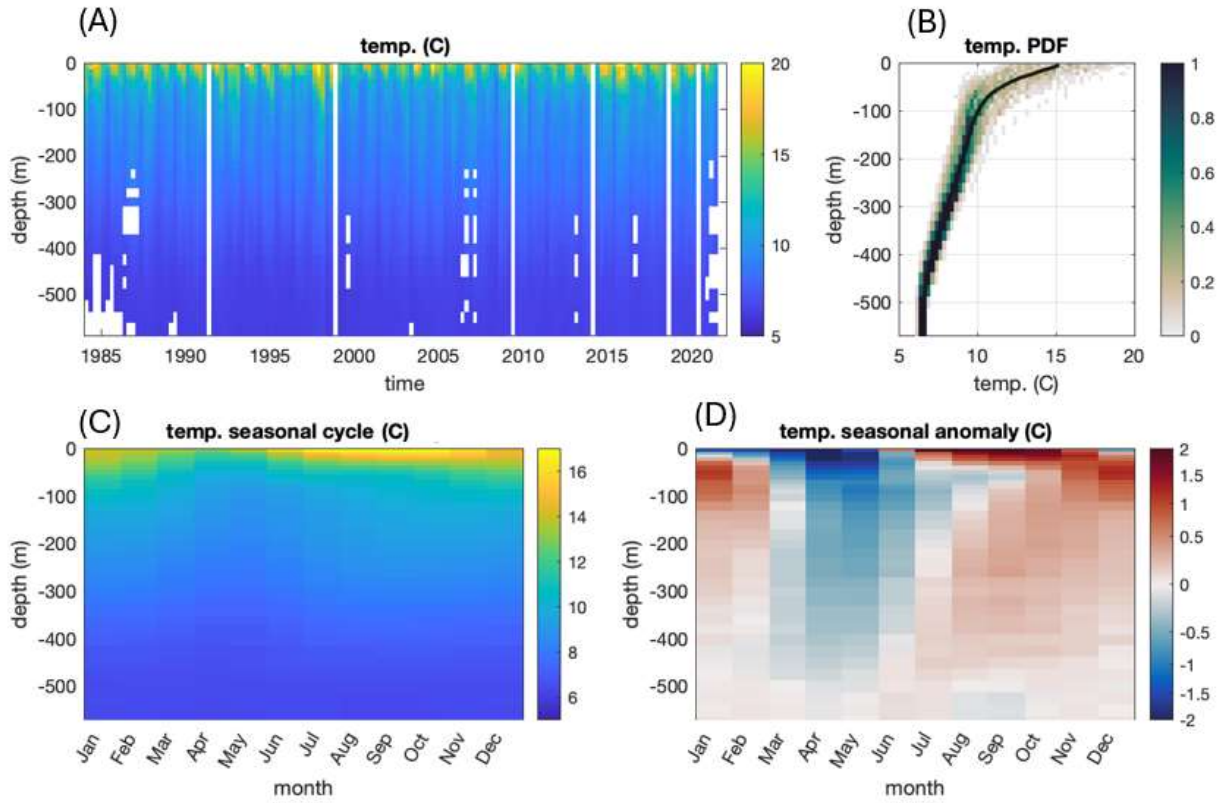


**Figure S3- 5.** Temporal variability of temperature (°C) the for the SBC only. (A) Hovmöller diagram of temperature at 4-month (seasonal) intervals. Note the uneven vertical bin width. (B) Profile showing the "probability distribution function" of temperature as a function of depth, essentially the variability, and the mean. (C) The seasonal cycle at 2 months resolution, and (D) the seasonal anomalies relative to the mean.

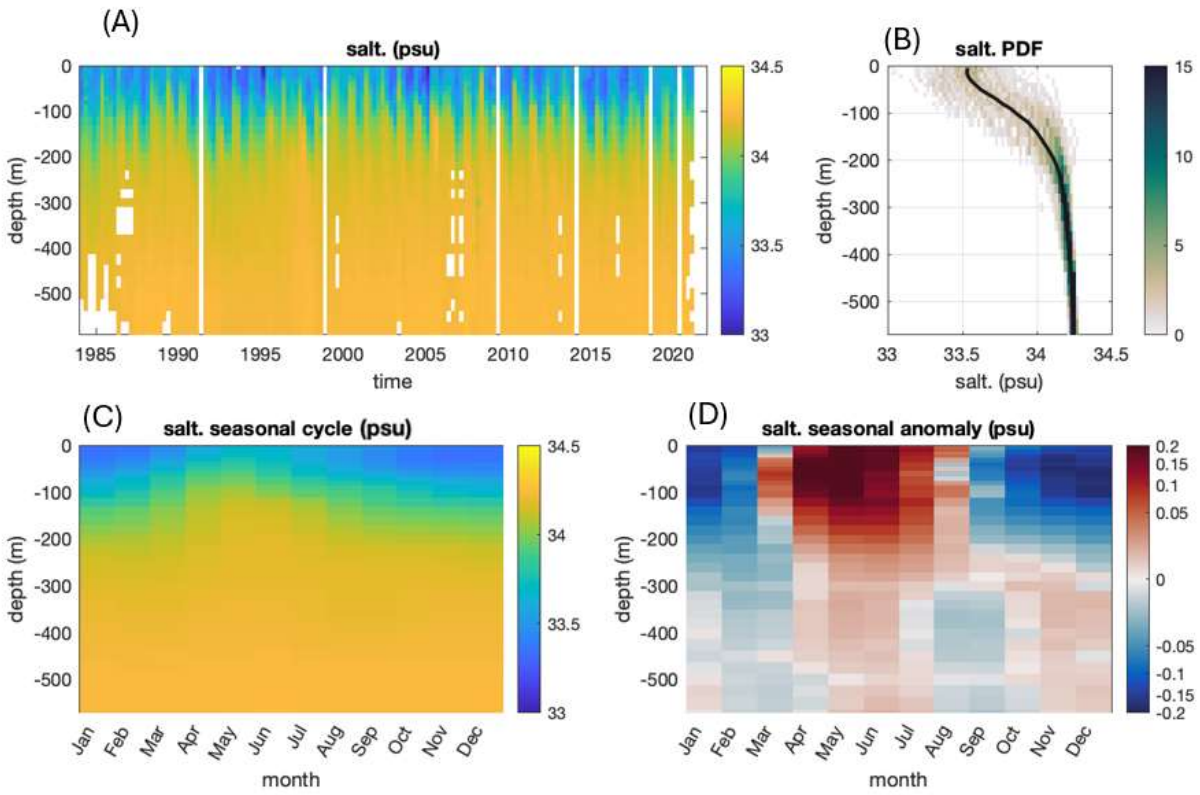


**Figure S3- 6.** Temporal variability of salinity (PSU) the for the SBC only. (A) Hovmöller diagram of salinity at 4-month (seasonal) intervals. Note the uneven vertical bin width. (B) profile showing the "probability distribution function" of salinity as a function of depth, essentially the variability, and the mean. (C) The seasonal cycle at 2 months resolution, and (D) the seasonal anomalies relative to the mean.

## References

Berg, J. S., Ahmerkamp, S., Pjevac, P., Hausmann, B., Milucka, J., and Kuypers, M. M. M.: How low can they go? Aerobic respiration by microorganisms under apparent anoxia, FEMS Microbiol. Rev., 46, fuac006, https://doi.org/10.1093/femsre/fuac006, 2022.

Bernhard, J. M., Casciotti, K. L., McIlvin, M. R., Beaudoin, D. J., Visscher, P. T., and Edgcomb, V. P.: Potential importance of physiologically diverse benthic foraminifera in sedimentary nitrate storage and respiration, J. Geophys. Res. Biogeosciences, 117, https://doi.org/10.1029/2012JG001949, 2012.

Bianchi, D., Dunne, J. P., Sarmiento, J. L., and Galbraith, E. D.: Data-based estimates of suboxia, denitrification, and N2O production in the ocean and their sensitivities to dissolved O2, Glob. Biogeochem. Cycles, 26, https://doi.org/10.1029/2011GB004209, 2012.

Bograd, S. J., Schwing, F. B., Castro, C. G., and Timothy, D. A.: Bottom water renewal in the Santa Barbara Basin, J. Geophys. Res. Oceans, 107, 9-1-9–9, https://doi.org/10.1029/2001JC001291, 2002.

Bograd, S. J., Castro, C. G., Di Lorenzo, E., Palacios, D. M., Bailey, H., Gilly, W., and Chavez, F. P.: Oxygen declines and the shoaling of the hypoxic boundary in the California Current, Geophys. Res. Lett., 35, https://doi.org/10.1029/2008GL034185, 2008.

Bray, N. A., Keyes, A., and Morawitz, W. M. L.: The California Current system in the Southern California Bight and the Santa Barbara Channel, J. Geophys. Res. Oceans, 104, 7695–7714, https://doi.org/10.1029/1998JC900038, 1999.

Brzezinski, M. A. and Washburn, L.: Phytoplankton primary productivity in the Santa Barbara Channel: Effects of wind-driven upwelling and mesoscale eddies, J. Geophys. Res. Oceans, 116, https://doi.org/10.1029/2011JC007397, 2011.

Burdige, D. J., Komada, T., Magen, C., and Chanton, J. P.: Modeling studies of dissolved organic matter cycling in Santa Barbara Basin (CA, USA) sediments, Geochim. Cosmochim. Acta, 195, 100–119, https://doi.org/10.1016/j.gca.2016.09.007, 2016.

Chanton, J. P., Martens, C. S., and Goldhaber, M. B.: Biogeochemical cycling in an organic-rich coastal marine basin. 7. Sulfur mass balance, oxygen uptake and sulfide retention, Geochim. Cosmochim. Acta, 51, 1187–1199, https://doi.org/10.1016/0016-7037(87)90211-0, 1987.

Checkley, D. M. and Barth, J. A.: Patterns and processes in the California Current System, Prog. Oceanogr., 83, 49–64, https://doi.org/10.1016/j.pocean.2009.07.028, 2009.

Chhak, K. and Di Lorenzo, E.: Decadal variations in the California Current upwelling cells, Geophys. Res. Lett., 34, https://doi.org/10.1029/2007GL030203, 2007.

Evans, N., Schroeder, I. D., Pozo Buil, M., Jacox, M. G., and Bograd, S. J.: Drivers of Subsurface Deoxygenation in the Southern California Current System, Geophys. Res. Lett., 47, e2020GL089274, https://doi.org/10.1029/2020GL089274, 2020.

Franco, A. C., Kim, H., Frenzel, H., Deutsch, C., Ianson, D., Sumaila, U. R., and Tortell, P. D.: Impact of warming and deoxygenation on the habitat distribution of Pacific halibut in the Northeast Pacific, Fish. Oceanogr., 31, 601–614, https://doi.org/10.1111/fog.12610, 2022.

García-Reyes, M. and Largier, J.: Observations of increased wind-driven coastal upwelling off central California, J. Geophys. Res., 115, C04011, https://doi.org/10.1029/2009JC005576, 2010.

Goericke, R., Bograd, S. J., and Grundle, D. S.: Denitrification and flushing of the Santa Barbara Basin bottom waters, Deep Sea Res. Part II Top. Stud. Oceanogr., 112, 53–60, https://doi.org/10.1016/j.dsr2.2014.07.012, 2015.

Hendershott and Winant: Surface Circulation in the Santa Barbara Channel, Oceanography, 9, 114–121, https://doi.org/10.5670/oceanog.1996.14, 1996.

Keeling, R. F., Körtzinger, A., and Gruber, N.: Ocean Deoxygenation in a Warming World, Annu. Rev. Mar. Sci., 2, 199–229, https://doi.org/10.1146/annurev.marine.010908.163855, 2010.

Kessouri, F., Renault, L., McWilliams, J. C., Damien, P., and Bianchi, D.: Enhancement of Oceanic Eddy Activity by Fine-Scale Orographic Winds Drives High Productivity, Low Oxygen, and Low pH Conditions in the Santa Barbara Channel, J. Geophys. Res. Oceans, 127, e2022JC018947, https://doi.org/10.1029/2022JC018947, 2022.

Krause, S. J. E., Liu, J., Yousavich, D. J., Robinson, D., Hoyt, D. W., Qin, Q., Wenzhöfer, F., Janssen, F., Valentine, D. L., and Treude, T.: Evidence of cryptic methane cycling and non-methanogenic methylamine consumption in the sulfate-reducing zone of sediment in the Santa Barbara Basin, California, Biogeosciences, 20, 4377–4390, https://doi.org/10.5194/bg-20-4377-2023, 2023.

Laufkötter, C., John, J. G., Stock, C. A., and Dunne, J. P.: Temperature and oxygen dependence of the remineralization of organic matter, Glob. Biogeochem. Cycles, 31, 1038–1050, https://doi.org/10.1002/2017GB005643, 2017.

Levin, L. A. and Breitburg, D. L.: Linking coasts and seas to address ocean deoxygenation, Nat. Clim. Change, 5, 401–403, https://doi.org/10.1038/nclimate2595, 2015.

Levitus, S.: Climatological Atlas of the World Ocean, Eos Trans. Am. Geophys. Union, 64, 962–963, https://doi.org/10.1029/EO064i049p00962-02, 1983.

Llapapasca, M. A., Pardo, M. A., Grados, D., and Quiñones, J.: The oxygen minimum zone relative depth is a key driver of dolphin habitats in the northern Humboldt Current System, Front. Mar. Sci., 9, 2022.

Low, N. H. N., Micheli, F., Aguilar, J. D., Arce, D. R., Boch, C. A., Bonilla, J. C., Bracamontes, M. Á., De Leo, G., Diaz, E., Enríquez, E., Hernandez, A., Martinez, R., Mendoza, R., Miranda, C., Monismith, S., Ramade, M., Rogers-Bennett, L., Romero, A., Salinas, C., Smith, A. E., Torre, J., Villavicencio, G., and Woodson, C. B.: Variable coastal hypoxia exposure and drivers across the southern California Current, Sci. Rep., 11, 10929, https://doi.org/10.1038/s41598-021-89928-4, 2021.

McCormick, L. R. and Levin, L. A.: Physiological and ecological implications of ocean deoxygenation for vision in marine organisms, Philos. Transact. A Math. Phys. Eng. Sci., 375, 20160322, https://doi.org/10.1098/rsta.2016.0322, 2017.

McWilliams, J. C., Damien, P., and Kessouri, F.: Circulation and Dispersal in California's Borderland Basins, https://doi.org/10.22541/essoar.171017133.39619177/v1, 11 March 2024.

Morée, A. L., Clarke, T. M., Cheung, W. W. L., and Frölicher, T. L.: Impact of deoxygenation and warming on global marine species in the 21st century, Biogeosciences, 20, 2425–2454, https://doi.org/10.5194/bg-20-2425-2023, 2023.

Myhre, S. E., Pak, D., Borreggine, M., Kennett, J. P., Nicholson, C., Hill, T. M., and Deutsch, C.: Oxygen minimum zone biotic baseline transects for paleoceanographic reconstructions in Santa Barbara Basin, CA, Deep Sea Res. Part II Top. Stud. Oceanogr., 150, 118–131, https://doi.org/10.1016/j.dsr2.2017.12.009, 2018.

Oschlies, A., Brandt, P., Stramma, L., and Schmidtko, S.: Drivers and mechanisms of ocean deoxygenation, Nat. Geosci., 11, 467–473, https://doi.org/10.1038/s41561-018-0152-2, 2018.

Peng, X., Yousavich, D. J., Bourbonnais, A., Wenzhoefer, F., Janssen, F., Treude, T., and Valentine, D. L.: The fate of fixed nitrogen in Santa Barbara Basin sediments during seasonal anoxia, EGUsphere, 1–26, https://doi.org/10.5194/egusphere-2023-1498, 2023.

Pozo Buil, M. and Di Lorenzo, E.: Decadal dynamics and predictability of oxygen and subsurface tracers in the California Current System, Geophys. Res. Lett., 44, 4204–4213, https://doi.org/10.1002/2017GL072931, 2017.

Qin, Q., Kinnaman, F. S., Gosselin, K. M., Liu, N., Treude, T., and Valentine, D. L.: Seasonality of water column methane oxidation and deoxygenation in a dynamic marine environment, Geochim. Cosmochim. Acta, 336, 219–230, https://doi.org/10.1016/j.gca.2022.09.017, 2022.

Reimers, C. E., Lange, C. B., Tabak, M., and Bernhard, J. M.: Seasonal spillover and varve formation in the Santa Barbara Basin, California, Limnol. Oceanogr., 35, 1577–1585, https://doi.org/10.4319/lo.1990.35.7.1577, 1990.

Renault, L., Deutsch, C., McWilliams, J. C., Frenzel, H., Liang, J.-H., and Colas, F.: Partial decoupling of primary productivity from upwelling in the California Current system, Nat. Geosci., 9, 505–508, https://doi.org/10.1038/ngeo2722, 2016.

Robinson, C.: Microbial Respiration, the Engine of Ocean Deoxygenation, Front. Mar. Sci., 5, 2019.

Robinson, D., Pham, A. L. D., Yousavich, D. J., Janssen, F., Wenzhöfer, F., Arrington, E. C., Gosselin, K. M., Sandoval-Belmar, M., Mar, M., Valentine, D. L., Bianchi, D., and Treude, T.: Iron “Ore” Nothing: Benthic iron fluxes from the oxygen-deficient Santa Barbara Basin enhance phytoplankton productivity in surface waters, Biogeosciences Discuss., 1–36, https://doi.org/10.5194/bg-2022-237, 2022.

Robinson, D., Pham, A. L. D., Yousavich, D. J., Janssen, F., Wenzhöfer, F., Arrington, E. C., Gosselin, K. M., Sandoval-Belmar, M., Mar, M., Valentine, D. L., Bianchi, D., and Treude, T.: Iron “ore” nothing: benthic iron fluxes from the oxygen-deficient Santa Barbara Basin enhance phytoplankton productivity in surface waters, Biogeosciences, 21, 773–788, https://doi.org/10.5194/bg-21-773-2024, 2024.

Sánchez-Velasco, L., Godínez, V. M., Ruvalcaba-Aroche, E. D., Márquez-Artavia, A., Beier, E., Barton, E. D., and Jiménez-Rosenberg, S. P. A.: Larval Fish Habitats and Deoxygenation in the Northern Limit of the Oxygen Minimum Zone off Mexico, J. Geophys. Res. Oceans, 124, 9690–9705, https://doi.org/10.1029/2019JC015414, 2019.

Sandoval-Belmar, M., Smith, J., Moreno, A. R., Anderson, C., Kudela, R. M., Sutula, M., Kessouri, F., Caron, D. A., Chavez, F. P., and Bianchi, D.: A cross-regional examination of patterns and environmental drivers of *Pseudo-nitzschia* harmful algal blooms along the California coast, Harmful Algae, 126, 102435, https://doi.org/10.1016/j.hal.2023.102435, 2023.

Schmidtko, S., Stramma, L., and Visbeck, M.: Decline in global oceanic oxygen content during the past five decades, Nature, 542, 335–339, https://doi.org/10.1038/nature21399, 2017.

Severmann, S., McManus, J., Berelson, W. M., and Hammond, D. E.: The continental shelf benthic iron flux and its isotope composition, Geochim. Cosmochim. Acta, 74, 3984–4004, https://doi.org/10.1016/j.gca.2010.04.022, 2010a.

Severmann, S., McManus, J., Berelson, W. M., and Hammond, D. E.: The continental shelf benthic iron flux and its isotope composition, Geochim. Cosmochim. Acta, 74, 3984–4004, https://doi.org/10.1016/j.gca.2010.04.022, 2010b.

Shepherd, J. G., Brewer, P. G., Oschlies, A., and Watson, A. J.: Ocean ventilation and deoxygenation in a warming world: introduction and overview, Philos. Trans. R. Soc. Math. Phys. Eng. Sci., 375, 20170240, https://doi.org/10.1098/rsta.2017.0240, 2017.

Sholkovitz, E. R. and Gieskes, J. M.: A PHYSICAL-CHEMICAL STUDY OF THE FLUSHING OF THE SANTA BARBARA BASIN1: FLUSHING OF THE SANTA BARBARA BASIN, Limnol. Oceanogr., 16, 479–489, https://doi.org/10.4319/lo.1971.16.3.0479, 1971.

Sigman, D. M., Robinson, R., Knapp, A. N., van Geen, A., McCorkle, D. C., Brandes, J. A., and Thunell, R. C.: Distinguishing between water column and sedimentary denitrification in the Santa Barbara Basin using the stable isotopes of nitrate, Geochem. Geophys. Geosystems, 4, https://doi.org/10.1029/2002GC000384, 2003.

Stramma, L., Schmidtko, S., Levin, L. A., and Johnson, G. C.: Ocean oxygen minima expansions and their biological impacts, Deep Sea Res. Part Oceanogr. Res. Pap., 57, 587–595, https://doi.org/10.1016/j.dsr.2010.01.005, 2010.

Stramma, L., Prince, E. D., Schmidtko, S., Luo, J., Hoolihan, J. P., Visbeck, M., Wallace, D. W. R., Brandt, P., and Körtzinger, A.: Expansion of oxygen minimum zones may reduce available habitat for tropical pelagic fishes, Nat. Clim. Change, 2, 33–37, https://doi.org/10.1038/nclimate1304, 2012.

Thunell, R. C.: Particle fluxes in a coastal upwelling zone: sediment trap results from Santa Barbara Basin, California, Deep Sea Res. Part II Top. Stud. Oceanogr., 45, 1863–1884, https://doi.org/10.1016/S0967-0645(98)80020-9, 1998.

Tiano, L., Garcia-Robledo, E., Dalsgaard, T., Devol, A. H., Ward, B. B., Ulloa, O., Canfield, D. E., and Peter Revsbech, N.: Oxygen distribution and aerobic respiration in the north and south eastern tropical Pacific oxygen minimum zones, Deep Sea Res. Part Oceanogr. Res. Pap., 94, 173–183, https://doi.org/10.1016/j.dsr.2014.10.001, 2014.

Valentine, D. L., Fisher, G. B., Pizarro, O., Kaiser, C. L., Yoerger, D., Breier, J. A., and Tarn, J.: Autonomous Marine Robotic Technology Reveals an Expansive Benthic Bacterial Community Relevant to Regional Nitrogen Biogeochemistry, Environ. Sci. Technol., 50, 11057–11065, https://doi.org/10.1021/acs.est.6b03584, 2016.

Wallmann, K., José, Y. S., Hopwood, M. J., Somes, C. J., Dale, A. W., Scholz, F., Achterberg, E. P., and Oschlies, A.: Biogeochemical feedbacks may amplify ongoing and future ocean deoxygenation: a case study from the Peruvian oxygen minimum zone, Biogeochemistry, 159, 45–67, https://doi.org/10.1007/s10533-022-00908-w, 2022.

White, M. E., Rafter, P. A., Stephens, B. M., Wankel, S. D., and Aluwihare, L. I.: Recent Increases in Water Column Denitrification in the Seasonally Suboxic Bottom Waters of the Santa Barbara Basin, Geophys. Res. Lett., 46, 6786–6795, https://doi.org/10.1029/2019GL082075, 2019.

World Ocean Atlas: https://www.ncei.noaa.gov/products/world-ocean-atlas, last access: 29 May 2024.

Yamamoto, A., Hajima, T., Yamazaki, D., Noguchi Aita, M., Ito, A., and Kawamiya, M.: Competing and accelerating effects of anthropogenic nutrient inputs on climate-driven changes in ocean carbon and oxygen cycles, Sci. Adv., 8, eabl9207, https://doi.org/10.1126/sciadv.abl9207, 2022.

Yousavich, D. J., Robinson, D., Peng, X., Krause, S. J. E., Wenzhöfer, F., Janssen, F., Liu, N., Tarn, J., Kinnaman, F., Valentine, D. L., and Treude, T.: Marine anoxia initiates giant sulfur-oxidizing bacterial mat proliferation and associated changes in benthic nitrogen, sulfur, and iron cycling in the Santa Barbara Basin, California Borderland, Biogeosciences, 21, 789–809, https://doi.org/10.5194/bg-21-789-2024, 2024.

## Chapter 4: Implementing deoxygenation for Biodiversity Beyond National Jurisdiction Treaty: Opportunities for governance and management across scales and levels

**De'Marcus Robinson**[1*], Richard Gragg[2], Daniele Bianchi[1], Tina Treude[1,3*]

[1]Department of Atmospheric and Oceanic Sciences, University of California Los Angeles, Los Angeles, CA, USA

[2]Florida Agricultural and Mechanical University,
Tallahassee, FL

[3]Department of Earth, Planetary, and Space Sciences, University of California Los Angeles, Los Angeles, CA, USA

**Abstract**

Global deoxygenation is an emerging issue in ocean policy that intersects with other ocean issues such as ocean acidification, climate impacts on marine species and marine conservation. However, deoxygenation has not appeared in international ocean policy even though the loss of oxygen transcends national and international jurisdiction. The Biodiversity Beyond National Jurisdiction Treaty (BBNJ) or "High Seas Treaty" provides an opportunity to implement deoxygenation for the High Seas. To do so we developed a framework for deoxygenation using scale and levels based on scientific understanding and consensus on the loss of oxygen that intersect with ocean governance. We identify that advancing science and technology using $GO_2DAT$ to implement deoxygenation policy in BBNJ agreement could address deoxygenation globally. Our framework illustrates how ocean governance can advance ocean policy for deoxygenation that intersects with the initiative in BBNJ.

## 1. Introduction

The governance and management structure of the ocean is multifaceted, with a myriad of governments in territorial states and countries with jurisdictional regulations and laws that manage, protect, and utilize the ocean for overall ocean sustainability and human benefit (Adewumi, 2021; Barbier, 2017; Carvalho et al., 2023; Haas et al., 2022; Intergovernmental Panel On Climate Change (IPCC), 2023; Palumbi et al., 2009; Young et al., 2007)

However, governance and management of the ocean can be complex, because of the transboundary nature of the ocean and its marine inhabitants. Complexities involving impacts of pollution, fisheries management disputes, and climate change can spillover and transcend beyond nation-states jurisdictions, or into areas beyond national jurisdiction (Adler, 2005; Halpern et al., 2019; Palacios-Abrantes et al., 2020; van Tatenhove, 2017).

To address some of these challenges, international laws and regulations through the United Nation Convention on the Law of the Sea (UNCLOS), provide the overall legal framework for international and national maritime law and security (United Nations Convention on the Law of the Sea, 1982) along with International Maritime Organization, London Convention, and Regional Fisheries Management Organization. UNCLOS also governs over matters relating maritime security, energy production, conservations, fisheries management, environment regulations, and laws for establishing jurisdictional boundaries from the Exclusive Economic Zones (EEZ) to the high-seas (United Nations Convention on the Law of the Sea, 1982). Furthermore, maritime law has also been accompanied by international cooperation though multi-national initiatives including the High Ocean Panel for a Sustainable Ocean Economy, United Nation Ocean Decade for Ocean Sustainability, Ocean Acidification Alliance, ocean and climate dialogue at the United Nations Framework Convention on Climate Change, and the Intergovernmental Oceanographic

Commission (IOC); along with outside cooperation from non-governmental organizations, academic and research institutions, Indigenous and Tribal communities, and the public. However, with a myriad of stakeholder engagement, and national and international cooperation, challenges still arise for ocean governance and management, that is similar to other types of environmental management efforts across human-environmental systems, like forestry management and agriculture (von Braun and Birner, 2017; Schultz et al., 2019).

The ocean's dissolved oxygen is essential to the marine environment that supports aquatic life at all trophic levels within the terrestrial and marine food web, including migratory birds, marine mammals, fish, invertebrates, zooplankton and microbes (Franco et al., 2022; McCormick and Levin, 2017; Sánchez-Velasco et al., 2019). However, global ocean oxygen concentrations have decreased by approximately 2% since the 1950's ((Schmidtko et al., 2017). Moreover, since the 1950's, 500 coastal areas have undergone hypoxia, which here is defined as dissolved oxygen concentrations below 2 mg $L^{-1}$ (= 63 μmol $L^{-1}$ or ≅61 μmol $kg^{-1}$) (Breitburg et al., 2018). The main driver for the decline of oxygen in coastal waters is eutrophication caused by excess nutrient loading from anthropogenic sources, such as agriculture, which is particular severe in upwelling regions, and the resulting oxygen consumption caused by the decay of excess phytoplankton biomass. In contrast, deoxygenation in the open ocean is caused by a combination of increase in sea surface temperature, increase in remineralization, and slow-down in circulation, which remain uncertain (Levin and Breitburg, 2015; Limburg et al., 2020; Fennel and Testa, 2019).

Deoxygenation is an emerging issue for ocean policy that overlaps with ocean biodiversity, management of marine protected areas, ocean sustainability (Haas et al., 2022) and ocean acidification (Bates and Johnson, 2020). Both deoxygenation and acidification are coupled to ocean (biogeo)chemistry. Planetary Boundaries, an influential policy framework, defines the nine

environmental limits within which humanity can safely operate. Deoxygenation intersects with six of these planetary boundaries ('E. Ferrer, unpubl. data.'), that include ocean acidification, biogeochemical flows, land-systems change, biosphere integrity and climate change (Richardson et al., 2023; Steffen et al., 2015).

Calls to include and advance deoxygenation science and policy have been echoed by scientists through various channels, including local efforts, through monitoring and research (Grégoire et al., 2021); nationally, through laws like the Harmful Algal Bloom and Hypoxia Research Control Act in the United States (The Harmful Algal Bloom and Hypoxia Research and Control Amendments Act (HABHRCA), 2021); and internationally through the Global Ocean Oxygen Network (Global Ocean Oxygen Network, 2016), Keil Declaration (Kiel Declaration on Ocean Deoxygenation, 2018) and IOC Intergovernmental Panel on Harmful Algal Blooms. However, not until recently, through the signing of the Biodiversity Beyond National Jurisdiction (BBNJ) Agreement, adopted June 19th, 2023, by the Intergovernmental Conference on Marine Biodiversity on Areas Beyond National Jurisdiction, has deoxygenation been structurally embedded into international ocean policy (Agreement under the United Nations Convention on the Law of the Sea on the conservation and sustainable use of marine biological diversity of areas beyond national jurisdiction, 2023) .

A systematic framework is required to implement deoxygenation governance and management in the High Seas called for in the BBNJ. This implementation could include the following initiatives: deploying a multinational oxygen observation program; advance technology for ocean observation; advancing our understanding of the synergistic relationship of deoxygenation with marine biodiversity, climate change and sustainable development. Lastly

implementation would need multilateral communication on the impact of deoxygenation on fisheries management, to prevent future fisheries disputes.

To properly implement deoxygenation governance and management into ocean policy regarding social-environmental dynamics, there needs to be more attention to the intersection of natural and human-social systems. Analyzing such intersection can be achieved by analyzing the spatial, temporal, quantitative, or analytical dimensions used to study or measure the specific phenomenon, or system. Political and social scientists call these dimensions "scales" (Cash et al., 2006): "Scales are accompanied by levels, which are units of analysis located at different positions on a scale, over which certain processes operate". For instance, a scale for an institution as a category can include multiple levels, e.g., from student to president of a university, or jurisdictional scale, with levels from localities to international. Identifying a scale for a system and assessing the levels can be useful for simplifying understanding of the dynamics and interaction of a system. For instance, instead of analyzing a global marine food web, it may be advantageous to assess a marine food chain in a certain region, and then expand from there. Simplifying scales can reduce the overburden and complexity that arises in human-environmental interactions and policies and allows for the reassessment of intersection of scales and levels. Recognizing and exploiting scales and levels provides an important understanding of the interactions between natural and human systems and the cross-scale and cross-level interactions over time and space. Implementation of scales and levels has been applied to fisheries management, forest industry and water quality (May, 2013; Patrick et al., 2014; Schultz et al., 2019).

However, misalignment of scales and levels between social-environmental systems contributes to scale challenges. These are defined as conditions in which cross-scale and cross-level interactions interact in such a way that the resilience of a human-environment system is

threatened or undermined (Cumming et al., 2006; Schultz et al., 2019). An example of misalignment is the decline of local fish stocks because of climate change, and the resulting impact to local communities, which can conflict with local and federal policy relating to outdated fisheries management. Another example are local activities to mitigate global carbon dioxide emissions with small scale marine carbon dioxide removal technologies (Pomeroy et al., 2019; Yang et al., 2023). However, scale challenges can be addressed with the proper alignment between social and natural systems, in which the scales and levels complement each other. For example, marine spatial planning for a marine protected area designed to match the spatial habitat for a protected species (Cash et al., 2006; Cumming et al., 2006; Schultz et al., 2019).

Scales and levels can be developed and implemented for deoxygenation under the BBNJ framework to address global deoxygenation and its detrimental impacts on marine species and chemistry. The goal of this present study is to analyze the factors that are most relevant to the development of an ocean deoxygenation policy for the BBNJ Agreement, based upon the framework developed by Cash et al. (2006). The following sections are organized as follows: first, we provide a brief overview of deoxygenation and the establishment of hypoxia in the ocean; second, we develop scales and levels for the most relevant factors that influence deoxygenation and social-human governance structure; and third, we apply these scales and levels to the four issues addressed by BBNJ, which include: Environmental Impact Assessment, Marine Genetic Resource, Area Based Management Tools, and Capacity Building and Transfer of Marine Technology.

## 2. Brief overview of Ocean Deoxygenation

Oxygen is essential for aerobic respiration for marine organisms in marine ecosystems. The causes of the ongoing oceanic oxygen decline are multifaceted and can be attributed to warming at the surface because of anthropogenic climate change, increases in nutrients such as nitrate and phosphate in coastal waters, and a slowdown in ocean circulation that reduces ventilation and increases the residence time of water masses below the ocean's surface (Keeling et al., 2010; Oschlies et al., 2018; Rabalais et al., 2014). Deoxygenation can cause habitat compression and mortality for aerobic pelagic and benthic organisms, amplify ocean acidification, and stimulate the release of nutrients and trace elements from the sediment into the water column (Bates and Johnson, 2020; Franco et al., 2022; Sánchez-Velasco et al., 2019). Under declining oxygen concentrations, certain areas of the ocean can also be pushed to hypoxic (< 65 μM) or anoxic (> 0 μM) conditions (Morée et al., 2023; Craig, 2020; Kwiatkowski et al., 2020; Breitburg et al., 2018; Ekau et al., 2010; Noffke et al., 2012).

The historical decline in coastal oxygen is generally attributed to eutrophication of coastal waters (Rabalais et al., 2014), caused by the growing input of nutrients from terrestrial sources such as river runoff (Rabalais et al., 2014). Deoxygenation is particularly relevant in regions that are naturally characterized by elevated nutrient inputs and low oxygen, such as coastal upwelling systems (Chan et al., 2008). Globally, 50% of open-ocean oxygen loss has been attributed to the decrease in oxygen solubility caused by ocean warming (Schmidtko et al., 2017). The other half of oxygen loss is caused by a combination of physical and biological processes.

Warming of surface waters also increases ocean stratification by enhancing the density contrast between surface and deep waters. This in turn reduces wind-driven mixing and shoals the

surface mixed layer, contributing to a decline in the turbulent transfer of oxygen from the surface to the ocean interior (Oschlies et al., 2018). Below the mixed layer, a decline in the rate of subduction of oxygen-rich waters and transport by ocean currents, also referred to as ventilation, decreases the supply of oxygen to the oceanic thermocline. This is accompanied by a slowdown in the formation and flow rates of deep waters that form the global meridional overturning circulation, deeper in the water column (Shepherd et al., 2017). A slowdown in the shallow and deep circulation rates increases the residence time of oceanic water masses, which, coupled to interior remineralization, causes a progressive decline in oxygen concentrations. These processes may be locally exacerbated by increasing remineralization rates as the ocean warms. Over shorter timescales, interannual to decadal climate variability can be an additional contributor to oxygen loss. This is for example observed during different phases of El Niño-Southern Oscillation (ENSO), the dominant recurring climate pattern across the tropical Pacific Ocean. During the warm El Niño phase, a decrease in equatorial and coastal upwelling reduces oxygen loss in the eastern tropical Pacific, while warming conditions in the central and western tropical Pacific cause a reduction in oxygen because of decreased solubility. In contrast, during the cold La Niña phase increased upwelling drives rapid oxygen loss in subsurface waters in the eastern side of the Pacific basin (Yang et al., 2017). On multi-decadal timescales, climate fluctuations such as the Pacific Decadal Oscillation drive widespread changes in thermocline oxygen, with progressive expansion and contractions of hypoxic waters in the tropical Pacific Ocean (Deutsch et al., 2011).

While the economic impact of global deoxygenation has not been quantified, we can assume that it is in the trillion (USD) dollars when considering open ocean and coastal oxygen loss. Understanding deoxygenation as a stressor in combination with other stressors like ocean acidification and ocean warming is paramount in management, mitigation, and impact on marine

species (Bates and Johnson, 2020). To address the impacts of deoxygenation, national and international efforts through the IOC Intergovernmental Panel on Harmful Algal Blooms, have been undertaken. These efforts are specifically aimed at mitigating and reducing the occurrence of human-induced deoxygenation, while current scientific studies are underway to understand the broader impacts of deoxygenation (Grégoire et al., 2021).

## 3. Developing scales and levels for ocean deoxygenation and ocean policy

To implement deoxygenation for the BBNJ Agreement, scales need to be developed for deoxygenation, along with the scales for governance (Fig 4-1). The drivers of deoxygenation in the ocean are complex and numerous, but can be reduced and homogenized into scales of biogeochemistry, temperature, ocean physical variability and temporality with levels that reflect changes in condition (Fig. 4-1 (A, D)), or the increase in magnitude and duration of a process (Fig 4-1 **(**B,D)). These chosen scales for deoxygenation can also have cross-scale interactions, for instance the physical aspect of the ocean can be represented at various temporal levels, where changes in stratification can be a contributor to loss of oxygen.

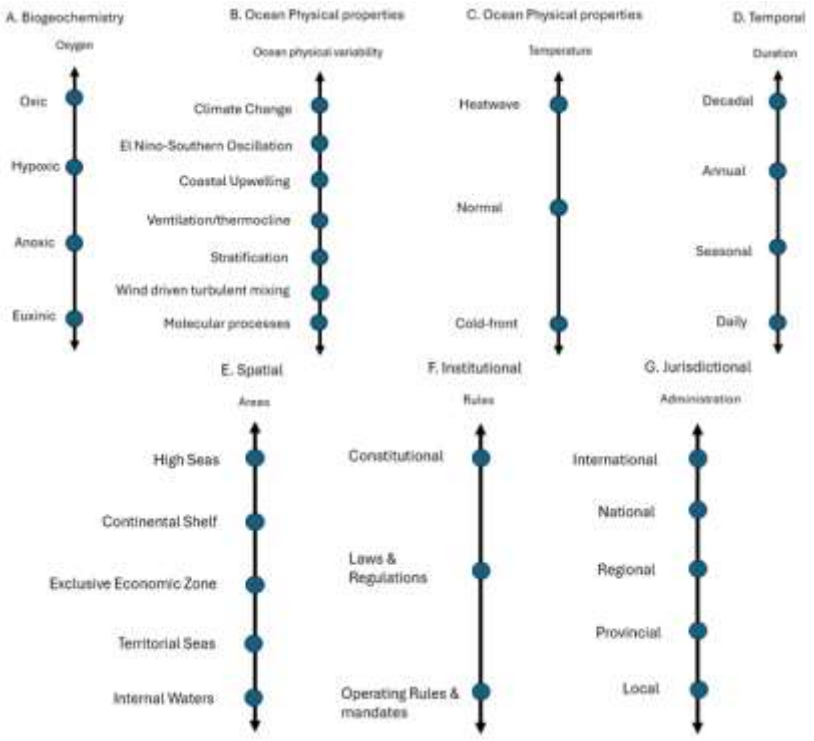


**Figure 4- 1.** Schematic illustrating the scales and levels relevant to ocean science and policy that are critical to understanding and responding to social-environmental interactions related to deoxygenation. Schematic is based on Cash et al. (2006).

For scale development, various ocean processes can be siloed into scales for biogeochemistry and temperature, but these ocean processes can also have cross-scale interaction for scale development. For instance, microbial remineralization can be siloed into the biogeochemical scale, because microbial remineralization contributes to oxygen loss, creating hypoxic or anoxic conditions in the ocean (Fig. 4-1 (A)). Microbial remineralization can also increase with temperature, especially in the upper ocean, so there is a cross-scale interaction between temperature and oxygen through remineralization. The scale for temperature can reflect the alternance of warm and cold periods that can have cross scale-interaction with the other scales previously mentioned (Fig. 4-1 (B)). The scale of oxygen represents various levels of oxygen concentrations that include thresholds for oxic, hypoxic, anoxic and euxinic conditions. Lastly, the ocean physical variability scale contains levels that represent small to large-scale ocean physical

variability that contributes to mixing, circulation and overall oxygen dynamics (Fig. 4-1 (A -C)). The spatial scale is important for both ocean process and governance, similar to the temporal scale (Fig 4-1 (E)). Different ocean processes can occur in various areas that overlap with the spatial jurisdiction developed by UNCLOS. Since the BBNJ Agreement focuses on the High Seas, more attention can be given to the High Seas level, which represents international governance.

The scales for governance represent institutional rules and jurisdictional administration for ocean policy. The levels for institutional rules are the legal governing documents and procedures for governing bodies, while administration represents the various levels of government from local to international (Fig. 3-1 (F-G)). Lastly, scales and levels are bidirectional (as shown by the arrows in Fig. (4-1)) and do not necessarily need to be static, but can change or adjust in direction (Cohen and Bakker, 2014). For instance, a scale for temperature can change over time based on seasonality and duration of warming and cooling on the ocean surface (Fig. (4-1)). The scales and levels for deoxygenation developed here provide a foundation for understanding the processes that influence and govern the interaction between oxygen loss, changes in marine resources, and human responses in the ocean.

## 4. Cross scale and cross level dynamics of Scale challenges: Ignorance, Plurality, and Mismatch

Interactions between different scales and levels illustrate the complex dynamics of coupled natural and human systems (Fig. (4-2)). The overlap illustrates how social interactions through institutional and jurisdictional scales influence oxygen dynamics along with changes in oxygen through ocean processes. An example can be seen in the Gulf of Mexico, where nutrient run-off from agricultural lands through the Mississippi river exacerbates hypoxia in the Gulf (Rabalais et al., 2014; Turner and Rabalais, 1994), while the Gulf also receives heat from the Caribbean Ocean through transport by the Loop Current. Both effects contribute to oxygen depletion, with nutrient run-off being the dominant feature, along with changes in stratification because of freshwater input and seasonal temperature changes. Management and monitoring of nutrient utilization on land and ocean biogeochemistry in the Gulf is facilitated by the collaboration between Federal agencies such as the Environmental Protection Agency, and multiple state government along the Mississippi River, and states that border the Gulf coast, to reduce nutrient loading and hypoxia in the Gulf ( Suddleson et al ., 2021).

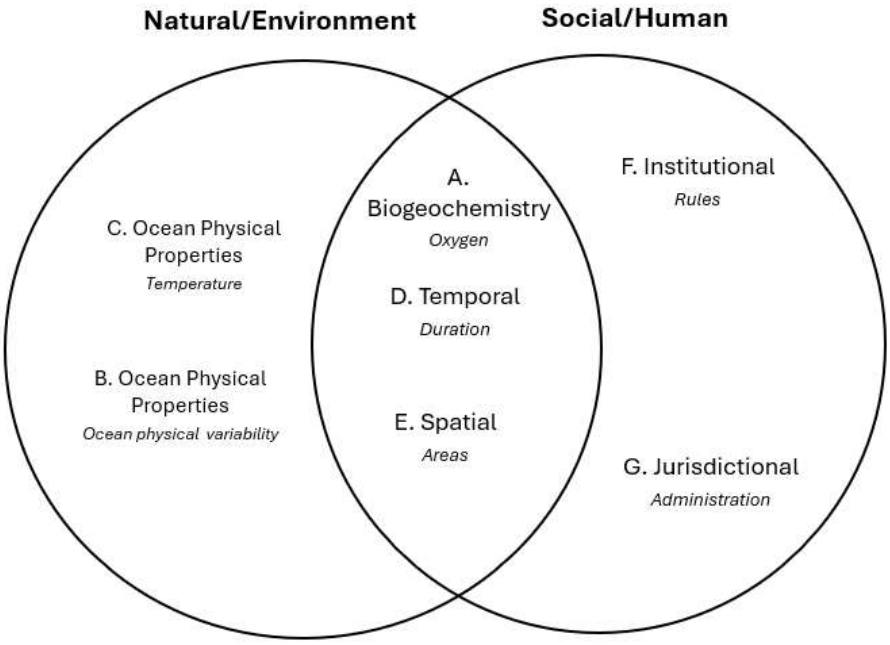


**Figure 4- 2**. Cross-scale interactions between natural and social constructed systems demonstrates how social constructed systems and scales for the ocean intersect with changes in ocean biogeochemistry, temporal duration, seasonal durations, and spatial jurisdiction.

The cross-scale interaction provides an illustration of the competing social-environmental effects taking place in the ocean. The cross-scale dynamic for oxygen decline can be visualized by examining how temporal variability intersects with both natural and human systems because of the seasonality and time scale that oxygen can undergo, which ranges from days to decades (Fig. 4-2). Simultaneously, environmental planning and monitoring of the ocean can undergo a similar time frame, but environmental managers and ocean policy need to consider the spatial impact and temporal variability of oxygen when planning policy actions and initiatives.

Temperature and ocean physical variability (as shown in Fig. 4-1) are categorized as a natural/environmental scale without overlap with the social/human scale, because of natural climate variability modes such as El Niño. However, temperature could overlap with the social/human scale because of the growing influence of climate change. An important aspect of deciding whether to have temperature, or other scales, to overlap needs to be centered around

scientific data and duration of policy implementation, with effective policies to mitigate climate change that occur on decadal or longer timescale.

Understanding and recognizing scale and level interactions are important to reduce management problems contributing to scale challenges of ignorance, mismatch, and plurality. Cash et al. (2006) defines ignorance as the perception of human-environmental systems only at one level within one scale that tries to influence cross-level and cross-scale interactions. However, recent work has further defined ignorance associated with the lack of knowledge in science policy, either purposedly, because of political views ignoring objective evidence, or unavoidably because of the absence of information, because it has not been produced (Andone and Lomelí Hernández, 2022; Medvecky, 2022; Paul and Haddad, 2019; Perl et al., 2018). Nevertheless, both views can be applied together, and illustrate the lack of perspective when policy and science interact with human-environmental systems.

The limited perception constricts and reduces the contributing factors of the cause and solution of a problem causing more difficulty along the way. An example of ignorance can be the perception of solution at only an international level, without any perspective from other levels within a jurisdiction (Fig. 4-3). This limited perception can be accompanied by a "one-size fits all" approach where the solution to address a particular problem does not take into account other factors such as temporal variability of the ocean systems, spatial and geographical differences, and contrast in economic and governance structure of different nations. An example of ignorance that can occur with ocean management is if international agreements or multinational alliances only plan strategies and initiatives for El Niño. Additionally, considering only one viewpoint of scientific information to inform policy provides limited background to address an ocean issue. For example, management that only considers nutrient loading and marine heatwaves as the

determining causes of oxygen loss while ignoring other factors such as changes in ocean circulation and acidification.

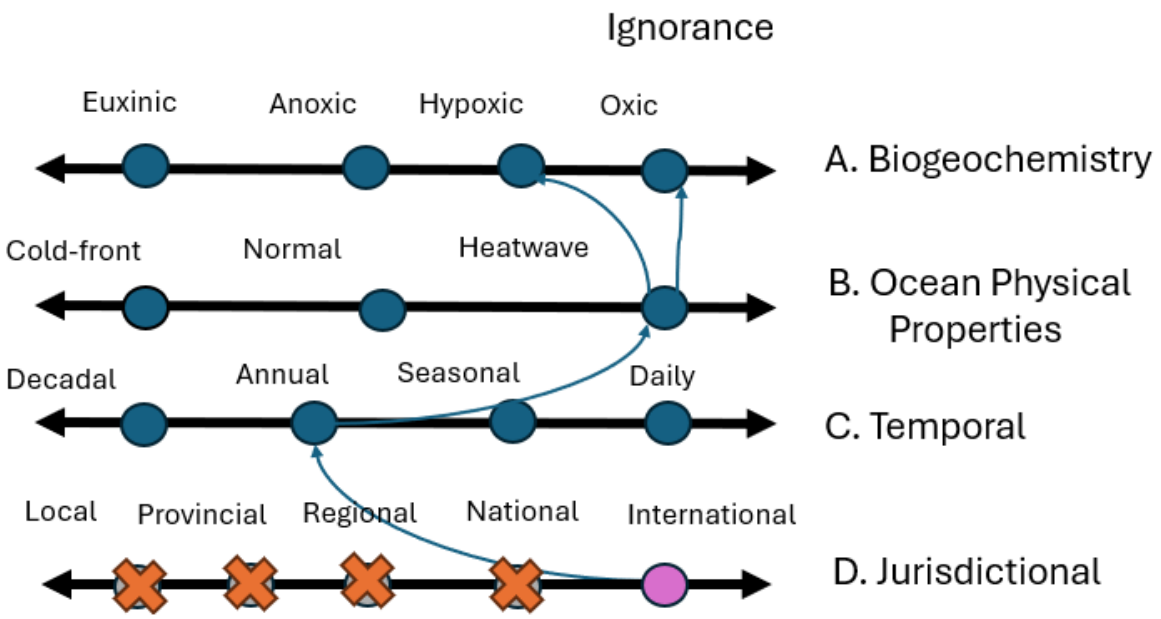


**Figure 4- 3.** Schematic illustrating an example of ignorance in levels in the jurisdictional scale along with the cross-scale interaction between (A) biogeochemistry, (B) ocean physical properties, (C) temporality, and (D) jurisdiction. This illustration shows that by only viewing information and planning at the international level, that results in only considering annual variability of temperature causing hypoxia, can cause ignorance because the decision underestimates the influence and inclusion of other levels and scales.

Mismatch occurs when regulation and policy intervention are not coterminous with space and time of environmental impact and management capabilities (Cash et al., 2006; Cumming, 2022). Mismatch can underestimate or overestimate the management solutions needed to mitigate, or adapt to a changing environment, negatively impact human infrastructure and ecological systems, and complicate financial investment for ocean solutions and management. Ideally, the scale of the problem should be met with the scale of the solution, but because of exogenous and endogenous dynamics within the social-ecological systems, these dynamics can create mismatches.

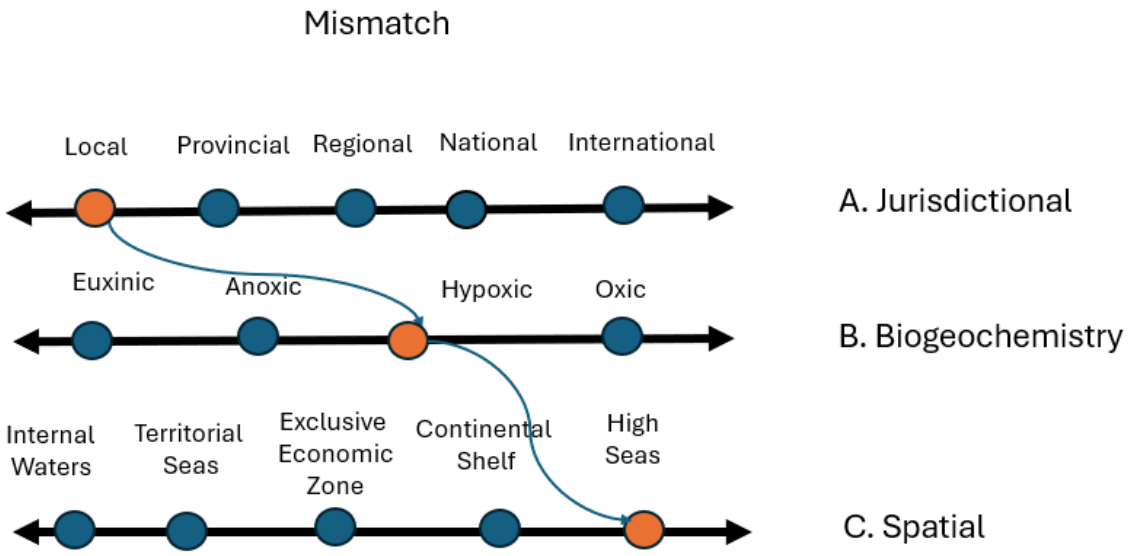


**Figure 4- 4.** Schematic illustrates an example of mismatch between levels in the spatial scale and jurisdictional scale along with the cross-scale interaction between (A) jurisdictional, (B) biogeochemistry, (C) spatiality. Mismatch occurs because local jurisdiction typically would not have the ability to address hypoxia in the High Seas. Mismatch results in incompatibility between jurisdictional and spatial scales.

Fig. 4-4 shows an example of a mismatch that occurs when local enforcement is utilized to address hypoxia in High Seas. Local jurisdiction would not have the legal authority to address ocean issues in the High Seas, and if local jurisdictions did, the resources needed to address a large spatial scale would likely be inadequate. This example of mismatch shows an underestimation of intervention needed to address an issue at a large scale.

Lastly, plurality arises when there is an assumed single, correct, and/or best characterization of the scales and levels. The approach assumes that the single characterization applies for the system as a whole and for all actors, with the view that actors hope to gain something from one's perspective (Cash et al., 2006). An example would be viewing an ocean problem only globally, without considering the impacts at local levels. If the only solution for deoxygenation includes only the open ocean, then global deoxygenation unfortunately cannot be fully addressed without considering the occurrence of hypoxia at the local level within a country's EEZ.

## 5. Discussion: Addressing scale challenges of deoxygenation using co-monitoring, institutional interplay, and bridging organizations in the BBNJ Agreement

Scales and levels for deoxygenation and governance can be integrated to understand how ocean oxygen loss can be related to the governance over space and time, what type of governance level is needed to address the oxygen loss directly, and the process that influences the decline of oxygen (Fig. 4-5). Changes in global deoxygenation can occur on decadal timescales, within the EEZ and in the High Seas. Governance would need national and international deoxygenation policies and resources to address the issue of global deoxygenation over space and time (Fig. 4-5). Additionally, there needs to be consistent and active ocean monitoring and knowledge sharing when it comes to understanding and communicating processes that influence continued oxygen loss as it occurs spatially. Deoxygenation effects marine species and coastal economies, while also being coupled to ocean acidification, ocean warming and climate change. To address the overlapping effects of deoxygenation, a synergistic relationship needs to be established that brings together existing research, program and initiatives, the general public, and government infrastructure, to holistically address the current problems that face the ocean with scales and levels that have proper alignment.

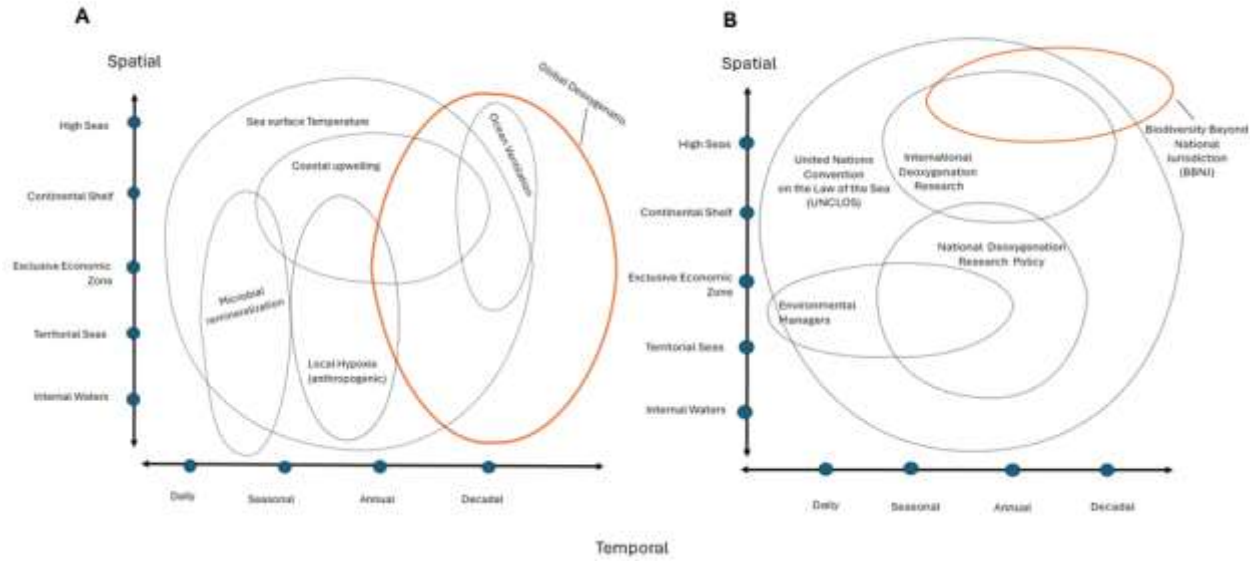


**Figure 4- 5.** Schematic illustrating the spatial and temporal scale of deoxygenation in the ocean and the policies to address deoxygenation. (A) Combination of local to global deoxygenation events that occurs at various times along with the chemical, physical and biological processes that contribute to deoxygenation. (B) Policies and research at various spatial and temporal levels to address deoxygenation, along with the international (UNCLOS) and national (Environmental Management) governing and management bodies. While global deoxygenation occurs at all spatial levels, policies will need a combination of international cooperation through BBNJ and national deoxygenation policies to address global oxygen loss.

To provide a solution for deoxygenation while addressing scale challenges of mismatch, plurality, and ignorance, there needs to be a combined approach of tools and resources to prevent scale challenges that uses co-management, institutional interplay, and bridging organizations as a solution (Cash et al., 2006). Co-management is a continuum of arrangements that rely on various degrees of power and responsibility-sharing between governments and local communities (Cash et al., 2006). An example would be shared resources and data use between developed countries, small island and developing nations when addressing oxygen loss and the effect on marine sustainability. Institutional interplay is the cross-level interaction among resource regimes that occur when there is vertical interplay between, or among regimes located at higher and lower levels on the jurisdictional scale. Institutional interplay can be seen with the duties of environmental managers addressing oxygen loss within the EEZ and the interplay with national deoxygenation

policy. Lastly, organizations focus on intermediary function or processes are known as bridging organizations, because they play intermediary roles, or act as mediators between different levels, or scales, while facilitating the co-production of knowledge (Cash et al., 2006). This type of organization, similar to a state agency, can act as mediators to conflict. For instance, since nutrient run-off influence hypoxia and Harmful Algal Bloom (HAB) formation, contributing to a reduction in fish harvest from mass die off, national policy may want to enforce nutrient reduction to decrease the effects of HAB and hypoxia. In contrast, local actors, like agricultural farmers, may see the reduction of nutrients not in their favor, of the potential negative impact on crop yield. The bridging organization could act as a mediator and facilitate knowledge sharing to find a solution.

For deoxygenation, resources and tools relating to advancement in ocean technology and monitoring provide an opportunity to implement deoxygenation in BBNJ. The framework development of BBNJ has already incorporated elements of co-management, with knowledge sharing between international governance, indigenous communities, and small island nations; institutional interplay between national and international governing bodies that facilitates collaboration; and boundary organizations where disputes on the implementation of the treaty are discussed in Article 60 of the Agreement. However, scale challenges can still develop, “when (1) the failure to recognize important interactions altogether, (2) the persistence of mismatches between levels and scales in human- environment systems, and (3) the failure to recognize the way that scales are perceived and valued by different actors, even at the same level” (Cash et al.,2016).

Implementing deoxygenation through the Agreement by recognizing the important scale and level interactions, will support addressing deoxygenation and the impact deoxygenation has on marine species and chemistry. Section 5.2 and 5.3 address how the main themes of BBNJ

intersect with deoxygenation that promotes synergistic relationship, and advancement in ocean technology through existing initiatives to address deoxygenation.

## 5.2 Application of deoxygenation scales and levels in the implementation of the BBNJ Agreement

Providing a policy approach that addresses deoxygenation requires examining how deoxygenation intersects with BBNJ (Fig. 4-6).

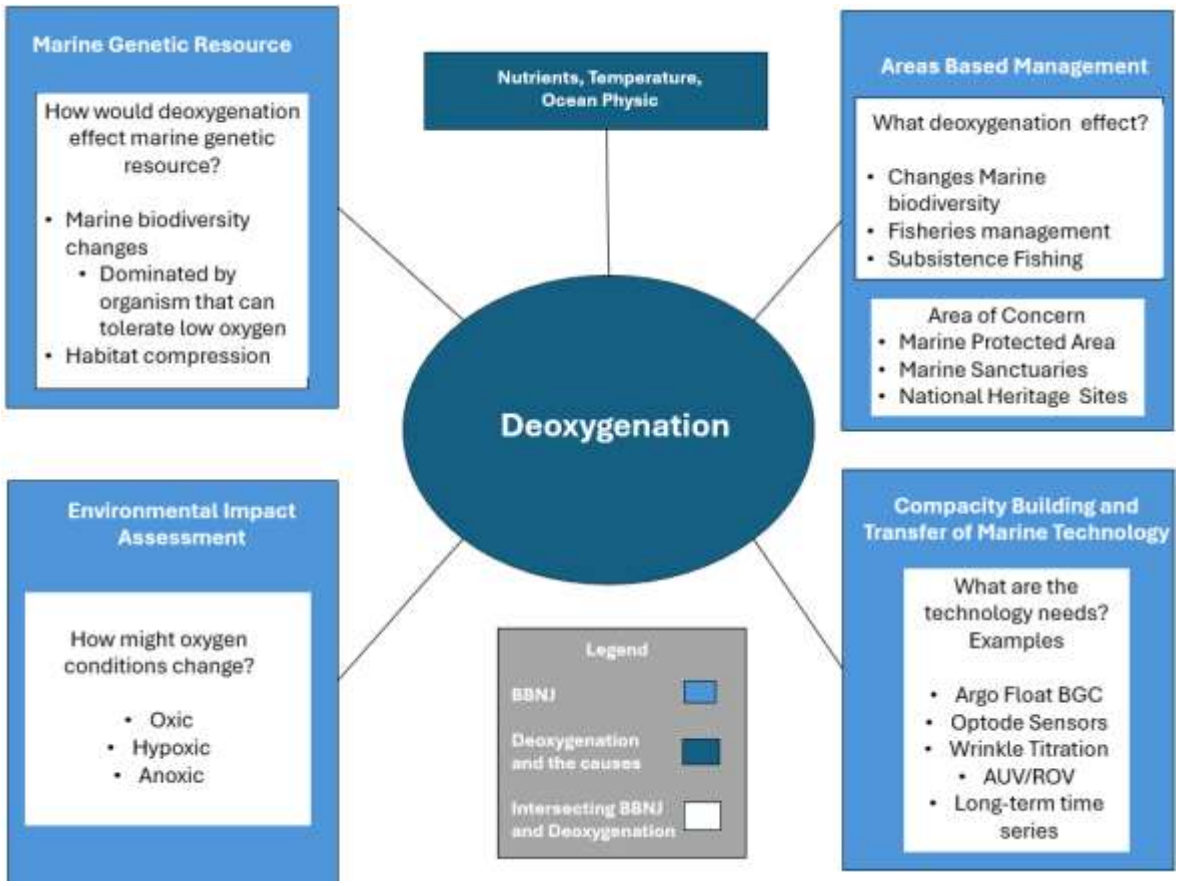


**Figure 4- 6.** Schematic illustrating the intersection between deoxygenation and BBNJ. The components of the agreement include area-based management, capacity building transfer of marine technology, environmental impact assessment, and marine genetic resource. Smaller boxes inside each component are prompts that relate to deoxygenation and components of the treaty.

The purpose of BBNJ is to protect marine biodiversity in the High Seas. BBNJ covers four main issues, (1) marine genetic resources, (2) area-based management tools (3) environmental impact assessment, and (4) capacity building and transfer of marine technology. Under each issue, parties to this agreement are guided by general principles and approaches outlined in Article 7 and international cooperation in Article 8. The intersection of oxygen is an attribute for the four main issues that the agreement seeks to address (Fig. 4-6). The loss of oxygen has a direct impact on marine protected areas and biodiversity in the High Seas that can influence migratory fish and other marine species. Additionally, BBNJ authorizes parties, or countries, to perform an environmental impact assessment when needed. Assessing oxygen conditions can be an important indicator for ecosystem health. Lastly, monitoring oxygen conditions along with the marine fish species metabolic index, requires advancement in ocean technology and open-source data sharing between nations (Bilawal Khaskheli et al., 2023; Deutsch et al., 2015; Grégoire et al., 2021; Seibel, 2011). These advances, for example, includes advancing the Biogeochemical Argo Float program to provide measurements of ocean biogeochemistry across the open-ocean and ways to facilitate data sharing between nations and non-governmental organizations (Grégoire et al., 2021).

Even though the text of the Agreement can be interpreted ambiguously, BBNJ can incorporate deoxygenation scales and levels. Cross-scale and cross-level dynamics developed in Section 3 can be applied to address scale challenges in the agreement along with applying a framework to intersect with the main issues in the agreement. This approach can foster further dialogue and cooperation though outside multilateral initiatives for specific purposes and objectives under the agreement. Since the Agreement is yet to be enacted, it is important to consider where ignorance, mismatch and plurality can develop, and provide the appropriate scale to address them.

### 5.3 Advancing Science and Technology using $GO_2DAT$ to implement deoxygenation policy in BBNJ agreement

The BBNJ agreement itself does not specify the technology types needed or conflict resolution on technology use and data sharing, which could provide some difficulty in multilateral negotiations on data sharing, storage, security and accessibility (Bilawal Khaskheli et al., 2023; Vierros and Harden-Davies, 2020). For example, according to Cash et al. (2006), these problems can result in mismatch, ignorance and plurality in data management, where the scale of data volume from complex measurements does not match with the ability of individual actors to access and use the data, including tribal nations and less developed countries.

Ocean technology and observation has been transformative in understanding the processes of the ocean, from satellite altimetry analyzing surface currents, to autonomous underwater vehicles measuring physical parameters in the deep ocean. Technology and data sharing has been revolutionary in understanding chemical, physical, and biological processes in the ocean that support marine ecosystem management (Bilawal Khaskheli et al., 2023; Grégoire et al., 2021). Ocean technology and data sharing capacity are components of the main themes in the Agreement, especially in Part IV of the Agreement, *Capacity Building and the Transfer of Marine Environmental* (Agreement under the United Nations Convention on the Law of the Sea on the conservation and sustainable use of marine biological diversity of areas beyond national jurisdiction, 2023). Technologies to measure ocean oxygen concentrations and the processes that influence oxygen decline are vital to monitoring ocean health and marine biodiversity. For this reason, technology advancement and international cooperation on data accessibility are important for understanding the interaction between oxygen loss and marine resources, and, as a consequence, for management and policy and decision-making. Recently, there has been an effort

undertaken to develop an international open-access Global Ocean Database Atlas ($GO_2DAT$) that will incorporate data from an array of ocean observatory systems, including data from the Argo-float program (Claustre et al., 2020; Grégoire et al., 2021; Le Traon et al., 2020). The $GO_2DAT$ is a framework developed under the UN Global Ocean Oxygen Decade (GOOD) endorsed by the Intergovernmental Oceanographic Commission. Because $GO_2DAT$ is an international program developed through multinational collaborations, BBNJ can benefit from implementing the existing $GO_2DAT$ framework, set to expire in 2030, under the UN Ocean Decade, so that there can be an overlap of priorities that benefits the Agreement and the goals of the UNGOOD.

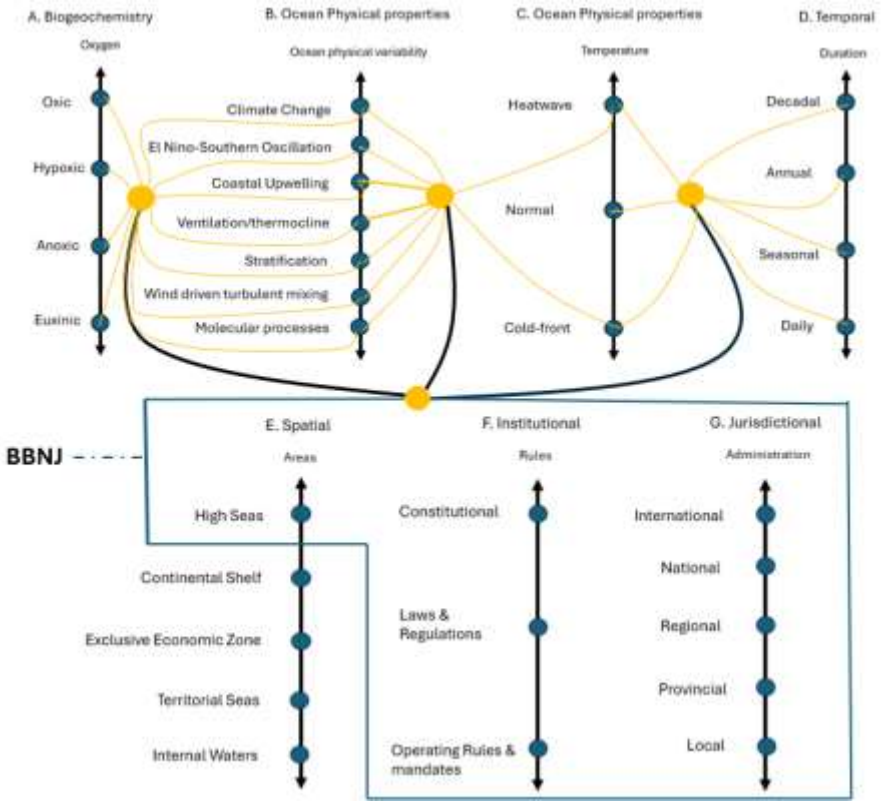


**Figure 4- 7.** Schematic illustrating the scales and levels relevant to BBNJ and deoxygenation. Yellow nodes represent ocean technology that is critical to understanding and responding to social-environmental interactions related to deoxygenation.

The advancement in ocean technology is essential for the cross-scale and cross-level interactions that occur in the context of ocean deoxygenation (Fig. 4-7). The scale developed for

judicial, institutional, and spatial scales in (Fig. 7 (E-G)), represent the governance and structural framework in the BBNJ agreement while the scales in (Fig. 7 (A-C)) represents the scales for ocean variability and processes that influence oxygen loss. The advancement in technology facilitates the cross-scale interaction between ocean variability and the agreement, by illustrating the connection between data that will be produced by monitoring changes in oxygen, and the science that is needed to influence policy in the High Seas. Deoxygenation then can be central to the main issues of the agreement and presents an opportunity to embed $GO_2DAT$ into the research scale that supports managing marine biodiversity (Fig. 4-6). This effort in the research scale would greatly lessen the impact of mismatch of technology and data accessibility with the spatial distribution of the High Seas or areas of interest.

## Conclusions

The loss of oxygen is a current issue for the oceanic ecosystem, blue economy, and ocean health but also for governance and management of marine resources. By understanding the scales and levels that cross between social structure and natural systems a proper way to address the current and future social–environmental challenges of ocean deoxygenation can be developed. Here we developed the necessary scales and levels to illustrate the natural and social dynamics that occur at various temporal and spatial scales for deoxygenation. Following Cash et al. (2006), we illustrate how scales and levels can have misalignments that present scale challenges of ignorance, mismatch and plurality in ocean deoxygenation and governance. We then apply these scales to the BBNJ agreement, which has four objectives that can implement deoxygenation for the High Seas. Using the existing initiative $GO_2DAT$, we suggest that advancing technology and data sharing can be implemented and intersect with the four main objectives in BBNJ while supporting marine biodiversity. As mentioned in the discussion, technology advancement and data sharing are paramount in understanding the dynamics of oxygen in the ocean and the impact that oxygen has ocean ecosystems, blue economy, and fisheries management, to name a few.

The implementation of deoxygenation in BBNJ can be a successful way to address deoxygenation in the ocean while coupling ocean marine biodiversity, ocean chemistry and ocean economics.

## References

Adewumi, I. J.: Exploring the Nexus and Utilities Between Regional and Global Ocean Governance Architecture, Front. Mar. Sci., 8, https://doi.org/10.3389/fmars.2021.645557, 2021.

Adler, J. H.: Jurisdictional Mismatch in Environmental Federalism, SSRN Electron. J., https://doi.org/10.2139/ssrn.770305, 2005.

Andone, C. and Lomelí Hernández, J. A.: On Arguments from Ignorance in Policy-Making, in: The Pandemic of Argumentation, vol. 43, edited by: Oswald, S., Lewiński, M., Greco, S., and Villata, S., Springer International Publishing, Cham, 105–123, https://doi.org/10.1007/978-3-030-91017-4_6, 2022.

Barbier, E. B.: Marine ecosystem services, Curr. Biol., 27, R507–R510, https://doi.org/10.1016/j.cub.2017.03.020, 2017.

Bates, N. R. and Johnson, R. J.: Acceleration of ocean warming, salinification, deoxygenation and acidification in the surface subtropical North Atlantic Ocean, Commun. Earth Environ., 1, 1–12, https://doi.org/10.1038/s43247-020-00030-5, 2020.

Bilawal Khaskheli, M., Wang, S., Zhang, X., Shamsi, I. H., Shen, C., Rasheed, S., Ibrahim, Z., and Baloch, D. M.: Technology advancement and international law in marine policy, challenges, solutions and future prospective, Front. Mar. Sci., 10, https://doi.org/10.3389/fmars.2023.1258924, 2023.

von Braun, J. and Birner, R.: Designing Global Governance for Agricultural Development and Food and Nutrition Security, Rev. Dev. Econ., 21, 265–284, https://doi.org/10.1111/rode.12261, 2017.

Breitburg, D., Levin, L. A., Oschlies, A., Grégoire, M., Chavez, F. P., Conley, D. J., Garçon, V., Gilbert, D., Gutiérrez, D., Isensee, K., Jacinto, G. S., Limburg, K. E., Montes, I., Naqvi, S. W. A., Pitcher, G. C., Rabalais, N. N., Roman, M. R., Rose, K. A., Seibel, B. A., Telszewski, M., Yasuhara, M., and Zhang, J.: Declining oxygen in the global ocean and coastal waters, Science, 359, eaam7240, https://doi.org/10.1126/science.aam7240, 2018.

Carvalho, M., Mathis, J., Hamzah, B. A., Forbes, V. L., Carlarne, C. P., and Manfredi, J. L.: Chapter 21 - Ocean law, policies, and regulation, in: Oceans and Human Health (Second Edition), edited by: Fleming, L. E., Alcantara Creencia, L. B., Gerwick, W. H., Goh, H. C., Gribble, M. O., Maycock, B., and Solo-Gabriele, H., Academic Press, San Diego, 643–685, https://doi.org/10.1016/B978-0-323-95227-9.00023-3, 2023.

Cash, D. W., Adger, W. N., Berkes, F., Garden, P., Lebel, L., Olsson, P., Pritchard, L., and Young, O.: Scale and Cross-Scale Dynamics: Governance and Information in a Multilevel World, Ecol. Soc., 11, 2006.

Chan, F., Barth, J. A., Lubchenco, J., Kirincich, A., Weeks, H., Peterson, W. T., and Menge, B. A.: Emergence of Anoxia in the California Current Large Marine Ecosystem, Science, 319, 920–920, https://doi.org/10.1126/science.1149016, 2008.

Claustre, H., Johnson, K. S., and Takeshita, Y.: Observing the Global Ocean with Biogeochemical-Argo, Annu. Rev. Mar. Sci., 12, 23–48, https://doi.org/10.1146/annurev-marine-010419-010956, 2020.

Cohen, A. and Bakker, K.: The Eco-Scalar Fix: Rescaling Environmental Governance and the Politics of Ecological Boundaries in Alberta, Canada, Environ. Plan. Soc. Space, 32, 128–146, https://doi.org/10.1068/d0813, 2014.

Cumming, G. S., Cumming, D. H. M., and Redman, C. L.: Scale Mismatches in Social-Ecological Systems: Causes, Consequences, and Solutions, Ecol. Soc., 11, 2006.

Deutsch, C., Brix, H., Ito, T., Frenzel, H., and Thompson, L.: Climate-Forced Variability of Ocean Hypoxia, Science, 333, 336–339, https://doi.org/10.1126/science.1202422, 2011.

Deutsch, C., Ferrel, A., Seibel, B., Pörtner, H.-O., and Huey, R. B.: Climate change tightens a metabolic constraint on marine habitats, Science, 348, 1132–1135, https://doi.org/10.1126/science.aaa1605, 2015.

Franco, A. C., Kim, H., Frenzel, H., Deutsch, C., Ianson, D., Sumaila, U. R., and Tortell, P. D.: Impact of warming and deoxygenation on the habitat distribution of Pacific halibut in the Northeast Pacific, Fish. Oceanogr., 31, 601–614, https://doi.org/10.1111/fog.12610, 2022.

Global Ocean Oxygen Network, 2018: https://www.ioc.unesco.org/en/go2ne, last access: 27 May 2024.

Grégoire, M., Garçon, V., Garcia, H., Breitburg, D., Isensee, K., Oschlies, A., Telszewski, M., Barth, A., Bittig, H. C., Carstensen, J., Carval, T., Chai, F., Chavez, F., Conley, D., Coppola, L., Crowe, S., Currie, K., Dai, M., Deflandre, B., Dewitte, B., Diaz, R., Garcia-Robledo, E., Gilbert, D., Giorgetti, A., Glud, R., Gutierrez, D., Hosoda, S., Ishii, M., Jacinto, G., Langdon, C., Lauvset, S. K., Levin, L. A., Limburg, K. E., Mehrtens, H., Montes, I., Naqvi, W., Paulmier, A., Pfeil, B., Pitcher, G., Pouliquen, S., Rabalais, N., Rabouille, C., Recape, V., Roman, M., Rose, K., Rudnick, D., Rummer, J., Schmechtig, C., Schmidtko, S., Seibel, B., Slomp, C., Sumalia, U. R., Tanhua, T., Thierry, V., Uchida, H., Wanninkhof, R., and Yasuhara, M.: A Global Ocean Oxygen Database and Atlas for Assessing and Predicting Deoxygenation and Ocean Health in the Open and Coastal Ocean, Front. Mar. Sci., 8, 2021.

Haas, B., Mackay, M., Novaglio, C., Fullbrook, L., Murunga, M., Sbrocchi, C., McDonald, J., McCormack, P. C., Alexander, K., Fudge, M., Goldsworthy, L., Boschetti, F., Dutton, I., Dutra, L., McGee, J., Rousseau, Y., Spain, E., Stephenson, R., Vince, J., Wilcox, C., and Haward, M.: The future of ocean governance, Rev. Fish Biol. Fish., 32, 253–270, https://doi.org/10.1007/s11160-020-09631-x, 2022.

Halpern, B. S., Frazier, M., Afflerbach, J., Lowndes, J. S., Micheli, F., O'Hara, C., Scarborough, C., and Selkoe, K. A.: Recent pace of change in human impact on the world's ocean, Sci. Rep., 9, 11609, https://doi.org/10.1038/s41598-019-47201-9, 2019.

Intergovernmental Panel On Climate Change (Ipcc): Climate Change 2022 – Impacts, Adaptation and Vulnerability: Working Group II Contribution to the Sixth Assessment Report of

the Intergovernmental Panel on Climate Change, 1st ed., Cambridge University Press, https://doi.org/10.1017/9781009325844, 2023.

Keeling, R. F., Körtzinger, A., and Gruber, N.: Ocean Deoxygenation in a Warming World, Annu. Rev. Mar. Sci., 2, 199–229, https://doi.org/10.1146/annurev.marine.010908.163855, 2010.

Kiel Declaration on Ocean Deoxygenation 2016: https://www.ocean-oxygen.org/declaration, last access: 27 May 2024.

Le Traon, P.-Y., D'Ortenzio, F., Babin, M., Leymarie, E., Marec, C., Pouliquen, S., Thierry, V., Cabanes, C., Claustre, H., Desbruyères, D., Lacour, L., Lagunas, J.-L., Maze, G., Mercier, H., Penkerc'h, C., Poffa, N., Poteau, A., Prieur, L., Racapé, V., Randelhoff, A., Rehm, E., Schmechtig, C. M., Taillandier, V., Wagener, T., and Xing, X.: Preparing the New Phase of Argo: Scientific Achievements of the NAOS Project, Front. Mar. Sci., 7, https://doi.org/10.3389/fmars.2020.577408, 2020.

May, C. K.: Power across scales and levels of fisheries governance: Explaining the active non-participation of fishers in Two Rivers, North Carolina, J. Rural Stud., 32, 26–37, https://doi.org/10.1016/j.jrurstud.2013.04.002, 2013.

McCormick, L. R. and Levin, L. A.: Physiological and ecological implications of ocean deoxygenation for vision in marine organisms, Philos. Transact. A Math. Phys. Eng. Sci., 375, 20160322, https://doi.org/10.1098/rsta.2016.0322, 2017.

Medvecky, F.: Public Understanding of Ignorance as Critical Science Literacy, Sustainability, 14, 5920, https://doi.org/10.3390/su14105920, 2022.

Oschlies, A., Brandt, P., Stramma, L., and Schmidtko, S.: Drivers and mechanisms of ocean deoxygenation, Nat. Geosci., 11, 467–473, https://doi.org/10.1038/s41561-018-0152-2, 2018.

Palacios-Abrantes, J., Reygondeau, G., Wabnitz, C. C. C., and Cheung, W. W. L.: The transboundary nature of the world's exploited marine species, Sci. Rep., 10, 17668, https://doi.org/10.1038/s41598-020-74644-2, 2020.

Palumbi, S. R., Sandifer, P. A., Allan, J. D., Beck, M. W., Fautin, D. G., Fogarty, M. J., Halpern, B. S., Incze, L. S., Leong, J.-A., Norse, E., Stachowicz, J. J., and Wall, D. H.: Managing for ocean biodiversity to sustain marine ecosystem services, Front. Ecol. Environ., 7, 204–211, https://doi.org/10.1890/070135, 2009.

Patrick, M. J., Syme, G. J., and Horwitz, P.: How reframing a water management issue across scales and levels impacts on perceptions of justice and injustice, J. Hydrol., 519, 2475–2482, https://doi.org/10.1016/j.jhydrol.2014.09.002, 2014.

Paul, K. T. and Haddad, C.: Beyond evidence versus truthiness: toward a symmetrical approach to knowledge and ignorance in policy studies, Policy Sci., 52, 299–314, https://doi.org/10.1007/s11077-019-09352-4, 2019.

Perl, A., Howlett, M., and Ramesh, M.: Policy-making and truthiness: Can existing policy models cope with politicized evidence and willful ignorance in a “post-fact” world?, Policy Sci., 51, 581–600, https://doi.org/10.1007/s11077-018-9334-4, 2018.

Pomeroy, R. S., Garces, L. R., Pido, M. D., Parks, J. E., and Silvestre, G.: The role of scale within an Ecosystem Approach to fisheries management: Policy and practice in Southeast Asian seas, Mar. Policy, 106, 103531, https://doi.org/10.1016/j.marpol.2019.103531, 2019.

Rabalais, N. N., Cai, W.-J., Carstensen, J., Conley, D. J., Fry, B., Hu, X., Quiñones-Rivera, Z., Rosenberg, R., Slomp, C. P., Turner, R. E., Voss, M., Wissel, B., and Zhang, J.: Eutrophication-Driven Deoxygenation in the Coastal Ocean, Oceanography, 27, 172–183, 2014.

Richardson, K., Steffen, W., Lucht, W., Bendtsen, J., Cornell, S. E., Donges, J. F., Drüke, M., Fetzer, I., Bala, G., von Bloh, W., Feulner, G., Fiedler, S., Gerten, D., Gleeson, T., Hofmann, M., Huiskamp, W., Kummu, M., Mohan, C., Nogués-Bravo, D., Petri, S., Porkka, M., Rahmstorf, S., Schaphoff, S., Thonicke, K., Tobian, A., Virkki, V., Wang-Erlandsson, L., Weber, L., and Rockström, J.: Earth beyond six of nine planetary boundaries, Sci. Adv., 9, eadh2458, https://doi.org/10.1126/sciadv.adh2458, 2023.

Sánchez-Velasco, L., Godínez, V. M., Ruvalcaba-Aroche, E. D., Márquez-Artavia, A., Beier, E., Barton, E. D., and Jiménez-Rosenberg, S. P. A.: Larval Fish Habitats and Deoxygenation in the Northern Limit of the Oxygen Minimum Zone off Mexico, J. Geophys. Res. Oceans, 124, 9690–9705, https://doi.org/10.1029/2019JC015414, 2019.

Schmidtko, S., Stramma, L., and Visbeck, M.: Decline in global oceanic oxygen content during the past five decades, Nature, 542, 335–339, https://doi.org/10.1038/nature21399, 2017.

Schultz, C. A., Timberlake, T. J., Wurtzebach, Z., McIntyre, K. B., Moseley, C., and Huber-Stearns, H. R.: Policy tools to address scale mismatches: insights from U.S. forest governance, Ecol. Soc., 24, 2019.

Seibel, B. A.: Critical oxygen levels and metabolic suppression in oceanic oxygen minimum zones, J. Exp. Biol., 214, 326–336, https://doi.org/10.1242/jeb.049171, 2011.

Shepherd, J. G., Brewer, P. G., Oschlies, A., and Watson, A. J.: Ocean ventilation and deoxygenation in a warming world: introduction and overview, Philos. Trans. R. Soc. Math. Phys. Eng. Sci., 375, 20170240, https://doi.org/10.1098/rsta.2017.0240, 2017.

Steffen, W., Richardson, K., Rockström, J., Cornell, S. E., Fetzer, I., Bennett, E. M., Biggs, R., Carpenter, S. R., de Vries, W., de Wit, C. A., Folke, C., Gerten, D., Heinke, J., Mace, G. M., Persson, L. M., Ramanathan, V., Reyers, B., and Sörlin, S.: Planetary boundaries: Guiding human development on a changing planet, Science, 347, 1259855, https://doi.org/10.1126/science.1259855, 2015.

van Tatenhove, J. P. M.: Transboundary marine spatial planning: a reflexive marine governance experiment?, J. Environ. Policy Plan., 19, 783–794, https://doi.org/10.1080/1523908X.2017.1292120, 2017.

Turner, R. E. and Rabalais, N. N.: Coastal eutrophication near the Mississippi river delta, Nature, 368, 619–621, https://doi.org/10.1038/368619a0, 1994.

The Harmful Algal Bloom and Hypoxia Research and Control Amendments Act (HABHRCA): https://www.epa.gov/habs/harmful-algal-bloom-and-hypoxia-research-and-control-amendments-act-habhrca, last access: 1 April 2024.

United Nations Convention on the Law of the Sea 1986: https://legal.un.org/avl/ha/uncls/uncls.html, last access: 28 March 2024.

Vierros, M. K. and Harden-Davies, H.: Capacity building and technology transfer for improving governance of marine areas both beyond and within national jurisdiction, Mar. Policy, 122, 104158, https://doi.org/10.1016/j.marpol.2020.104158, 2020.

Yang, P., Mi, Z., Wei, Y.-M., Hanssen, S. V., Liu, L.-C., Coffman, D., Sun, X., Liao, H., Yao, Y.-F., Kang, J.-N., Wang, P.-T., and Davis, S. J.: The global mismatch between equitable carbon dioxide removal liability and capacity, Natl. Sci. Rev., 10, nwad254, https://doi.org/10.1093/nsr/nwad254, 2023.

Yang, S., Gruber, N., Long, M. C., and Vogt, M.: ENSO-Driven Variability of Denitrification and Suboxia in the Eastern Tropical Pacific Ocean, Glob. Biogeochem. Cycles, 31, 1470–1487, https://doi.org/10.1002/2016GB005596, 2017.

Young, O. R., Osherenko, G., Ekstrom, J., Crowder, L. B., Ogden, J., Wilson, J. A., Day, J. C., Douvere, F., Ehler, C. N., McLeod, K. L., Halpren, B. S., and Peach, R.: Solving the Crisis in Ocean Governance: Place-Based Management of Marine Ecosystems, Environ. Sci. Policy Sustain. Dev., 49, 20–32, https://doi.org/10.3200/ENVT.49.4.20-33, 2007.

# Chapter 5: Summary

## 5.1 Summary

In this dissertation, I have demonstrated the impact of deoxygenation in the Santa Barbara Channel (SBC) on benthic Fe flux, and its impact on phytoplankton growth in the SBC and the greater California Current System (CCS). Additionally, I created a new compiled dissolved oxygen dataset, utilizing underwater vehicles and hydrographic data for the SBC, and the deep basin to map the spatial distribution and temporal variability of oxygen in the channel. Lastly, I have investigated how a new international ocean agreement can be utilized to address global deoxygenation through technology advancement, data-sharing and utilizing existing international ocean programs to advance ocean observation of dissolved oxygen for the benefit of ocean ecosystem and coastal economies.

Chapter 2 explored the impact of benthic Fe flux on phytoplankton growth in the SBC and CCS. I recorded the highest amount of benthic Fe flux in the Santa Barbara Basin (0.23 – 4.9 mmol $m^{-2}$ $d^{-1}$), greater than reported from previous studies from this region (Severmann et al., 2010) and from other oxygen minimum zones (Dale et al. 2015; Homoky et al. 2021). I was also able to apply these benthic Fe flux measurements to an existing iron parameterization in the ROMS-BEC model. My results showed that benthic Fe flux supports phytoplankton growth while also changing surface nitrate and iron dynamics. My simulations also suggested that Fe inputs from atmospheric deposition are mostly important in the northern Pacific ocean (40°N-48°N) near the CCS and Oregon coast, where phytoplankton rely on Fe delivery by dust. However, I also showed that changes in atmospheric Fe deposition can affect ocean productivity in the southern CCS by altering $NO_3^-$ utilization further downstream. My results supported the idea that benthic Fe fluxes are the

major source of Fe in the southern CCS and are supplemented by atmospheric deposition in northwestern and offshore waters, leading to relatively high NPP coastwide.

Chapter 3 explored the spatial and temporal variability of oxygen in the SBC. I was able to develop a compiled oxygen dataset for the SBC, along with utilizing underwater vehicles equipped with optode sensors to measure high-resolution oxygen concentrations in the SBC. I was able to show that the deep basin has an "out of sync" seasonal cycle with the upper ocean due to its bathymetry. I finally, demonstrated that anoxia is concentrated below the sill depth, and oxygen gradually declines from the surface to the deep ocean.

Chapter 4 explored the development of a framework to implement deoxygenation into the Biodiversity Beyond National Jurisdiction (BBNJ) Agreement. I constructed scales and levels for deoxygenation that has not been done before, to understand the social-human dynamics of ocean governance and the factors that contribute to global oxygen loss. I then determined how deoxygenation intersects with ocean governance relating to spatial, jurisdictional, and temporal scales. My results showed that deoxygenation can be addressed within the Agreement's *Capacity Building and the Transfer of Marine Environmental,* by utilizing and advancing the Global Ocean Database Atlas. Advancing technology and data sharing can be implemented and intersect with the four main objectives in BBNJ while supporting marine biodiversity. The implementation of deoxygenation in BBNJ can be a successful way to address deoxygenation in the ocean while coupling ocean marine biodiversity, ocean chemistry and blue economies.

## 5.2 Future work

The work presented in this dissertation addresses questions on dFe impacts on phytoplankton growth in the channel, the distribution of oxygen in the channel, and how to implement deoxygenation into ocean policy. While providing new original data, our studies also stimulate new questions that demand future research. In this section I discuss suggested future work and new research directions for studying processes in the Santa Barbara Channel.

The impact of Fe on phytoplankton growth in the Santa Barbara Basin and CCS provides new knowledge on the connection between sediments and the surface ocean, but also leaves some unopen questions. Dissolved Fe is known to stimulate phytoplankton growth, that fosters a positive feedback loop between low oxygen sediments, benthic Fe flux, phytoplankton growth, organic matter production, remineralization and settling of particulate Fe to the sediment-water interface (Robinson et al., 2024). However, Fe(II) that reaches the surface ocean would oxidize under oxic conditions, restricting phytoplankton growth. But the impact of dFe(II) ligands in the ocean may play a role in dFe(II) binding to organic matter, dFe(II) dynamics, and the growth of phytoplankton communities in the channel (Bundy et al., 2015, 2016). It is possible that in the Santa Barbara Channel, dFe(II) retains its reduced state well into the interior of the water column (200-300 m ) after being fluxed from the sediments. Once dFe(II) reaches oxic conditions ( > 100 μM) in the subsurface, photo-oxidation can occur either before, or after ligands bind to Fe(II). The process of photo-oxidation either may make Fe(III) more biologically soluble for phytoplankton growth as a ligand complex Fe(III)-L, or stimulate the photo-reduction of Fe(III)/Fe(III)-L in which the dFe(II) that's produced from photo-reduction can be taken up by phytoplankton (Barbeau, 2006; Huang et al., 2021).

From Chapter 3, we were able to reconstruct near bottom oxygen concentrations and extrapolate the hypoxic and anoxic concentrations to benthic Fe flux. It is possible that this extrapolation method could be applied to other nutrients like phosphate, reactive nitrogen species (especially ammonium and nitrous oxide), and inorganic carbon that would help better constrain production and consumption rates of nutrients within the water column and sediments. For instance, this oxygen dataset provides new opportunities to investigate the temporal variability and spatial distribution of nitrogen in the basin and relate that to a nitrogen budget. This nitrogen budget would be important in distinguishing the sources and sinks of nitrogen that are present throughout the basin and expand on previous work on nitrate dynamics in the basin (Sigman et al., 2003; Valentine et al., 2016; Yousavich et al., 2023). This extrapolation method could also be applied to the Southern California Bight, which would provide insight on the total estimated nutrient flux in the Bight that can aid in constraining nutrient budgets for sources and sinks between the sediments and water column along with physical transport from the CCS, and extrapolating the volume of hypoxia and anoxia that is present in the Bight. This compiled data-set also presents an opportunity to support efforts on the application of the Global Oxygen Database Atlas, by using the SBC data-set created here, as a case study on the importance of having a historical long time series coupled with high resolution observation, that can provide a more holistic and accurate view of oxygen dynamics in low oxygen regions (Grégoire et al., 2021)

The Santa Barbara Basin hosts microbial mats of sulfur-oxidizing bacteria in the sediment. The presence of these mats were observed during several research cruises including in 2013 (Valentine et al., 2016) where microbial mats created a ring around the sill depth; 2019 with partially-full microbial mat present in the depocenter (Yousavich et al., 2024) and unpublished data from 2021, 2022 and 2023. By utilizing the spatial distribution of hypoxic/anoxic conditions

at 560 m in Chapter 3, the spatial distribution of the microbial mats can be estimated by coupling and overlaying the gridded oxygen dataset and photo surveys of the benthic microbial mat. This combination of data would provide an estimate of the potential microbial mat cover as a function of oxygen, and expand on previous work on nutrient cycling (Sigman et al., 2003; Valentine et al., 2016; Yousavich et al., 2023) by extrapolating the impact on the nitrogen cycle, sulfide oxidation and sulfate reduction that occur in the sediment and water column.

## Reference

Barbeau, K.: Photochemistry of Organic Iron(III) Complexing Ligands in Oceanic Systems, Photochem. Photobiol., 82, 1505–1516, https://doi.org/10.1111/j.1751-1097.2006.tb09806.x, 2006.

Bundy, R. M., Abdulla, H. A. N., Hatcher, P. G., Biller, D. V., Buck, K. N., and Barbeau, K. A.: Iron-binding ligands and humic substances in the San Francisco Bay estuary and estuarine-influenced shelf regions of coastal California, Mar. Chem., 173, 183–194, https://doi.org/10.1016/j.marchem.2014.11.005, 2015.

Bundy, R. M., Jiang, M., Carter, M., and Barbeau, K. A.: Iron-Binding Ligands in the Southern California Current System: Mechanistic Studies, Front. Mar. Sci., 3, https://doi.org/10.3389/fmars.2016.00027, 2016.

Dale, A. W., Nickelsen, L., Scholz, F., Hensen, C., Oschlies, A., and Wallmann, K.: A revised global estimate of dissolved iron fluxes from marine sediments: GLOBAL BENTHIC IRON FLUXES, Glob. Biogeochem. Cycles, 29, 691–707, https://doi.org/10.1002/2014GB005017, 2015.

Grégoire, M., Garçon, V., Garcia, H., Breitburg, D., Isensee, K., Oschlies, A., Telszewski, M., Barth, A., Bittig, H. C., Carstensen, J., Carval, T., Chai, F., Chavez, F., Conley, D., Coppola, L., Crowe, S., Currie, K., Dai, M., Deflandre, B., Dewitte, B., Diaz, R., Garcia-Robledo, E., Gilbert, D., Giorgetti, A., Glud, R., Gutierrez, D., Hosoda, S., Ishii, M., Jacinto, G., Langdon, C., Lauvset, S. K., Levin, L. A., Limburg, K. E., Mehrtens, H., Montes, I., Naqvi, W., Paulmier, A., Pfeil, B., Pitcher, G., Pouliquen, S., Rabalais, N., Rabouille, C., Recape, V., Roman, M., Rose, K., Rudnick, D., Rummer, J., Schmechtig, C., Schmidtko, S., Seibel, B., Slomp, C., Sumalia, U. R., Tanhua, T., Thierry, V., Uchida, H., Wanninkhof, R., and Yasuhara, M.: A Global Ocean Oxygen Database and Atlas for Assessing and Predicting Deoxygenation and Ocean Health in the Open and Coastal Ocean, Front. Mar. Sci., 8, 2021.

Homoky, W. B., Conway, T. M., John, S. G., König, D., Deng, F., Tagliabue, A., and Mills, R. A.: Iron colloids dominate sedimentary supply to the ocean interior, Proc. Natl. Acad. Sci., 118, e2016078118, https://doi.org/10.1073/pnas.2016078118, 2021.

Huang, J., Jones, A., Waite, T. D., Chen, Y., Huang, X., Rosso, K. M., Kappler, A., Mansor, M., Tratnyek, P. G., and Zhang, H.: Fe(II) Redox Chemistry in the Environment, Chem. Rev., 121, 8161–8233, https://doi.org/10.1021/acs.chemrev.0c01286, 2021.

Robinson, D., Pham, A. L. D., Yousavich, D. J., Janssen, F., Wenzhöfer, F., Arrington, E. C., Gosselin, K. M., Sandoval-Belmar, M., Mar, M., Valentine, D. L., Bianchi, D., and Treude, T.: Iron “ore” nothing: benthic iron fluxes from the oxygen-deficient Santa Barbara Basin enhance phytoplankton productivity in surface waters, Biogeosciences, 21, 773–788, https://doi.org/10.5194/bg-21-773-2024, 2024.

Severmann, S., McManus, J., Berelson, W. M., and Hammond, D. E.: The continental shelf benthic iron flux and its isotope composition, Geochim. Cosmochim. Acta, 74, 3984–4004, https://doi.org/10.1016/j.gca.2010.04.022, 2010.

Sigman, D. M., Robinson, R., Knapp, A. N., van Geen, A., McCorkle, D. C., Brandes, J. A., and Thunell, R. C.: Distinguishing between water column and sedimentary denitrification in the Santa Barbara Basin using the stable isotopes of nitrate, Geochem. Geophys. Geosystems, 4, https://doi.org/10.1029/2002GC000384, 2003.

Sommer, S., Gier, J., Treude, T., Lomnitz, U., Dengler, M., Cardich, J., and Dale, A. W.: Depletion of oxygen, nitrate and nitrite in the Peruvian oxygen minimum zone cause an imbalance of benthic nitrogen

fluxes, Deep Sea Res. Part Oceanogr. Res. Pap., 112, 113–122, https://doi.org/10.1016/j.dsr.2016.03.001, 2016.

Valentine, D. L., Fisher, G. B., Pizarro, O., Kaiser, C. L., Yoerger, D., Breier, J. A., and Tarn, J.: Autonomous Marine Robotic Technology Reveals an Expansive Benthic Bacterial Community Relevant to Regional Nitrogen Biogeochemistry, Environ. Sci. Technol., 50, 11057–11065, https://doi.org/10.1021/acs.est.6b03584, 2016.

Yousavich, D. J., Robinson, D., Peng, X., Krause, S. J. E., Wenzhoefer, F., Janßen, F., Liu, N., Tarn, J., Kinnaman, F., Valentine, D. L., and Treude, T.: Marine anoxia initiates giant sulfur-bacteria mat proliferation and associated changes in benthic nitrogen, sulfur, and iron cycling in the Santa Barbara Basin, California Borderland, EGUsphere, 1–48, https://doi.org/10.5194/egusphere-2023-1198, 2023.